

AD-A032 868

WEBB INST OF NAVAL ARCHITECTURE GLEN COVE N Y
NON-STRUCTURAL BULKHEADS TO CONTROL TANKER OIL SPILLS.(U)
AUG 74 N A HAMLIN

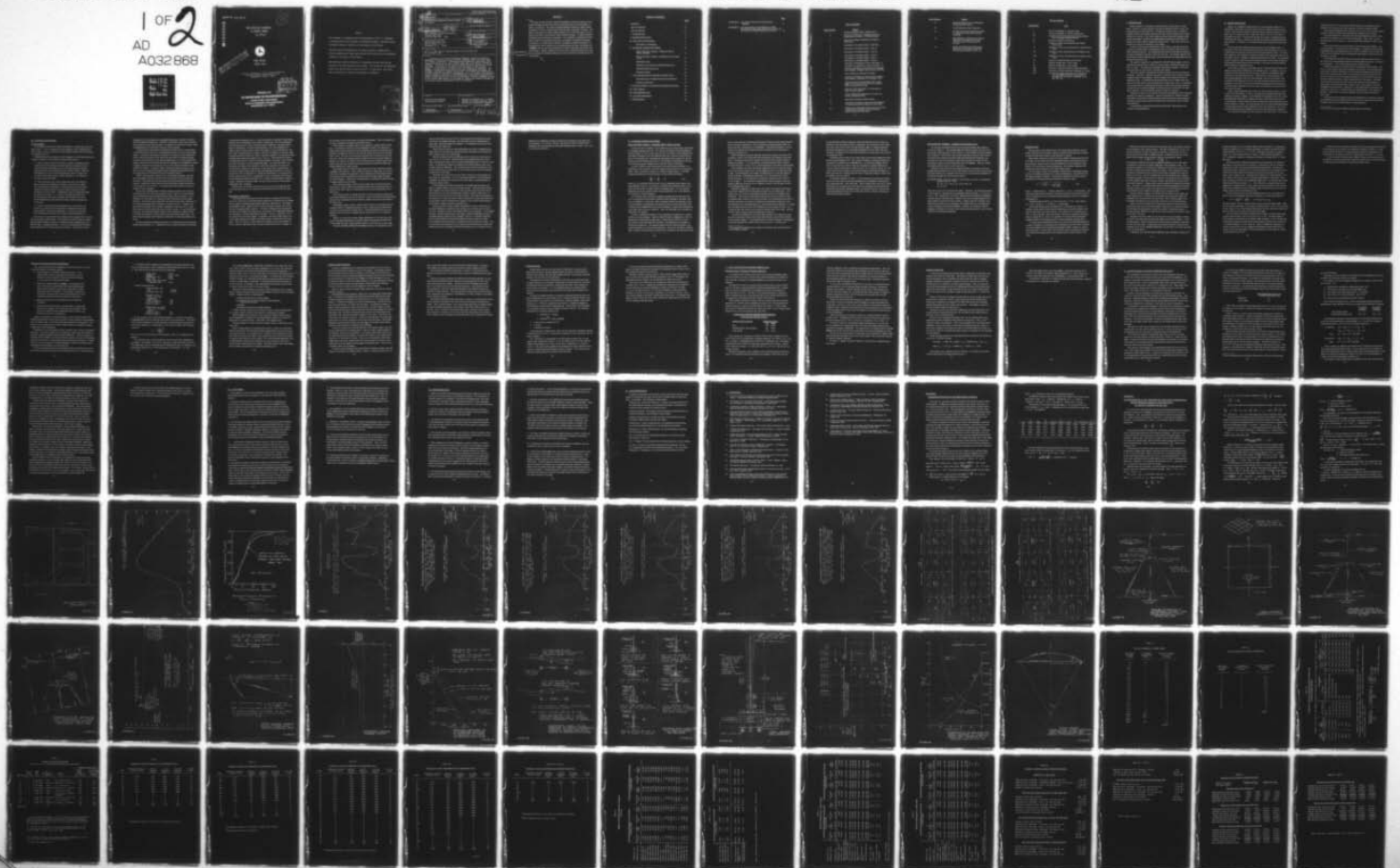
F/G 13/10

UNCLASSIFIED

USCG-D-112-76

DOT-CG-41015-A
NL

1 OF 2
AD
A032 868



REPORT NO. CG-D-112-76

ADA 032868

13

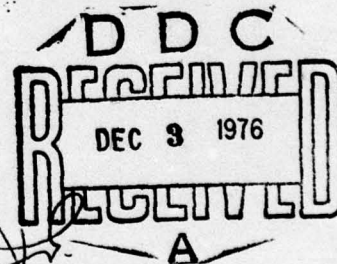
NON-STRUCTURAL BULKHEADS
TO CONTROL TANKER
OIL SPILLS



FINAL REPORT
AUGUST 1974

COPY AVAILABLE TO DDG DOES NOT
PERMIT FULLY LEGIBLE PRODUCTION

Document is available to the U.S. Public through the
National Technical Information Service,
Springfield, Virginia 22161



PREPARED FOR

U.S. DEPARTMENT OF TRANSPORTATION
UNITED STATES COAST GUARD
OFFICE OF RESEARCH AND DEVELOPMENT
WASHINGTON, D.C. 20590

NOTICE

This document is disseminated under the sponsorship of the U. S. Department of Transportation in the interest of information exchange. The United States Government assumes no liability for the contents or use thereof.

The United States Government does not endorse products or manufacturers. Trade or manufacturers' names appear herein solely because they are considered essential to the object of this report.

Webb Institute of Naval Architecture is responsible for the facts and the accuracy of the data presented in this report. The contents do not necessarily reflect the official views or policy of the U. S. Coast Guard. This report does not constitute a standard, specification or regulation.

ACCESSION for	
THIS	White Section <input checked="" type="checkbox"/>
DDO	Full Section <input type="checkbox"/>
UNREPRODUCED	<input type="checkbox"/>
JUSTIFICATION.....	
BY.....	
ORIGINATOR'S AVAILABILITY CODES	
APPROL. DRUG. SPECIAL	
A	

1342

1. Report No. 18 USCG D-112-76	2. Government Accession No.	3. Recipient's Catalog No.
4. Title and Subtitle Non-Structural Bulkheads to Control Tanker Oil Spills.		5. Report Date August 1974
6. Performing Organization Code		7. Author(s) Norman A. Hamlin
8. Performing Organization Report No.		9. Work Unit No. (TRAIS)
10. Sponsoring Agency Name and Address Webb Institute of Naval Architecture Crescent Beach Road Glen Cove, New York 11542		11. Contract or Grant No. DOT-CG-41015A
12. Sponsoring Agency Name and Address United States Coast Guard 400 7th Street, S. W. Washington, D. C. 20590		13. Type of Report and Period Covered Final Report.
14. Sponsoring Agency Code G-DST-2		
15. Supplementary Notes The U. S. Coast Guard's technical monitor on this project was Mr. Jonathan R. Amy.		
16. Abstract A system of non-structural transverse bulkheads, formed by transverse membranes enclosing the open space between transverse webs in the cargo tanks of a tanker, is presented. The system provides additional subdivision, which reduces the outflow of oil from a loaded cargo tank if the tank is ruptured in collision. The ability of the system to reduce collision outflows on a 75,000 DWT tanker is evaluated on the basis of the statistics of past collision damages. A design method for sizing sheet steel membranes is developed. Cost estimates, and Required Freight Rate to recover the increased investment, are included, predicated on Japanese construction. It is shown that a reduction of probable accidental discharge of approximately 9% can be achieved by an estimated annual increase in operating cost of \$26,000 when non-structural bulkheads are fitted in wing tanks only and at every second frame. Finally, estimates are made of the overall effectiveness of the system is reducing the probable discharge of oil from all sources, operational as well as accidental.		
17. Key Words Non-Structural Bulkheads Controlling Oil Spills		18. Distribution Statement Document is available to U. S. Public through the National Technical Information Service, Springfield, Virginia 22161
19. Security Classif. (of this report) Unclassified	20. Security Classif. (of this page) Unclassified	21. No. of Pages 95
		22. Price

ABSTRACT

↙ A system of non-structural transverse bulkheads, formed by transverse membranes enclosing the open space between transverse webs in the cargo tanks of a tanker, is presented. The system provides additional subdivision, which reduces the outflow of oil from a loaded cargo tank if the tank is ruptured in collision. The ability of the system to reduce collision outflows on a 75,000 DWT tanker is evaluated on the basis of the statistics of past collision damages. A design method for sizing sheet steel membranes is developed. Cost estimates, and Required Freight Rate to recover the increased investment, are included, predicated on Japanese construction. It is shown that a reduction of probable accidental discharge of approximately 9% can be achieved by an estimated annual increase in operating cost of ~~\$20,000~~ when non-structural bulkheads are fitted in wing tanks only and at every second frame. Finally, estimates are made of the overall effectiveness of the system in reducing the probable discharge of oil from all sources, operational as well as accidental.

U

↖

TABLE OF CONTENTS

	<u>Page</u>
ABSTRACT	i
LIST OF FIGURES	iv
LIST OF TABLES	vi
I. INTRODUCTION	1
II. SYSTEM DESCRIPTION	2
III. OUTFLOW CALCULATIONS	4
Base Ship for Calculations	6
IV. BULKHEAD LOADING AND STRESS	10
Static Loads after Collision - Bulkheads Tight at Bottom and Sides	10
Static Loads after Collision - Bulkheads Free-Flooding at Foot	13
Seakeeping Loads	14
Material for Non-Structural Bulkhead Membranes	18
Membrane Edge Connections	21
Membrane Design	23
V. COST ESTIMATES AND REQUIRED FREIGHT RATE	25
Estimated Costs of Fitting Non-Structural Bulkheads	25
Required Freight Rate	27
VI. EFFECTIVENESS OF SYSTEM IN REDUCING POLLUTION	29
VII. CONCLUSIONS	34
VIII. RECOMMENDATIONS	36
IX. ACKNOWLEDGEMENTS	38
X. REFERENCES	39

	<u>Page</u>
APPENDIX A - "As-Failed" Distortion of Non-Structural Bulkhead	41
APPENDIX B - An Approximation to the Thickness of a Mild Steel Clamped-Edge Square Membrane Loaded to the Yield Point by Constant Pressure on One Face	43

LIST OF FIGURES

<u>Figure Number</u>	<u>Caption</u>
1	Simplified Midship Section, Design D75-A
2	Percent of Collisions vs. Damage Location for Longitudinal Increments = 5% of Ship Length
3	Observed Cumulative Distribution of Depth of Penetration
4	Distribution of Probable Outflow - Base Ship
5	Distribution of Probable Outflow - Case II
6	Distribution of Probable Outflow - Case III
7	Distribution of Probable Outflow - Case IV
8	Distribution of Probable Outflow - Case V
9	Distribution of Probable Outflow - Case VI
10	Alternative Arrangement of Cargo Tank Space - I
11	Alternative Arrangement of Cargo Tank Space - II
12	Pressure Distribution on Non-Structural Bulkhead After Damage - Bulkhead Tight at Bottom and Sides
13	Square Membrane Clamped at All Edges
14	Pressure Distribution on Non-Structural Bulkhead After Damage - Bulkhead Free Flooding at Foot
15	Hydrostatic Pressure Distribution Due to Pitch Angle on 2-Frame Cell Non-Structural Bulkhead When Carrying Partial Cargo
16	Maximum Pitch Amplitudes vs. Deadweight for Ships of Large Fullness
17	Vector Diagram Showing Motion at Frame 98 at Instant of Maximum Pitch
18	Hydrostatic Pressure Increase Factor
19	Hydrostatic Pressures on Non-Structural Bulkhead at Frame 98 at Instant of Maximum Pitch Angle
20	Diagrammatic Sketch Showing Directions of Vertical Acceleration Components Forward and Aft at Instant of Maximum Pitch Angle

Figure Number

Caption

- | | |
|----|---|
| 21 | Membrane Edge-Connections That Were Considered and Rejected |
| 22 | Typical Membrane Edge Connection |
| 23 | Increase in Required Freight Rate (RFR) vs. Reduction in Expected Accidental Discharge |
| 24 | Approximation to Work Done and Energy Absorbed in Yielding of Center Tank Membrane Due to Pressure Load of 6.23 psi |
| 25 | Section Through Clamped-Edge Square Membrane with Pressure on One Face Showing Approximating Circular Arc |

LIST OF TABLES

<u>Table Number</u>	<u>Title</u>
I	Percent of Damages vs. Damage Length
II	Percent of Damages vs. Depth of Penetration
III	Calculation Form for Determining Probable Outflow from 5% Length Damage Increment
IV	Summary of Outflow Calculations
V	Thickness of Wing Tank Membranes for Double- Frame Cells
VI	Thickness of Center Tank Membranes for Double-Frame Cells
VII	Thickness of Wing Tank Membranes for Single-Frame Cells
VIII	Thickness of Center Tank Membranes for Single-Frame Cells
IX	Summary of Estimated Ship Cost Increases
X	Required Freight Rate - Short Voyage
XI	Required Freight Rate - Long Voyage
XII	Decrease in Expected Annual Accidental Discharge
XIII	Calculation of Mean Operational Discharge per Voyage
XIV	Fleetwise Oil Outflow Estimates from Operational and Accidental Discharges Apportioned on a Per Ship, Per Year Basis, Assuming 12 Voy- ages Per Year

I. INTRODUCTION

Modern tankers are customarily constructed with a small number of large tanks. Therefore, a large quantity of oil may be spilled from such a vessel, following puncture of a full cargo tank. The objective of this report is to explain a possible method of reducing the amount of oil which would be spilled from a tanker involved in a collision. The method makes use of non-structural bulkheads which extend athwartships, effectively providing additional subdivision and limiting the amount of oil which would be replaced by flooding water. This report may be considered as a study of the feasibility of the method.

In order to determine the effectiveness of the system, it has been necessary to develop a rational method of finding the amount of oil which would flow out of a tanker following collision. The calculational procedure is based upon the statistics of collision damages as they have occurred in the past. The damage statistics utilized include records of damage length, depth of penetration and longitudinal location, largely from Reference (1).

The method is applied to a conventional 75,000 DWT tanker design, on the assumption the ship will carry crude oil on some voyages, and dirty petroleum products on others. The design has substantial clean ballast capability, in that only two cargo tanks are also used for carrying water ballast.

The study considers scantlings and material selection for the non-structural bulkheads. Therefore, it has been necessary to estimate both in-service and after-damage loadings on the bulkheads, and the strength of the material of which the bulkhead is built. The bulkhead design adopted makes use of a double-layer laminate of thin sheet metal, which can support only tensile loads, that is, a membrane. An important detail in implementing the system is found to be the edge connection, by which the non-structural bulkhead membrane material is attached to the fixed ship's structure, such that bending stresses are kept to a minimum.

Estimates of the cost of the system are made by assessing the cost of materials and labor for separate components. Using the estimated cost, Required Freight Rate (RFR) is calculated, the RFR increase beyond the base ship representing the increased monetary income which would have to be recovered in order to justify the investment.

A final portion of the report deals with the estimated effectiveness of the system in reducing pollution.

II. SYSTEM DESCRIPTION

Figure 1 is a simplified midship section of a modern tanker typical of U. S. construction, showing the web frame which serves to stiffen the structure transversely. Such webs are located in transverse planes, typically spaced 12 to 15 ft. apart; thus, in a cargo tank 100 ft. long, there may be 6 or more such webs in the length of the tank. It may be seen that the web occupies a significant portion of the transverse space, especially in the wing tank between the longitudinal bulkhead and shell. In addition, two horizontal struts further subdivide the wing tank space.

The non-structural bulkhead proposed consists of an unstiffened sheet, or membrane, which would extend transversely to fill in the open space up to a level at least above the waterline between the web face plates and the struts. For structural simplicity, the membrane is assumed to fill the entire open space between web face plates, thereby providing a continuous attachment at all edges. The membrane is able to support a moderate pressure difference across its two faces through the development of tensile stress in the membrane, in the same way that an inflated balloon contains an internal pressure.

In the event of a puncture in the shell, all oil in the space formed between the adjacent non-structural bulkheads is lost through outflow. In addition, oil in the remainder of the tank above the level of upper openings in the bulkheads (which must be above the waterline) flows out. Furthermore, in the event there are free-flooding openings at the foot of the bulkheads, then oil at the bottom of the remainder of the tanks will be lost; an oil-water interface will then form in the remainder of the tank at or above the free-flooding openings such that the pressure of the head of contained oil at the interface is balanced by the external hydrostatic water pressure.

Figure 1 shows lightening holes in the web, which would be omitted or closed in way of the oiltight space on webs at which non-structural bulkheads are fitted. Although not shown on Figure 1, most shipyards fit longitudinals at the deck, shell and longitudinal bulkheads as continuous members, which pass through the web in open cutouts. These cutouts must also be closed in way of the membrane at all levels intended to be tight. (It is assumed that the ease of assembling longitudinals in cutouts would result in their continuance in new ship construction, but with the shipyard taking steps after assembly to close the cutout openings as necessary).

Non-structural bulkheads may also be fitted in the center tanks. For reasons

outlined in Section IV, it is assumed that such center tank membranes would be supported by a vertical strut on the centerline, as well as around its edges.

Non-structural bulkheads may be fitted on every web or at more widely-spaced intervals; single and double-frame spacings are considered in this report.

The space between two successive non-structural bulkheads is called a "cell", and these are identified by a letter with two subscripts. Thus, cell a₄₂ means the forwardmost cell in tank No. 4, with non-structural bulkheads at every second frame.*

Access into the tank must be provided for tank cleaning and "mucking". For pricing purposes, it is assumed that internal ladders, a cylindrical plate coaming, a personnel hatch, and hinged hatch cover would be provided for every second cell, with access into alternate cells accomplished through dogged oil-tight doors in the membrane at its foot.

Tank washing in tanks fitted with non-structural bulkheads would be done in the normal way, using washing machines inserted through deck plates -- or "Butterworth openings" -- or by fixed washing machines within the tank.

Filling and pumping out the tank would be accomplished without change. However, to avoid separate cargo pipe connections in each cell, it is assumed the web at the foot of a non-free-flooding type of non-structural bulkhead would be fitted with a motor-operated sluice valve, so that cargo oil could flow freely from cell to cell. (Obviously, this valve should be placed at the foot of the web as close to the bottom shell as possible, perhaps opening directly at the shell). The sluice valves would be closed at all times, except when cargo oil is being loaded or pumped out, at which time the valves would be open. This appears to be a disadvantage for this alternative, inasmuch as a ship lightering off into barges at the entrance to a busy port, or transferring cargo while underway, when collision is possible, would not have the desired additional outflow protection activated at these times.

In the case of free-flooding non-structural bulkheads also considered, generous free-flooding ducts are provided at the foot of the web to assure that cargo oil flows smoothly from cell to cell when filling, or when pumping out.

* See Table IV for rigorous definition used for outflow calculations.

III. OUTFLOW CALCULATIONS

Assumed Damage

The principle upon which the outflow calculations -- and the merit of the proposed system -- rests is dependent upon the tendency of oil of a light density to float on water, not to mix with water, and to establish a stable oil-water interface at the bottom of the oil.

Manifestations of this principle are well explained in the following excerpt from a report of model tests of oil outflows in Japan, Reference (2):

"1. Where a break occurs in the bottom of a tanker, the pressure of the crude oil at the ship's bottom is greater than that of outside sea water, and therefore the crude begins to go out and keeps flowing till the head difference between crude oil and sea water would be relieved. When the head difference in way of the break disappears, the oil no longer flows out except where ship's motion, rolling, pitching etc. or moving in of sea water excites the outflow."

"2. When the break occurs in ship's side under water, the crude oil above the water line would flow out quickly, and in this case, unlike the case described in paragraph 1, the pressure does not come to equilibrium all around the break, because the specific gravity of crude oil differs from that of water. Consequently, the oil is displaced through the break by sea water, i. e., oil flows out through the upper half of the break and sea water flows in through the lower half of the break, and the displacement ceases when the seawater reaches the upper end of the break."

"3. Where a break at the ship side extends above the water line, the oil flows out at first by the head difference and afterwards by the displacement effect mentioned in paragraph 2. The total oil in the tank flows out because oil and water never balance during displacement..."

Any system to reduce outflow from collision must be supported by a valid method of assessing its effectiveness. This requires a realistic method of calculating the probable outflow of cargo oil for different system configurations, and different ships. Simplified formulae -- such as the assumption that the depth of damage penetration is a fixed percentage of the beam -- generally do not lend

themselves to the determination of meaningful differences in outflow for different tank and bulkhead arrangements. Therefore, calculations in this report are based upon the history of past ship collisions, as manifest in the statistics of length, depth of penetration, and of longitudinal location of collision damage.

Considering first the question of longitudinal damage location, it was decided to divide the length of ship into 20 equally-spaced intervals, each of 5% ship length. Figure 2, showing the percentage of collisions to be expected in each longitudinal interval, has been prepared on the basis of the past history of collision damages reported in Reference (1) for cargo and passenger ships. It is tacitly assumed that similar statistical trends would be shown by an examination of the statistics of tanker collisions, inasmuch as such statistics are not to the writer's knowledge readily available for tankers. In general, Figure 2 shows that collision damage is most likely to be experienced by the middle portions of the ship; also such damage has been experienced more frequently forward of amidships than aft.

Table I, also from data in Reference (1), lists lengths of damage, generally for 5-foot length increments, and the percent of damages occurring within each increment. These data are also based upon cargo and passenger ship collision records. Inspection of Table I shows that the most frequent length of damage lies in the range of 17.5 to 22.5 feet. It is assumed that these statistics are also applicable to tanker collisions.

Similar data regarding depth of collision damage penetration can be derived from Reference (1) for cargo and passenger vessels. However, we are fortunate to have available the tanker collision analysis results shown on Figure 3, from Reference (3), which shows the statistics of depth of penetration in past tanker collisions. Also shown is the comparable curve derived from data in Reference (1) for cargo and passenger ships, assuming a mean beam of 80 ft. It appears that about 50% of all damages from collision, regardless of ship type, led to a penetration inboard from the side of the ship of at least 6 meters. It may be noted that the deeper, less-frequent damages appear to have penetrated to a greater depth, in the case of the tankers, than was true for the cargo and passenger ships. The tanker data from Figure 3 are tabulated in Table II for 2-meter penetration increments.

In order to apply the foregoing information, it is assumed that each of the three damage characteristics, i. e., longitudinal location, length, and depth of penetration,

is statistically independent; that is, once the probability is specified of experiencing a damage with its longitudinal center within a certain range, then the probabilities that the damage will fall within a specified range of length and a specified range of depth are independent. Expressed mathematically, if P_1 is the probability of a specific range of damage center location from Figure 1, P_2 the probability of a specific range of damage length from Table I, and P_3 the probability of a specific range of damage penetration depth from Table II, then the probability of the specified ranges of damage being experienced together is $P_1 \times P_2 \times P_3$. This expression is subject to interpretation however, insofar as internal damage is concerned, and the athwartship extent of damage of a given longitudinal length. As a practical matter, the immediate importance of such statistics results from estimates of the amount of oil which may be spilled in a collision due to the outflow from a breached tank. In view of the relatively large width of wing tank (longitudinal bulkhead 10.82 meters inboard from side for Design D75-A, chosen for calculations), it is assumed in the present report that the bow of a colliding ship, were it to penetrate as far inboard as the longitudinal bulkhead of Design D75-A, would breach the bulkhead at only one location, regardless of damage length, and this location would be at the assumed longitudinal center of damage.

Furthermore, the damage is assumed to occur in way of the waterline, that is, the assumed puncture is not confined to areas wholly above or below the waterline.

Base Ship for Calculations

It was agreed that calculations would be made for a specific gravity of cargo oil of 0.85, and for the 75,000-DWT tanker design shown in Reference (4) as Design D75-A, which is a generally conventional single skin, single bottom, twin longitudinal bulkhead tanker, intended to carry crude oil and dirty cargoes, with a large amount of segregated ballast capacity. Transverse bulkheads divide the ship into five tanks in the length of the cargo space, but because of the longitudinal bulkheads, the cargo space is further subdivided into 15 tanks. The No. 3 wing tanks, P & S, are reserved for clean water ballast. In addition, clean water ballast may be carried in tanks outboard of and abaft the machinery space, and forward of the cargo space. The No. 2 and No. 4 center tanks are arranged to carry water ballast as well as cargo oil; this ballast water becomes contaminated from the "clingage" of

oil remaining on tank surfaces after the cargo is discharged. Thus, the design does not have a completely segregated clean ballast system.

Table III shows a completed tubular form adopted for making outflow calculations. For damages centered at a given longitudinal location, the principal variations which must be accounted for are the number and capacity of wing tank cells breached, the outflow from above cells, and the outflow from below free-flooding ducts, if any. The form is set up so that maximum effort is directed at the wing tank cells, owing to the range of numbers of these for various assumed lengths of damage. By contrast, the outflow from the center tanks is relatively easy to find, owing to the previously-mentioned assumed limitation of penetration of the longitudinal bulkhead at a single location.

The example shown on Table III demonstrates the way the variation of length of damage is accounted for. Thus, within the limits of a single tank, one or more cells may be breached; the probability of any combination of cells being breached is accounted for by the probability of experiencing the damage length that spans the cell combination. Outflow from adjoining tanks is accounted for when the length of damage extends into such tanks.

In the Table III example, outflow from the center tank is taken as the entire tank capacity, which is added to the probable outflow from the wing tank cells, inasmuch as the center tank is not subdivided by non-structural bulkheads for the case shown.

The probable outflow for damage centered at the point assumed is determined by the final calculation at the foot of Table III. It may be seen that only damage which penetrates the longitudinal bulkhead results in outflow from both the wing tank and the center tank.

Calculations similar to that in Table III were carried out for damage centered at approximately 27 longitudinal locations, and for 5 different ship modifications as well as for the base ship, Design D75-A. Limited calculations for other combinations were also made for damage centered at frame 72-1/2, for comparative purposes.

Figure 4 is a plot of the results of these calculations for the base ship, showing the longitudinal distribution of probable outflow from damage centered within 5% ship length intervals, plotted against distance as a decimal part of ship length.

To find the probable outflow from the ship as a whole, it is necessary to mul-

tively the mean value of the curve by 20, there being (20) ship-length increments of 5% each in the length of the ship. The area under the curve as plotted is its mean value, and may be found by integration. The integration of each curve was performed with a planimeter.

Table IV lists all cases for which calculations were made, including the probable outflow for the base ship, and the previously-mentioned five ship cases for which complete curves were determined.

Figures 5 through 9 show the distribution curves which were determined for Cases II, III, IV, V, and VI. Figures 10 and 11 are simplified plan views of the ship, showing frames where the non-structural bulkheads would be located for these cases. An inspection of Figures 5 through 9 shows discontinuities in the curves at main transverse bulkheads. This results from the convention adopted for handling the outflow from the center tank, by which outflow occurs only from damages centered in way of the tank.

The sharp dip in the curves in way of Tank 3 results from the assignment of Wing Tank 3 to clean ballast. In view of the high probability of collision damage amidships, the elimination of cargo oil from these tanks is obviously helpful in reducing probable outflow.

In accomplishing the outflow calculations, reasonable approximations were made as regards sinkage, heel and trim after damage. These generally assumed that a weight is lost from the ship as a result of cargo oil lost from above the initial waterline in way of the damaged tank, and that a weight is added due to replacement of oil by water below the initial waterline. Hydrostatic characteristics for Design D75-A which were used for these calculations are based upon Reference (5), inasmuch as ship G of Reference (5) appears to have similar characteristics (same length, breadth and depth) as Design D75-A.

Time did not allow complete outflow calculations for cases in which the non-structural bulkheads are tight at bottom and sides up to the deck, that is Case X. Nor were calculations made of the probable outflow from strandings. To accomplish the latter, statistical information on the length, width and longitudinal location of stranding damages would have to be compiled. However, it should be noted that the use of free-flooding non-structural bulkheads would not reduce oil outflow from strandings when the puncture is confined to the lower levels of the ship. This is so because a large quantity of oil is retained in any breached tank so punctured, whether there be free-flooding non-structural bulkheads or not, because of the es-

tablishment of equilibrium pressure at the oil-water interface at the upper level of the puncture. It is evident, however, that more oil would be retained after a stranding if non-free-flooding non-structural bulkheads tight at bottom, sides, and up to the deck were fitted.

IV. BULKHEAD LOADING AND STRESS

Static Loads After Collision -- Bulkheads Tight at Bottom and Sides

In this case the free surface of the contained oil is at a fixed height, determined by the highest opening in the web. The pressure distribution down the bulkhead is shown by Figure 12, and it may be noted that the net pressure on the bulkhead at its foot might be tending to force the bulkhead toward the contained oil, or toward the water in the damaged cell, depending upon the height of the contained oil, the difference in density between water and oil, and the depth of submergence at the foot. The maximum pressure loading occurs at the free surface of the water.

In order to find the stress distribution in the non-structural bulkhead, it is idealized as a thin membrane, which can support tensile loads but not compressive loads. Such a membrane is subject to a relatively simple analysis. The basic equation governing the stress distribution is given by Reference (6) as,

$$\frac{S_m}{R_m} + \frac{S_t}{R_t} = \frac{p}{t} \quad [1]$$

where S_m is a meridional tensile stress, and S_t a tangential tensile stress, both being principal stresses. R_m and R_t are meridional and tangential radii of curvature of section curves in planes normal to the tangent plane. P is the pressure of difference across the membrane which must be supported, and t is the thickness of the material, assumed constant.

In the present case, generally rectangular openings between wing tank webs are to be enclosed by the membrane material; larger openings in the center tanks are to be enclosed. In each case, since no bending stresses are assumed to exist in the membrane, the integration of all pressure forces normal to the plane of the membrane must be balanced by the normal component of tensile forces transmitted to the edge of the web by the membrane. Thus, the edge angle of the membrane is important to the analysis.

In order to simplify the problem, the web opening is treated first as a square, and then as a long rectangle. Figure 13 shows the square configuration. Since an initially plane membrane develops stress -- and also finite radii of curvature -- only because of the stretching of its elements, it is important that the degree of stretch be accounted for. The approach taken is that the material exhibits a pronounced yield point, as in the case of mild steel. Then in the "as-failed" condition, after a collision, the membrane is assumed to be stretched at the yield point stress, and it is only necessary to determine the amount of stretch.

and it is only necessary to determine the amount of stretch and the energy absorbed by the material in stretching, in order to find when conditions stabilize after the failure and static equilibrium is re-established. This approach appears to be generally in line with the limit design theory first presented to naval architects by Drucker in Reference (7).

Initial calculations using this approach assumed an arbitrary 1% stretch, without failure, which is well beyond the stretch associated with yielding of mild steel. Thus, if mild steel is assumed to yield at 30,000 psi in direct tension, and has a modulus of elasticity, $E = 30,000,000$ psi, the dimensionless stretch at yield is $30,000/30,000,000 = 0.001$ or 0.1%, provided the Poisson ratio effect is disregarded.

If one considers the load as carried by tangential forces only, then the tangential curves become circular arcs^{*}, and the tangential stress is constant from edge to edge. By introducing R_t into Equation [1] appropriate to a wing tank bulkhead with 0.1% stretch, by assuming P appropriate to an 8 foot head of oil, with $S_t = 30,000$ psi and $S_m = 0$, the thickness of membrane is found to be of the order of 0.1 in. or less. An 8 foot head is approximately the head needed to cause the pressure difference at the foot of the bulkhead to vanish, when the depth of water on the damaged side is 40 ft.

Inspection of Equation [1] shows that as the radius of curvature R_t decreases, the pressure supported by the membrane increases for a fixed thickness. In the present case, R_t can only be decreased by greater stretch of the initially-plane membrane. The amount of stretch which mild steel in the form of sheets is able to withstand before rupture is not known precisely, but is undoubtedly more than 1%. Standard references on strength of materials show substantial elongations of the test specimen in the standard tensile test, with dimensionless elongations, or stretch, up to 10% being shown by Figure 338 of Reference (9) for example; however, it is recognized that such strains occur beyond the constant yield stress range, when the stress is again rising and strain hardening has commenced.

Non-structural bulkheads in the center tanks present a more difficult problem than in the wing tanks because of the large width of panel involved and the absence of intermediate supports. A preliminary check of required thickness of unsupported membrane indicated this would be of the order of 0.36 in. A vertical strut

* The circular arc configuration is confirmed in Reference (8), which assumed a long rectangular opening.

on the centerline was then considered, and it was found that if such a strut were introduced, the total weight of steel (2 membranes, one on each side of the centerline, plus strut) would be about 25% less than the weight of a single unsupported membrane extending from one longitudinal bulkhead across the ship to the other. Therefore, scantlings of all center tank membranes are predicated on the presence of a centerline strut.

Considering the two panels of the center tank non-structural bulkhead as represented by long rectangles 27 ft. wide, and now tentatively accepting 10% stretch as a possible "as-yielded but not-ruptured" value, it is found (see Appendix A) that with a steel membrane 0.085 in. thick one can support a pressure difference of 6.23 psi, which is equivalent to a head of 16.9 ft. of 0.85 specific gravity oil. Such a head could only be developed on non free-flooding non-structural bulkheads if a filled cargo tank were ruptured with the ship in a light draft condition, which would be unlikely to occur in service.

A membrane thickness of 0.085 in. is that calculated as necessary for single-frame cell center tank non-structural bulkheads near amidships to withstand possible seakeeping loads. (See Table VIII). Thus it appears that if one were to select the thickness of the membranes on the basis of not exceeding the yield point when experiencing the highest seakeeping loads to be expected in service, then the non-structural bulkhead should be able to contain the oil after collision in almost any conceivable operating condition.

Static Loads After Collision -- Bulkheads Free-Flooding at Foot

The pressure distribution down the non-structural bulkhead after collision is shown by Figure 14. The principal difference between Figures 12 and 14 is that the pressure difference goes to zero at the foot of the bulkhead in the free-flooding case, Figure 14. At this level, the oil-water interface is achieved, and it may be seen that by directing the bellmouths of the free-flooding ducts downward, one can lower the level of the interface, and thereby minimize the outflow of oil by reducing the volume of free-flooding water below the interface. However, bottom web cutouts would also have to stop at this level.

Inasmuch as the depth from the damaged waterline to the bottom of the free-flooding ducts (assumed as 1 foot above the baseline) is about 40 feet for most cases for which outflows were calculated, the head of oil on non-structural bulkheads enclosing the damaged cell may be found as follows:

Let H be the height of oil from interface to free surface, and $S.G.$ be the specific gravity of the oil. Then,

$$64 \times 40 = S.G. \times 62.4 \times H = 0.85 \times 62.4 \times H$$

$$H = 48.2 \text{ ft.}$$

Thus, the oil level is 8.2 feet above the water. Therefore, the maximum pressure on the membrane, which occurs at the damaged waterline surface, is $0.85 \times 62.4 \times (48.2 - 40) = 370 \text{ lbs/ft}^2$ or 2.56 psi. Inasmuch as this loading is substantially less than might be developed after collision on non-free-flooding bulkheads in the light condition reported in the prior section, it appears that the "as-failed" case should not govern the choice of thickness of membrane either for free-flooding or non-free-flooding non-structural bulkheads. Instead, the membrane should be designed on the basis of in-service loads, using seakeeping criteria, such as those reported in the following paragraphs.

Seakeeping Loads

When the ship is fully loaded with oil, with cargo tanks pressed up, the free surface within the tank is minimal, and the membrane should experience virtually no pressure differences because of ship motions in a seaway.

When partial cargoes are carried, the oil is capable of surging back and forth in the tank, and one might expect that substantial dynamic loads would develop on the membrane, whether the non-structural bulkhead were free-flooding or tight. However, for such loads to become troublesome, the excitation frequency must approach the natural frequency of the motion being excited.

The first type of motion to be considered corresponds to longitudinal surging, such as is sometimes experienced in a ship's swimming pool, and sometimes called "cargo sloshing" on tankers. Abrahamsen in Reference (10) quotes Lamb's expression for the natural period of oscillation of liquid in a tank:

$$T_n = 2\pi \sqrt{\frac{l}{n\pi g} \times \frac{1}{\tanh\left(\frac{n\pi h}{l}\right)}} \quad [2]$$

where l = length of tank, h = depth of liquid and $n = 1, 2, 3, \dots$ = mode number. This is the same expression presented by Comstock in Reference (11) and also shown as curves in Reference (12) for the natural surging frequency of water in a shipboard swimming pool.

Evaluating Equation [2] for a 2-frame cell when $l = 27$ ft., with a depth of oil = 50 ft., and for $n = 1$, we find $T_n = 3.25$ seconds.

The natural pitching period of Design D75-A is estimated to be about 7-1/4 seconds, and the period at which severe pitching occurs would be expected on the basis of model tests to be more than this. So it appears the "swimming pool effect" or "cargo sloshing" may be discounted as the cause of significant membrane loads on Design D75-A. In fact, the presence of the non-structural bulkheads should eliminate the hydrodynamic need for swash bulkheads on Design D75-A.

A second dynamic loading could arise in the case of free-flooding bulkheads as a result of transfer of oil through the free-flooding ducts when the ship is pitching, in a mode analagous to the intentional athwartships transfer of liquid in a passive anti-rolling tank. It seems likely that such flows could be troublesome if the ship were pitching at the same period as the natural period of liquid transfer in this mode.

Reference (13) discusses the theory of the passive tank, and includes equations for calculating the tank natural frequency. The tank is idealized as a U-tube. As shown by Reference (14) and other texts on vibration, the natural period of a U-tube increases as the length of circuit increases. In Reference (13), the circular passive tank frequency ω_ϕ is expressed in terms of an integral S' , where

$$\omega_\phi^2 = \frac{2g}{S'} \text{ and } S' = \int_0^L \frac{A_0}{A(s)} ds.$$

The symbols in Reference (13) are not completely defined, but it is clear that S' is supposed to represent the length of fluid path of the equivalent U-tube. For numerical evaluation, S' is expressed in Reference (13) as the sum of three terms, the third of which includes duct length as one factor. This expression has been evaluated for adjoining 2-frame cells in the wing tanks of Design D75-A when the depth of oil is 50 ft., and it is concluded that if the free-flooding ducts consisted of 3 pipes of length 4 ft. and with 22 in. diameter, the natural period of oscillation would be slightly longer than 14 seconds, which is well beyond the period of maximum pitch response. A longer period could be achieved with longer free-flooding ducts. Therefore, it is believed that substantial bulkhead loadings due to dynamic transfer of cargo from one cell to the next in the case of free-flooding non-structural bulkheads can be avoided by reasonable care in sizing the ducts.

The final dynamic loading to be considered is that which occurs in high, generally regular waves, resulting from the combination of large pitch angles and substantial heave accelerations at the same time. Such a loading appears to be unavoidable and may be serious if the ship is allowed to carry partial cargoes.

Figure 15 shows the static shift of cargo free surfaces and associated pressures which result from a finite pitch angle in which there is no dynamic transfer of oil through free-flooding ducts and the free surface remains horizontal. A constant pressure difference is experienced by the membrane from the level of the low oil sided to its foot.

Inasmuch as the major effect for the case shown is pitch amplitude, a search was made of recorded cases of large pitch angles experienced by tankers, or tanker-type vessels. Of the few data found on extreme motion amplitudes, References (15) and (16) seem useful. In Reference (15) Aertssen reported a maximum pitch amplitude of 9.4° for the MINERAL SERAING, a 55,000-DWT ore carrier operating over a 10-month period.

In Reference (16), Dalzell obtained significant pitch amplitudes averaging 9.6°

(double-amplitude) for a 250,000-DWT tanker model in Sea State 7. Assuming the maximum amplitude is $1.8 \times$ significant amplitude, we obtain a probable maximum single amplitude $= (1/2) \times 9.6 \times 1.8 = 8.65^\circ$. Based upon these data, as plotted on Figure 16, a pitch amplitude (from the mean, or half the double amplitude) of 9.2° is adopted for purposes of sizing the membranes on Design D75-A, a 75,000-DWT ship.

To find the pressure difference experienced by the membrane, the pressure distribution on each side must be increased, or decreased, by the net vertical acceleration (as a part of gravity acceleration) being experienced. The Series 60 model tests in waves, Reference (17), were then referred to for the largest vertical accelerations which might be experienced by the ship at the instant of 9.2° pitch angle, when in regular waves. Maximum pitch response at a Froude Number $= 0.15$ (13.9 knots), and in waves to give a relatively high frequency of encounter, takes place in head seas and in a wave length/ship length ratio $= 1.2$, when the ratio, pitch angle slope/surface wave slope $= 1.1$. This would occur in regular waves 43.8 ft. high (crest to trough) and 915 ft. long, giving a period of encounter of 9.97 seconds. Under these conditions the heave amplitude is approximately the same as wave amplitude, giving a heave acceleration of $0.27g$.

At the forwardmost non-structural bulkhead (Frame 98 for a two-frame cell, 294 ft. forward of amidships), the pitch contribution to vertical acceleration is

$$294 \times \left(\frac{2\pi}{9.97}\right)^2 \times \frac{9.2}{57.3} = 18.74 \text{ ft/sec}^2 \text{ or } 0.58g.$$

The pitch motion, however, leads the heave motion by about 54° phase angle. Then the net vertical acceleration at the instant of maximum pitch $= (0.58 + 0.27 \cos 54^\circ)g = 0.74g$. Figure 17 is a vector diagram showing how the heave and pitch motions combine at Frame 98 at the instant of maximum pitch angle.

The net vertical acceleration amidships at the instant of maximum pitch angle results only from heave, and is $0.27g \times \cos 54^\circ$ or $0.16g$. The phase angles of pitch and heave acceleration are not additive abaft amidships, so one may then draw a hydrostatic pressure increase factor versus distance along the ship, rising from 1.16 abaft amidships to 1.74 at Frame 98. Figure 18 shows the resulting curve. Values from this curve are to be applied to hydrostatic pressures when the free surface in the cell is horizontal, but the ship experiences a pitch angle (or instantaneous angle of trim) of 9.2° .

In the case of the forwardmost two-frame cell, the resulting pressure distribution curves on the two sides of the membrane are shown on Figure 19. It will be seen that the net effect is a constant pressure difference experienced by the membrane over its depth from the low oil elevation of 402 lbs/ft.^2 , or 2.79 psi.

In order to clarify the above ideas, Figure 20 shows the ship in the wave at the instant of maximum pitch angle, both bow up and bow down, with the directions of pitch and heave contribution to vertical acceleration noted.

Material for Non-Structural Bulkhead Membranes

The only material which was considered in detail is sheet steel. This decision was made for the following reasons:

1. Modern tankers are invariably constructed of steel. To introduce another metallic element into the structure, such as aluminum, would be expected to cause accelerated corrosion of one or both of the metals near the joints.
2. Mild steel is endowed with the property of a pronounced yield point, which leads to good ductility and energy-absorbing capability in the membrane as plastic flow occurs after the yield point stress has been exceeded. "Limit design" or design of a structure at stresses in the vicinity of the yield point is a well-established technique which may be applied to sheet steel.
3. Shipyard personnel are well experienced in steel fabrication techniques.
4. Galvanized sheet steel provides a smooth surface, which should minimize the "clingage" of oil remaining on the structure. Such oil must be removed in tank cleaning and tends to become a pollutant when wash water is disposed of.

Rubber was considered a possible material, but was rejected because of the probable large thickness which would be needed to assure integrity of the membrane in the "as-failed" case, or when large seakeeping loads may be experienced. Furthermore, the compliant nature of rubber might be unable to withstand the impact of high velocity tank washing jets.

Fiberglass was not investigated in detail, because it does not have a pronounced yield point. It was also expected that the properties of steel noted above would outweigh any possible advantages which fiberglass might offer. Another potential disadvantage is the possibility that static electricity might be built up on the fiberglass, compared with the steel, causing sparking when tank washing is underway. Furthermore, the writer is unaware of a specific application of large, thin flexible sheets of fibreglassed cloth analagous to the present case.

The above arguments should not be considered as final, inasmuch as more detailed study could perhaps disclose unseen advantages for these or other materials.

The specific material suggested for membranes is hot-rolled steel sheet and strip, structural quality, which is specified by ASTM specification A570-72, Grade B. This material has the following chemical composition:

Carbon, max.	0.25%
Manganese	0.25% - .60%
Phosphorous, max.	0.04%
Sulfur, max.	0.04%
Copper, when copper steel is specified, min.	0.20%

Tensile requirements are:

Tensile strength, min. psi	49,000
Yield point, min., psi	30,000
Elongation in 2 in. or 50 mm., min., for thicknesses,	
0.2299 to 0.0972 in.	25%
0.0971 to 0.0636 in.	24%
0.0635 to 0.0255 in.	21%
Elongation in 8 in. or 203 mm., min., for thick- nesses,	
0.2299 to 0.0972 in.	19%
0.0971 to 0.0892 in.	17%

In order to gain an idea of the possible elongation, or stretch, of such material in long specimens, Oliver's analysis in Reference (18) was referred to. This states that the percent elongation of a ductile specimen stretched beyond the yield point to a permanent elongation ϵ_L in gage length L , and in which a single "neck" develops, is given by

$$\epsilon_L = K \left(\frac{L}{\sqrt{A}} \right)^{\alpha}$$

where A is the cross section area of the specimen. K and α are constants for the material.

The constants K and α may be found if one has test results from specimens of two lengths. For example, for 0.097 in. thick steel, taking conservative values of 25% elongation for the 2 in. specimen and 17% elongation for the 8 in. specimen, and assuming the standard 1/2 in. wide test specimen, we find that $K = 46.1$ and $\alpha = -.279$.

The resulting expression, evaluated for a "specimen" 20 ft. long, 20 ft. wide, and 0.0972 in. thick, gives a permanent elongation of 11.2%; thus, the previously-made assumption of 10% stretch-before-failure does not seem unreasonable. It should be noted, however, that this value takes no account of two-dimensional loading, such as would occur on a stretched membrane. To evaluate this more realistic method of loading, one would need tensile tests with specimens pulled in two directions, at right angles to each other. It is understood that testing machines exist for such tests, for example, at the Naval Research Laboratory, but the writer is unaware of such test results for the case at hand.

Sheet steel of the thicknesses of interest, whether furnished in rolls or single sheets, must be joined to be fabricated in large panels to form the size of membrane needed. Possible methods of joining include:

- a) Manual welding with the material lapped.
- b) Cementing, with the material lapped, using an adhesive such as epoxy cement.
- c) Riveting.
- d) Welding, using the laser welding technique.

Of these methods, riveting is not favored for seams, owing to the desirability of a relatively smooth surface on the interior of a double-sheet laminate.

Manual welding seems possible, but the manpower-intensive effort required, and the possibility of a welding arc burning through the material do not favor its application on a production basis. Either MIG or TIG might be used.

Cementing appears a possible attractive method, subject to verification in full scale tests.

Laser welding appears to be particularly attractive, owing to its ready adaptability to automation, and limited demonstrated applicability in auto body construction using sheet steel. There appears to be a minimum of heat-affected zone in the laser weld, but the absence of filler metal requires that care be used in the fitting of separate sheets before the weld is made. For a multi-bulkhead application, such as fabricating the membranes for Design D75-A, some investment in fixtures to hold the sheets would obviously be justified. The effects of laser power and welding speed on depth of penetration are discussed in Reference (19).

Membrane Edge Connections

A variety of configurations are considered in attempting to arrive at the best method of connecting the membrane to the web face plates. The multiple objective is an attachment which a) is able to transfer the full strength of the membrane to the web structures without introducing significant bending stresses into the membrane or the web structure, b) minimizes the clingage of oil after pumping out, but can be readily cleaned by normal tank washing methods, c) is easily fabricated, d) would not introduce problems when carrying granular cargoes rather than petroleum, e) would not tend to introduce sources of ignition, and f) is oiltight.

Figure 21 shows sketches of possible edge connections, and notes the reasons they were rejected.

The presently-favored connection, Figure 22, is a compromise of these objectives. It consists of an additional face plate which is bolted to the web face plate by high strength bolts in slightly oversized holes with a 1" x 1" neoprene gasket between. A sandwich consisting of two rolled boundary plates, with the thin membrane material between, is welded to the face plate. The sandwich is bolted together by high strength bolts close to the face plate. A specific radius is rolled into the two boundary plates, and the membrane material bears against one of these when under load, such that the bending stresses (tension and compression) in the outer fiber of the membrane material is limited to a low value -- one third of the yield stress was tentatively assumed -- when the membrane takes up an edge angle appropriate to its tensile strength as a membrane at the yield point. With further membrane tension and an increase in the edge angle, the boundary plates deflect, allowing a limited increase in bending of the membrane.

In order to minimize the width and thickness of the boundary plates, the membrane is fabricated of two adjoining sheets, which are tightly clamped together in the sandwich, but able to slip elsewhere. A few widely spaced bolts hold the double-sheet laminate loosely together to prevent voids between, which might become filled with oil, wash water or vapors. The use of two thin sheets rather than a single thicker one allows sharper bends and a reduced radius of curvature as the membrane leaves the sandwich bearing against the boundary plate. Thus, the size of boundary plate may be reduced.

In order to assure drainage and venting within the sandwich confines, generous holes are provided in the boundary plates. However, if granular cargoes are car-

ried, covers must be fitted over the tops of lower boundary plates, or the open areas between the boundary plates and membrane could be plugged with wood.

The membrane is installed without slack, or tension. If noticeable stretch develops in routine service, part of this can be removed by tightening the face plates bolts.

If the non-structural bulkheads are built with free-flooding capability, the maximum height of contained oil after collision in the undamaged cell is about 8 feet above the waterline after damage. Inasmuch as this level would be only about 5 feet or less below the bottom of the web under the deck, it was decided to extend the membrane up to the web, thus taking advantage of the additional support furnished by an upper boundary. The same approach is taken in the non free-flooding case, inasmuch as the possibility of containing more oil after collision in undamaged cells is thereby increased.

With regard to fitting the edge connections at corners, the rolled boundary plates may be faired into flat plates at the corners without harming their functional capability. This is allowed because of the reduced edge angle which an initially-square and plane membrane experiences at the corners, when loaded under pressure on one side. In fact, Reference (20) indicates that such a membrane tends to experience compressive stresses in the corners when large deformations are developed in the remainder of the membrane, and comments that "This is impossible in reality".

Membrane Design

Having decided that the membrane should be fabricated of a loosely-joined double-sheet laminate, allowing slippage between the sheets, and with edge connections which minimize the outer fiber bending stresses, the principal remaining question is the selection of sheet thickness.

The approach is to select a thickness for each frame on the ship which leads to tensile stresses in the membrane, determined in a conservative way, just below the yield point when the membrane is loaded under the effect of the maximum in-service load to be expected, i. e., the seakeeping load when carrying a partial cargo in the tank and when the ship experiences the largest pitch amplitude to be expected.

A search of available literature on strength of materials disclosed little work directly applicable to the case at hand, that is, a flexible membrane which is loaded by pressures on one side to the extent that the maximum stretch experienced is about 0.1%. Therefore, an approximate analysis, as outlined in Appendix B, is developed for a square panel of edge length $2a$. Also included are relationships for a membrane covering a long rectangular opening of width $2a$. The resulting expressions for membrane thickness are:

$$t = .00002862 \text{ Pa (square)}$$

and

$$t = .00003615 \text{ Pa (long rectangle)}$$

P is the pressure loading in lbs/ft^2

a is in feet

t is thickness in inches.

In the wing tank of Design D75-A, there are three generally rectangular openings of dimensions 24 ft. by 15 ft., formed by the existing two struts, and by the web, as shown on Figure 1.

If $P = 402 \text{ lbs/ft}^2$, as appropriate to the forwardmost 2-frame cell, we may evaluate these expressions, where $a = 12 \text{ ft.}$ (for square) and 7.5 ft. (for long rectangle), giving thickness of 0.138 in. and 0.109 in. respectively, or a mean of 0.124 in. This value is then modified by the Hydrostatic Pressure Increase Factor, Figure 18, giving membrane thickness as shown in Table V. Also shown are the appropriate gauge numbers for a double-sheet membrane.

It will be noted that evaluating the thickness expression for a square on the basis of the longer dimension is equivalent to introducing a factor of safety, thereby providing an element of conservatism.

Similarly-obtained results are given in Table VII when single-frame cells are used, in which case the static difference in head due to the 9.2° pitch angle, and associated pressure loadings, are one half those for double-frame cells.

In the case of the center tank, the two panels on either side of the centerline are about 45 ft. by 22 ft. Applying the preceding two expressions for thickness to the case when the non-structural bulkhead is located at Frame 98, and using $a = 22.5$ ft. (for square) and 13.5 ft. (for long rectangle) we obtain membrane thickness of 0.259 in. and 0.196 in. respectively, or a mean of 0.228 in., when the pressure loading is 402 lbs/ft^2 (forwardmost 2-frame cell). The thickness tabulated in Tables VI (for two-frame cells) and VIII (for single-frame cells) are then derived using the foregoing method.

V. COST ESTIMATES AND REQUIRED FREIGHT RATE

Estimated Costs of Fitting Non-Structural Bulkheads

It was agreed that estimates of the cost of a non-structural bulkhead installation be included in the study, both for cases when the bulkheads are tight at bottom and sides, and when free-flooding capability is provided at the foot of the bulkhead.

The objective has been to estimate costs on the same basis as used in Reference (4), and then to estimate Required Freight Rate using these costs. In Reference (4) a number of hypothetical ship designs are priced for construction in Japan and delivery in 1974. Therefore, in the present estimates, an attempt is made to evaluate the costs of materials and labor in 1973, during which much of the expenditures would likely have been made for 1974 delivery.

Where separate materials and labor costs are itemized, these are based upon estimated U.S. material prices multiplied by a factor of 0.8, based upon the following comparisons, which are excerpted below from Table 3, p. 786 of Annex III "Forecast of Attainable CDS Rates for Fiscal Year 1976", by D.M. Mack-Forlist, Reference (21), for the period fiscal year 1971-1973.

Comparison of Principal Material Prices Between the United States and Foreign Centers

<u>Materials and Components</u>	<u>Shipbuilding Center</u>	
	<u>U.S.</u>	<u>Japan</u>
Steel	100	75-80
Turbogenerators and Switchgear	100	70-80
Cargo pumps	100	80-95

Labor charges are estimated on the basis of direct labor in Japan at the rate of \$1.71/hour in 1972 (Transportation Equipment Industry), from Table 3.12, p. 113, Vol. II, Chapter 3 "Shipbuilding Costs and Prices" of Reference (21). This figure is increased by 20% to allow for annual wage cost growth (1972 to 1973) -- and by 115% to allow for overhead, or a total cost of $\$1.71 \times 1.2 \times 2.15 = \$4.41/\text{hour}$, including overhead.

Individual components, where available, such as high strength bolts and sluice valves, are estimated by phoned quotations from suppliers; other items are esti-

mated by judgement, and by comparison with standard shipyard tasks. Thus, the man-hours needed to fit membrane edge connections are assumed to be the same on an area basis as fitting bilge structure (or bilge keels) or $0.839 \text{ man-hours/ft}^2$, while man-hours needed to fabricate the membranes are assumed the same as for fabricating bulkheads, that is, $0.318 \text{ man-hours/ft}^2$, both figures being obtained from Table 6 of Reference (22).

In view of the vulnerability of sheet steel to corrosion, it is assumed that the membrane sheets in way of boundary plates and edge connections, and internal boundary plate surfaces, would be specially coated, such as with inorganic zinc. For open membrane panel areas, the galvanized sheet steel coating is considered sufficient protection by itself. Special coatings were estimated at $\$1.25/\text{ft}^2$, based upon Reference (4) and (23).

Design D75-A as described in Reference (4), makes no mention of an inert gas system to provide an explosion-proof atmosphere in empty and partially-full cargo tanks. However, in view of the common fitting of such protective measures on tankers today, a figure has been allowed for inert gas piping in the cost estimates, on the assumption that inert gas would be supplied to every cell formed by the non-structural bulkheads.

Table IX summarizes the ship cost estimates, including detailed breakdown of major items. The Shipyard Delivery Price at the foot of each column increases the Direct Shipyard Cost by 25%, to account for management costs, profits, etc.

The entry in Table IX, accounting for piping rearrangement, is to cover the cost of modifications to piping which otherwise would run through lightening holes, or would not encounter interference. It is assumed that such piping would run through stuffing boxes in the web when non free-flooding non-structural bulkheads are fitted.

The cost of web cutout closures is based upon the assumption that a lightly welded sheet metal plate would fill in most of the cutout opening, with the final seal achieved by a gunned caulking compound.

No credit, or charge, is given in Table IX for the omission of lightening holes in the webs.

Required Freight Rate

A criterion for assessing the economic effect of differences in alternative ship designs is the Required Freight Rate. The Required Freight Rate is the cost per unit of transporting a given commodity on a given trade route which a shipping company would have to charge its customers in order to amortize the cost of the ship and pay for her operation, but with no profit included. Thus, it one can determine the total operating cost per year (including amortization of the initial cost), and also the total tonnage of cargo delivered per year on a voyage of given length, RFR is the quotient of cost divided by weight of cargo delivered, i. e., dollars per ton.

Tables X and XI give the Required Freight Rate for a short voyage trade (5,000 nautical miles, round trip), and for a long voyage trade (22,000 nautical miles, round trip), respectively, for Design D75-A when fitted with the non-structural bulkhead alternatives used for making cost estimates. The lengths of voyage are the same as those adopted in Reference (4).

Inasmuch as we are only interested in differences between Design D75-A and the non-structural bulkhead alternatives, the calculations and economic bases in Reference (4) are not repeated here.

Of the various components of operating costs, the only changes which can be determined are those associated with the first cost of the ship -- that is, amortization of capital, and insurance. There is the possibility that a presently untried installation, such as the system of non-structural bulkheads proposed, might require more maintenance and repair work than a conventional ship not so fitted, but we know of no basis for evaluating this effect and have not included it in the operating cost calculations.

Annual insurance premiums are calculated using the expression from Reference (4), for the 75,000 DWT designs,

$$\text{Premium} = 0.905 ((F_1 \times \text{DWT}) + F_2 \times (\text{Capital Cost}) + F_3) + F_4$$

$$\text{where } F_1 = 3.55, F_2 = 0.00629, F_3 = 16,000, F_4 = 2,000.$$

Amortization costs, whether for 0 tax or 50% tax, are considered to increase in direct proportion to the shipyard delivery price.

The cargo delivered per year drops slightly, compared with Design D75-A, because of the weight of membranes, edge connections, etc., which results in increases in light ship weight and loss of deadweight -- in all cases less than 1%.

The Required Freight Rates in Tables X and XI show small increases, compared with Design D75-A, generally less than 5%.

VI. EFFECTIVENESS OF SYSTEM IN REDUCING POLLUTION

The calculations summarized in Table IV show that substantial reductions in outflow after collision would result from the use of non-structural bulkheads. For example, when using free-flooding non-structural bulkheads on every second frame and in wing tanks only, Case IV, the probable outflow after collision drops from 6576 (m)^3 for the base ship to 3829 (m)^3 , or a reduction of 42%. When single frame cells are provided, and these are located in wing tanks as well as center tanks, Case V, the outflow is 2378 (m)^3 , or a reduction of about 64%.

However, the total discharge of oil which may be expected to develop in the course of a ship's life arises from operational as well as accidental sources. Furthermore, accidental discharge results from strandings and rammings, as well as collisions. Reference (4) includes fleetwise annual outflow estimates from all such sources for Design D75-A, and these are used here as a basis of comparison.

Considering first accidental discharges, Table XII gives the Reference (4) values for Design D75-A, together with calculated values for the four free-flooding non-structural bulkhead alternatives for which Required Freight Rates are estimated. Discharges from rammings and strandings are assumed unchanged due to the presence of the non-structural bulkheads, the only reduction being in discharge from collisions. The collision discharges are found by multiplying the base ship values by the ratio of probable outflow after collision for the modified ship to that for the base ship.

Also shown on Table XII are increases in total operating costs from Table X, assuming the 0 tax case, and the quotient of the two -- that is, the increase in annual operating cost per cubic meter of estimated annual reduced discharge.

The increases in Required Freight Rates from Tables X and XI are plotted against the estimated reduction in annual discharge in Figure 23. Based upon this figure, it appears that fitting non-structural bulkheads in wing tanks is a relatively less costly way of reducing accidental discharges than fitting such increased subdivision in both center and wing tanks.

With regard to total discharge, the operational discharge must now be considered. This results from residual oil not removed from contaminated ballast water pumped from center tanks 2 and 4 -- and from oil remaining in the wash water used for washing both the all-cargo tanks and the two combined ballast and cargo tanks, center tanks 2 and 4, after slop oil is decanted.

It is obvious that additional structure in any of the cargo tanks tends to increase the "clingage" of oil remaining on tank surfaces when the oil is pumped out. Such clingage is carried into the wash water and must be accounted for as an increase in operational discharge. The presence of membranes in the cargo tanks results in an increase in tank surfaces. The membrane surface areas are readily calculated, but the basic tank structural surface areas are not readily available and must be estimated. It is understood that calculations of internal tank surface area for a large tanker had shown the following ratios of total internal tank surface area to projected areas:*

	<u>Total internal tank surface area</u> <u>Projected tank surface area</u>
Wing tanks	3.6
Center tanks	2.3

These ratios are applied to the projected tank areas (floor, roof, two ends and two sides) of the cargo tanks of Design D75-A giving the surface areas summarized in Table XIII.

Further analysis is needed to find the discharge resulting from residual oil remaining on these surfaces. Factors in the problem include the frequency with which cargo/ballast tanks are cleaned (all voyages), the frequency with which cargo only tanks are cleaned, and the tonnage of ballast carried in cargo/ballast tanks. From Reference (4), Design D75-A was assumed to carry crude oil on 75% of her voyages, and dirty products the rest of the voyages; cargo only tanks were to be washed every fourth voyage when carrying crude oil.

Having estimated the tank surface areas, and with the assumption that oil discharged due to dirty ballast varies directly as the weight of ballast, one can derive from Reference (4) a factor of proportionality to account for discharge from contaminated ballast from the base ship by referring to the difference in operational discharges for the 45% and 60% ballast conditions. The factor is found to be $6.25 \times 10^{-6} \text{ (m)}^3$ per ton of contaminated ballast for each pumpout of same. This is applied to the ballast water tonnages in Table XIII, and then increased in proportion to tank internal surface areas to give discharge due to dirty ballast per voyage

* Verbal communication from Maritime Administration, Division of Ship Design.

for each modification.

Discharge due to tank washings is calculated on the assumption that this varies directly as the total tank surface areas washed.

We consider a total of 16 voyages for Design D75-A, during 12 of which crude oil is carried. Let,

x = discharge per cleaning from cargo/ballast tanks, $(m)^3$

y = discharge per cleaning from cargo only tanks, $(m)^3$

S_b = total surface area cargo/ballast tanks = 143,970 $(ft)^2$

S_c = total surface area cargo only tanks = 858,410 $(ft)^2$

K = cubic meters of discharged oil per $(ft)^2$ cleaned.

From Table 10 of Reference (4), we have the following averaged operational discharge per voyage (discharge from many voyages divided by number of voyages):

	45% Ballast Condition		60% Ballast Condition	
Tank cleaning method	1	2	1	2
Operational discharge $(m)^3$	3.77	2.01	4.62	2.85

By deducting the discharge from dirty ballast in Table XIII for Design D75-A, we get the mean discharge due to tank washings, i.e., 3.44 $(m)^3$ per voyage for tank cleaning Method 1, and 1.68 $(m)^3$ per voyage for Method 2.

For Method 1, $16x = 16S_b \cdot K$; $3y = 3S_c \cdot K$

$$16S_b \cdot K + 3S_c \cdot K = 16 \times 3.44$$

$$\text{Then } K = 11.29 \times 10^{-6} (m)^3 / (ft)^2$$

For Method 2, $16S_b \cdot K + 3S_c \cdot K = 16 \cdot 1.68$

$$\text{Then } K = 5.51 \times 10^{-6} (m)^3 / (ft)^2$$

These constants are applied to the surface areas in Table XIII to calculate the mean operational discharge per voyage. It may be noted that the 60% ballast condition using single frame cells in wing and center tanks, tank cleaning Method 1 case, leads to an operational discharge in excess of 1/15,000 of cargo deadweight per voyage, and would be unacceptable, Reference (4).

The results of Tables XII and XIII are combined in Table XIV, giving the total

discharge per ship per year from all sources, assuming 12 voyages per year, and for both tank cleaning methods. This has been prepared by proportioning the per ship, per voyage operational discharge values, also given in Table XIV, to per ship, per year values on the basis of comparable data at the top of the table for Design D75-A, and adding the accidental discharge values from Table XII.

An inspection of the reduction in discharge, compared with Design D75-A, shows that in almost half the cases, the total discharge increases rather than decreases due to the presence of the non-structural bulkheads. The most favorable combination is found using tank cleaning Method 2 (which recycles the wash water), in the 45% ballast condition, and when the non-structural bulkheads are located on every other frame and in wing tanks only, in which case the calculated total discharge per year is reduced from 71.10 (m)^3 to 67.56 (m)^3 , or by 3.54 (m)^3 per year, a net reduction of 4.97%. Interestingly, this is the least costly of the various alternatives studied, leading to an annual operating cost increase of \$26,000 from the Required Freight Rate calculations, Table X (short voyages).

With regard to the several combinations of non-structural bulkheads which appear to increase total discharge, rather than reducing it, we should stress that the primary source of increased operational discharge which tends to offset the potential benefits from greater subdivision is the increased surface area within the tanks, and its effect on discharge from tank wash water. So long as tank washings are not permanently retained on the ship, it appears that any increase in internal tank surface area will have a negative effect on operational discharge, making this a greater source of pollution. For this reason, alternative methods of tank washing which reduce, or eliminate, this source should be vigorously encouraged. In this regard, a possible self-contained tank cleaning method which gave promising results in small scale tests, and avoids the overboard discharge of oil, is one based on magnesium sulfate brine as a washing medium, Reference (24).

Another technique which is understood to be finding favor with several tanker operating companies is to wash the tanks with crude oil. In the event either of the above techniques were adopted routinely, their effects could be incorporated in calculations of the type undertaken in this study, and increased gain in reduced outflow from the use of non-structural bulkheads would result. For example, with non-structural bulkheads on every frame, and in center tanks as well as wing tanks, the reduction in expected total discharge of oil from Design D75-A should approach 13%.

A further benefit in the use of the system not evaluated appears to be the reduction of impact of spilled oil on coastal communities in the event of a collision when approaching or leaving port. This effect is not accounted for in Reference (4) or the present report and must remain an intangible.

VII. CONCLUSIONS

1. The installation of non-structural bulkheads in the cargo tanks of tankers should significantly reduce the probable size of spill which would result from collision.
2. Despite the apparent greater accidental loss of oil from strandings than from collisions, the fitting of free-flooding non-structural bulkheads should lead to a reduction of total probable accidental discharge expected from Design D75-A varying from about 9 to about 13 percent, depending upon the extent of the system fitted. The corresponding annual operating cost increases resulting from fitting such non-structural bulkheads are estimated to be \$26,000 and \$103,000, respectively.
3. The estimated total shipyard delivery price for fitting non-structural bulkheads of the type considered, assuming Japanese construction and 1974 delivery, on the 75,000 DWT ship used as a base, range between \$230,000 and \$1,210,000, depending upon the degree of additional subdivision achieved, and whether free-flooding or non-free-flooding capability is provided. The non-free-flooding cases are significantly more costly than the free-flooding cases, owing to the expense of motor-operated sluice valves needed for each non-structural bulkhead.
4. The Required Freight Rate increases needed to offset the initial investment, amortization of capital and insurance increases called for by non-structural bulkheads are relatively small, but are greater for the long voyage (22,000 naut. mile round trip) operation of Design D75-A than for the short voyage trade (5,000 naut. mile round trip). In view of the greater number of harbor entries for the short voyage trade, when the chances of collision are increased, non-structural bulkheads should be particularly attractive to ships engaged in short-haul service.
5. Operational discharges resulting from pumping overboard partly contaminated water ballast and tank wash water which contains residual oil are increased on a ship with non-structural bulkheads, because of the additional surfaces within cargo tanks. The net effect, when combined with the decrease in outflow due to collisions, may be an increase or decrease in total outflow from all sources. In the case of Design D75-A, and using the assumptions adopted for Part 2 of Study 1, the use of free-flooding non-structural bulkheads on every 2nd frame in wing tanks only results in a slight decrease in total outflow expected (about 5%), for the short voyage, 45% ballast case, if tank cleaning Method 2 is followed.

6. This investigation disclosed no serious technical shortcomings of the system proposed. However, some reservations were expressed by an oil company representative about the ability of the thin sheet metal of which the membranes are fabricated to withstand the impact of high velocity tank washing jets. Also, the capability of developing the full tensile strength of the sheet metal membranes at seams, and the best way to form these seams to achieve oil tightness as well as strength has not been established.

7. The installation of non-structural bulkheads at the spacings considered in the report (single-frame cells or double-frame cells) should virtually eliminate the problem of liquid sloshing in cargo tanks, and the hydrodynamic need for swash bulkheads in long tanks.

8. Although not investigated in detail, it appears that longitudinal vents of limited size at the upper levels of each non-structural bulkhead should furnish increased fire protection after collision, provided inert gas is supplied to each cell and flame-arresting screens are fitted over each vent.

9. A non-structural bulkhead installation requires careful engineering to assure that membrane material and design are matched such that the membranes are strong enough to withstand expected seakeeping loads with partial cargoes, but thin enough to avoid high bending stresses at the boundaries. Thus, an overly conservative choice of membrane thickness to withstand direct tension requires wider, heavier boundary plates, rolled to a larger radius of curvature in order to keep such bending stresses within bounds.

10. Based upon statistical data available, the optimum location for a partial non-structural bulkhead installation would be in wing tanks amidships. Specifically, on Design D75-A, a greater reduction of probable outflow after collision occurs if Wing Tanks 4 are so fitted than if the system is installed in Wing Tanks 2.

VIII RECOMMENDATIONS

1. Studies of alternative tank arrangements and internal subdivision should take account of the statistical nature of the damage considered. The calculation of "probable outflow from collision" is one way of accomplishing this, but further work should be undertaken aimed at acquiring the statistics of the longitudinal extent of damage of a given penetration depth to allow one to refine the calculations.
2. Records of past tanker collisions should be further analyzed to determine whether the statistics of longitudinal location and length of collision damage on tankers agree with those on passenger and cargo ships.
3. The statistics of longitudinal and transverse location, and length and width of stranding damage on tankers are urgently needed, and should be acquired on a first priority basis; further data on the depth of penetration of stranding damages should be obtained.
4. After the data in Recommendation 3 are acquired, studies of probable outflow after stranding should be undertaken using alternative arrangements of non-structural bulkheads tight at bottom, sides and up to the deck.
5. When designing non-structural bulkheads to control oil spills, it is recommended that the height of contained oil after collision be set as high as possible, within the limits of physical constraints. With free-flooding bulkheads, this will be determined by the height of the free-flooding ducts and/or cutouts in bottom shell webs, together with the density difference between the water and the contained oil. In the case of non-free-flooding bulkheads, the height should be near the underside of the deck. Membranes designed to withstand probable seakeeping loads in the manner suggested in the report should be well able to support the resulting head of contained oil in the "as-failed" case after collision in almost all instances.
6. The development and application of alternative methods of tank washing, such as using crude oil or fully-contained solutions, should be pursued. The effectiveness of non-structural bulkheads in minimizing outflow from tankers -- accidental

as well as operational -- will be largely suppressed, or reversed, if the increased internal tank surfaces resulting from the system lead to substantial increases in the discharge of contaminated wash water and dirty ballast.

7. Hardware development in the application of non-structural bulkheads should be aimed at improved, less manpower-intensive methods of edge connection. While the edge connection proposed in this report appears on paper to perform satisfactorily, it may be possible to devise less expensive alternative designs which would do the job equally well.

8. Tensile tests should be conducted on sheet steel specimens with the load applied in two directions in the plane of the specimen, thereby simulating the bi-axial loading to which a membrane pressurized on one face is subjected. Such information would enable a non-structural bulkhead designer to design for the "as-failed" case after collision with more confidence than now possible. It is understood that the necessary bi-axial tensile test machines are in existence.

9. The theory of stretched membranes should be pursued, aimed at a better way of determining the stress distribution and deflection throughout the membrane when under a finite loading but below the yield point.

10. Development work should be undertaken with regard to finding the best way to fabricate seams in sheet steel for use as membranes.

11. A full-scale prototype application of non-structural bulkheads should be tested in a wing tank of a small tanker in conjunction with Recommendation 10. A generally midship tank is proposed in order to minimize seakeeping loads. For purposes of ready inspection, the tank adopted should perhaps be a permanent ballast tank. Frequent inspection should be made, aimed at determining whether there is evidence of stretching in the membranes beyond the yield point, whether seams in the membranes retain their integrity, and whether the edge connections perform as planned. In implementing such a system, seams should span the shortest dimension, inasmuch as maximum percentage stretch will be experienced by the shorter elements of the panel.

IX. ACKNOWLEDGMENTS

A number of individuals and firms have provided information and made suggestions in carrying out this study, and the writer extends thanks for this assistance. In particular, the following are acknowledged:

Professor R.B. Zubaly and Professor J. Femenia of the State University of New York Maritime College, who performed preliminary calculations and clarified the tank pumping and cleaning problem.

Exxon International, who furnished current information regarding tanker operational procedures, tank cleaning and tank inerting.

Professor George Winter of Cornell University who clarified the question of extension-before-failure of large steel sheets.

Professor E.V. Lewis of Webb Institute, who suggested the free-flooding non-structural bulkhead alternative, and furnished editorial review.

Professor L.W. Ward of Webb Institute, who provided guidance regarding the limit design technique.

Mr. D.M. Mack-Forlist, shipbuilding consultant, who furnished certain data relative to ship costs.

Mr. G. Whitney of United Aircraft who furnished information on laser welding.

Lt. Cdr. D. Folsom of the Office of Research and Development, and Cdr. R.A. Sutherland of the Office of Merchant Marine Safety, U.S. Coast Guard Headquarters, Washington, who recommended sponsorship of the study.

X. REFERENCES

1. "Survival of Collision Damage Versus the 1960 Convention on Safety of Life at Sea," Comstock and Robertson, SNAME Transactions 1961.
2. "Oil Outflow from a Breached Tank Model," submitted by Japan to IMCO, Sub-Committee on Ship Design and Equipment, 17 April 1970.
3. "Preliminary Analysis of Tanker Collisions," Bovet, U.S. Coast Guard Office of Research and Development, November 30, 1970.
4. "Segregated Ballast Aboard Product Tankers and Smaller Crude Carriers," Report on Part 2 of Study 1, a note by the United States of America, Department of Transportation, U.S. Coast Guard, February 1973.
5. "Ship Design and Construction," edited by D'Arcangelo, published by SNAME, 1969 -- Chapter I, "Basic Design," by E. Scott Dillon, Figure 8, p. 5 and Table 7, p. 31.
6. "Advanced Strength of Materials," Den Hartog, McGraw-Hill Book Co., 1952.
7. "Plastic Design Methods -- Advantages and Limitations," Drucker, SNAME Transactions, 1957.
8. "Finite Deformation of a Pressurized Membrane Strip," Wilson and Slick, ASME Transactions -- Journal of Applied Mechanics, June 1965.
9. "Elements of Strength of Materials," Timoshenko and McCullough, D. Van Nostrand Co., 1940.
10. "Tank Size and Dynamic Loads on Bulkheads in Tankers," Abrahamsen, Publ. No. 28, Det Norske Veritas, February 1962.
11. "Notes on the Dimensions of Shipboard Swimming Pools," Comstock, Chesapeake Section, SNAME, March 29, 1947.
12. "The Equipment and Methods Used in Operating the Newport News Hydraulic Laboratory," Hancock, SNAME Transactions, 1948.
13. "Roll Stabilization by Means of Passive Tanks," Vasta, Giddings, Taplin and Stillwell, SNAME Transactions, 1961.
14. "Mechanical Vibrations," Den Hartog, McGraw-Hill Book Co., 1947.
15. "Service Performance and Seakeeping Trials on a Large Ore Carrier," Aertssen, RINA, September 1968.
16. "Note on Seakeeping and Maneuvering Tests Performed on a 250,000 DWT Tanker Model in Various Ballasted Conditions," Dalzell, Symposium on Minimum Ballast Levels for Tankers, Stevens Institute, September 12, 1973.

17. "Experiments with Series 60 Models in Waves," Vossers, Swaan and Rijken, SNAME Transactions, 1960.
18. "Steel Ductility Measurements," Dhalla and Winter, ASCE Proceedings -- Journal of the Structural Division, Vol. 100, No. ST2, February 1974.
19. "Evaluation of CO₂ Laser Welding Capability in Rimmed Sheet Steel," Banas and Lessard, United Aircraft Research Laboratories, December 1971.
20. "Tensile Structures," Frei Otto, Editor (Volume One "Pneumatic Structures), the MIT Press, 1967.
21. "Report of the Commission on American Shipbuilding," Washington, DC, October 1973.
22. "Optimized Design of Midship Section Structure," Evans and Khoushy, SNAME Transactions, 1963.
23. "Segregated Ballast VLCCs: An Economic and Pollution Abatement Analysis," Kimon, Kiss and Porricelli, Marine Technology, October 1973.
24. "Development of a Pollution Free Cargo Tank Cleaning System for Use on Board Tankers," Femenia, NOAA Office of Sea Grant, Department of Commerce, Grant No. 2-35281, December 27, 1972.

APPENDIX A

"AS-FAILED" DISTORTION OF NON STRUCTURAL BULKHEAD

In this case the membrane material is stretched well beyond the point at which yielding begins. Following the procedure adopted in limit design, Reference (7), it is assumed that plastic flow beyond the yield point takes place at constant stress, i. e., at the yield point stress. The exact geometry at which such "failure" takes place need not be known; hence, the approximation is adopted that rectangular panels of constant thickness distort under plastic flow conditions as though the panel were long, in which case only tangential stresses are developed, as no support is provided by meridional stresses introduced by restraint of the panel ends.

It is shown in Reference (8) that sections across a long rectangular membrane clamped at its edges and subjected to a uniform pressure on one side are circular arcs. This provides a simple and conservative way to approximate the plastic flow deformation of rectangular membrane panels of finite proportions. According to Drucker's Upper Limit Theorem, Reference (7), failure takes place if the rate of energy input into the system exceeds the rate of energy absorption by plastic flow taking place during the yielding process. The energy input equals $P \int A \cdot dn$, where A is the area of a section through the segmental cylinder parallel to its axis and n is the normal to it; thus, the energy input equals the pressure loading multiplied by the volume formed between the initially-plane membrane and the circular cylindrical surface into which it distorts.

The energy absorption is found as the cross section of the membrane (thickness \times panel length) multiplied by the increase in length of tangential section (extension of width of panel into circular arc) and multiplied by the yield stress.

Thus, assume a center tank panel of width 27 ft. Then $2a = 27$. Let $\theta =$ edge angle and $R =$ radius of arc. Then arc length $= \frac{2\pi R \times 2\theta}{2\pi} = 2R\theta$. Chord length $2a = 2R \sin \theta$. Then for 10% stretch, $\frac{2R\theta - 2R \sin \theta}{2R \sin \theta} = .1$ or $\theta = 1.1 \sin \theta$. This occurs for $\theta = 43.2^\circ$. The volume of the segmental cylinder per unit length

is $\frac{1}{2}R^2 (2\theta - \sin 2\theta)$. Input work per unit length $W = \frac{PR^2}{2} (2\theta - \sin 2\theta)$.

Strain energy, or energy absorbed, per unit length,

$$E = 2R (\theta - \sin \theta) \times \sigma_{yp} \times t ,$$

where σ_{yp} is yield point stress, and t is membrane thickness.

The pressure loading P which would produce 10% stretch may be found by equating W and E , when $\sigma_{yp} = 32,000 \text{ psi} = 4608000 \text{ lbs./ft.}^2$, $t = 0.085 \text{ ins.} = 0.00708 \text{ ft.}$, and when $\theta = 43.2^\circ$. This gives $P = 897 \text{ lbs./ft.}^2 = 6.23 \text{ psi}$.

Alternatively, by assuming various edge angles θ , we can find W and E for the given values of σ_{yp} , t and a . Plotting these it is seen that they are equal when $\theta = 43.2^\circ$. See Figure 24.

θ	θ rad.	$\sin\theta$	R ft.	$(\theta - \sin\theta)$	E lbs x ft	$\sin 2\theta$	R^2	$(2\theta - \sin 2\theta)$	W lbs x ft
10°	.1745	.1736	77.8	.0009	4500	.3420	6052	.0070	19000
20°	.3491	.3420	39.5	.0071	18300	.6428	1560	.0554	38800
30°	.5236	.5000	27.0	.0236	41600	.8660	729	.1812	59200
40°	.6981	.6428	21.0	.0553	75800	.9848	441	.4114	81400
50°	.8727	.7660	17.6	.1067	122500	.9848	310	.7606	105800

The static equilibrium stress following failure results when the normal component of tension equals the applied load. In this case if σ_e is the equilibrium stress, then $2\sigma_e t \sin \theta = 2aP$. If $\theta = 43.2^\circ$, $\sin \theta = .6845$.

$$\text{Then } \sigma_e = \frac{13.5 \times 897}{.00708 \times .6845} = 2498000 \text{ lbs./ft.}^2 = 17350 \text{ psi.}$$

APPENDIX B

AN APPROXIMATION TO THE THICKNESS OF A MILD STEEL CLAMPED-EDGE SQUARE MEMBRANE LOADED TO THE YIELD POINT BY CONSTANT PRESSURE ON ONE FACE

It is assumed the membrane stresses are all tensile (bending stresses from flexure are assumed to be negligible), and such tensile stresses are at or below the yield point. Also, the elasticity of the material is assumed to follow Hooke's law. Figure 13 shows the membrane in plan view. At any point the tangential or x stress σ_x and meridional or y stress σ_y are related by equation [1] which is repeated here,

$$\frac{\sigma_x}{R_x} + \frac{\sigma_y}{R_y} = \frac{P}{t}.$$

By common observation and inspection, the maximum deflection of the membrane from its initial plane takes place at the origin of coordinates. Therefore, it may be assumed that the section of maximum stretch passes through the origin. By symmetry, shear forces, if they exist, on sides qr and sp of the element p q r s are equal and of opposite sign, since the initially-square element does not distort into a rhomboidal shape. Hence, the shear stress gradient $\frac{\partial \sigma}{\partial x}$ must be zero along the y axis.

The distortion of an initially-square grid on the surface of the membrane resulting from a loading small enough to keep the stretch of sections along the axes to .1% or less will be small. Hence, the tensile force experienced by side pq must be the same as that experienced by side rs to a very close approximation. In the limit, as the distortion becomes infinitesimally small, the tensile forces approach each other. Therefore, it is reasonable that the tensile stress σ_y along the y axis and σ_x along the x axis may be taken as constant.

Along an edge of the membrane, a section parallel to the edge experiences no stretch, since it is completely restrained at the edge. Then $\sigma_y = 0$ at $x = \pm a$ and $\sigma_x = 0$ at $y = \pm a$.

Let σ_x and σ_y be σ_o at the origin. Also, let $\sigma_x = \sigma_e$ at $x = \pm a, y = 0$. Then $\sigma_y = \sigma_e$ at $x = 0, y = \pm a$. Then at the origin,

$$\frac{\sigma_o}{R_x} + \frac{\sigma_o}{R_y} = \frac{P}{t}.$$

But $R_x = R_y = R_c$ at the origin, by inspection, so $\frac{2\sigma_c}{R_c} = \frac{P}{t}$. Therefore,

$$\sigma_c = \frac{R_c}{2} \times \frac{P}{t}.$$

Let R_e be the radius of curvature of the section at the edge. Now at the edge,

$$\frac{\sigma_e}{R_e} + 0 = \frac{P}{t} \text{ or } \sigma_e = R_e \times \frac{P}{t}. \text{ But } \sigma_c = \sigma_e. \text{ Hence, } \frac{R_c}{2} \times \frac{P}{t} =$$

$$R_e \times \frac{P}{t} \text{ and } R_c = 2R_e, \text{ or the edge radius of curvature is half that at the origin.}$$

We do not know the variation of normal stresses on the element, or tensile loads on sides qr and sp, as the element moves from the edge to the center. However, for purposes of calculating stretch, it will be a conservative assumption that the mean dimensionless strain -- or stretch -- along the y axis, $\epsilon_y = \frac{1}{E} (\sigma_y - \mu \sigma_x)$ may be found on the basis that σ_x is constant all along the axis and equals σ_c .

Then if E, the modulus of elasticity = 30000000 psi, if μ , Poisson's ratio = .3 and if $\sigma_x = \sigma_y = \sigma_c = \sigma_{yp} = 30000$ psi, we may write as the average dimensionless stretch along either axis,

$$\epsilon = \frac{(30000 - .3 \times 30000)}{30000000} = .0007.$$

Shown on Figure 25 is a section cut through the distorted membrane along either axis. A circle of constant radius R is taken as an approximation to the theoretical curve representing the distorted section, whose radius of curvature varies. Then the ratio, length of circular arc to length of chord -- or ratio of stretched to unstretched section length $= (\frac{2\pi R \times 2\theta}{360}) / 2R \sin \theta$, where θ is the edge angle in degrees of the approximating circle. If we let this ratio $= \frac{1.0007}{1}$, we have $\frac{\theta}{\sin \theta} = 57.3359$. Then $\theta = 3.71^\circ$.

The assumption is now made that the radius of curvature R of the approximating circle is the mean of the central and edge radii, or $R = (1/2)(R_c + R_e)$. Then $R = (1/2)(R_c + (1/2)R_c)$ or $R_c = \frac{4}{3}R$. But the unstretched section length $2a = 2R \sin \theta = 2R \times .06470$. Then $R = 15.456a$, and so $R_c = 20.607a$. We may now substitute in the expression for stress at the origin, found above, $\sigma_c = \frac{R_c}{2} \times \frac{P}{t}$, getting, $\sigma_c = \frac{20.607a}{2} \times \frac{P}{t} = 10.304 \frac{P}{t} \times a$, which applies when σ_c equals the yield point stress previously assumed, i.e., when $\sigma_c = 30000$ psi. This gives,

$$t = \frac{10.304}{30000} \times P \times a$$

Now let t = required thickness in inches

P = pressure in lbs/ft²

a = half width of square in feet.

$$\text{Then } t = \frac{10.304}{12 \times 30000} \times P \times a = .00002862 \text{ Pa.}$$

For completeness, the case of a long rectangle is now developed, based upon the preceding expressions.

In the case of the long rectangle, sections normal to the long sides are circular arcs, Reference (8). Let R be the radius, and assume the sides are parallel to the y axis, and located at $x = \pm a$. Then σ_x = tangential stress,

$$\frac{\sigma_x}{R} = \frac{P}{t}, \text{ or } \sigma_x = R \times \frac{P}{t}. \text{ In the case of this long rectangle, } \sigma_y = 0. \text{ Then}$$

$$\epsilon_x = \frac{1}{E} (\sigma_x).$$

If we now let σ_x be the yield point stress, 30000 psi, then $\sigma_x = \frac{30000}{30000000} = .001$. Then the ratio, length of circular arc to length of chord =

$$\frac{1.001}{1}. \text{ Using symbols as before, we have } \frac{\theta}{\sin \theta} = 57.3531. \text{ Then } \theta = 4.41^\circ, \text{ and } 2a = 2R \sin \theta = 2R \times .07684.$$

Then $R = 13.014a$. Therefore, $\sigma = 13.014 \times \frac{P}{t} \times a$, which applies when σ equals the yield point stress 30000 psi.

As before, let t = required thickness in inches

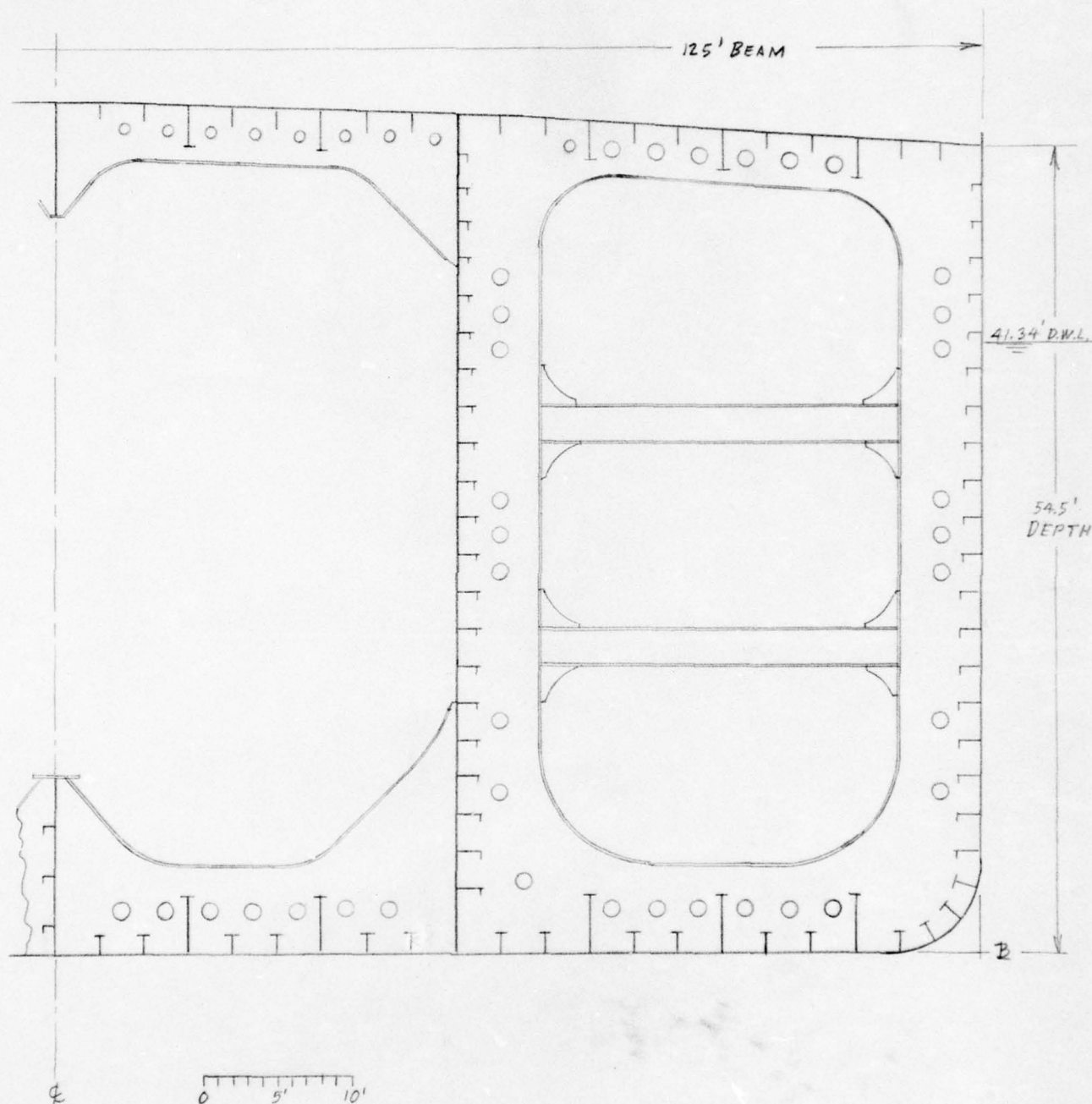
P = pressure in lbs/ft²

a = half spacing between long sides in feet.

$$\text{Then } t = \frac{13.014}{12 \times 30000} \times P \times a = .00003615 \text{ Pa.}$$

To check that this satisfies equilibrium requirements, the components of tension (per foot of length) normal to the initial plane = $2 \sigma t \sin \theta \times 12$. This must equal $2Pa$ for equilibrium.

By direct substitution, the normal components become,
 $2 \times 30000 \times .00003615 \text{ Pa} \times .07684 \times 12 = 1.9922 \text{ Pa}$, which is considered a reasonable check. It may be noted in passing that this tension is the familiar "hoop stress" tension, derived in elementary strength of materials when considering pipe stress.



SIMPLIFIED MIDSHIP SECTION
DESIGN D75-A

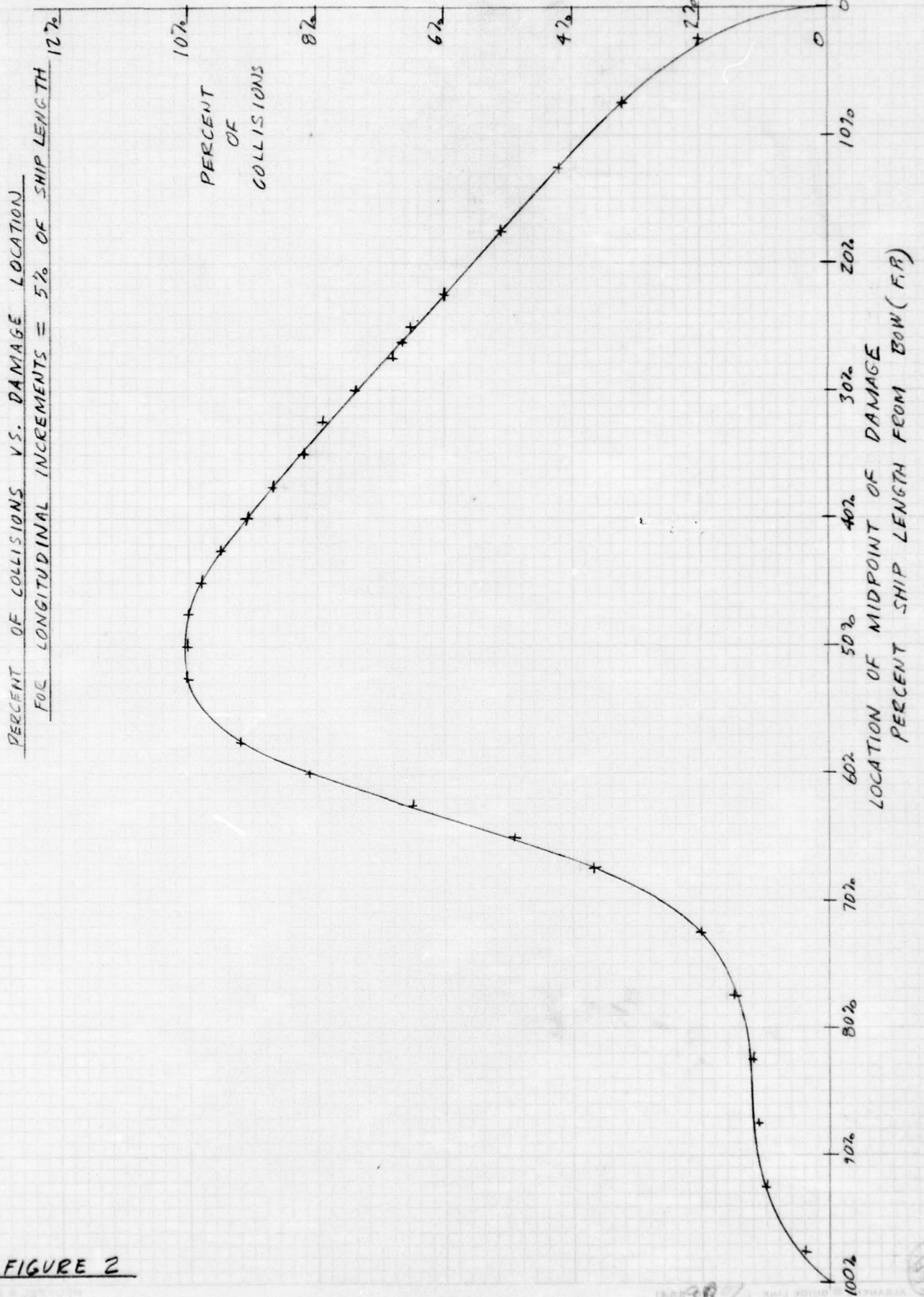
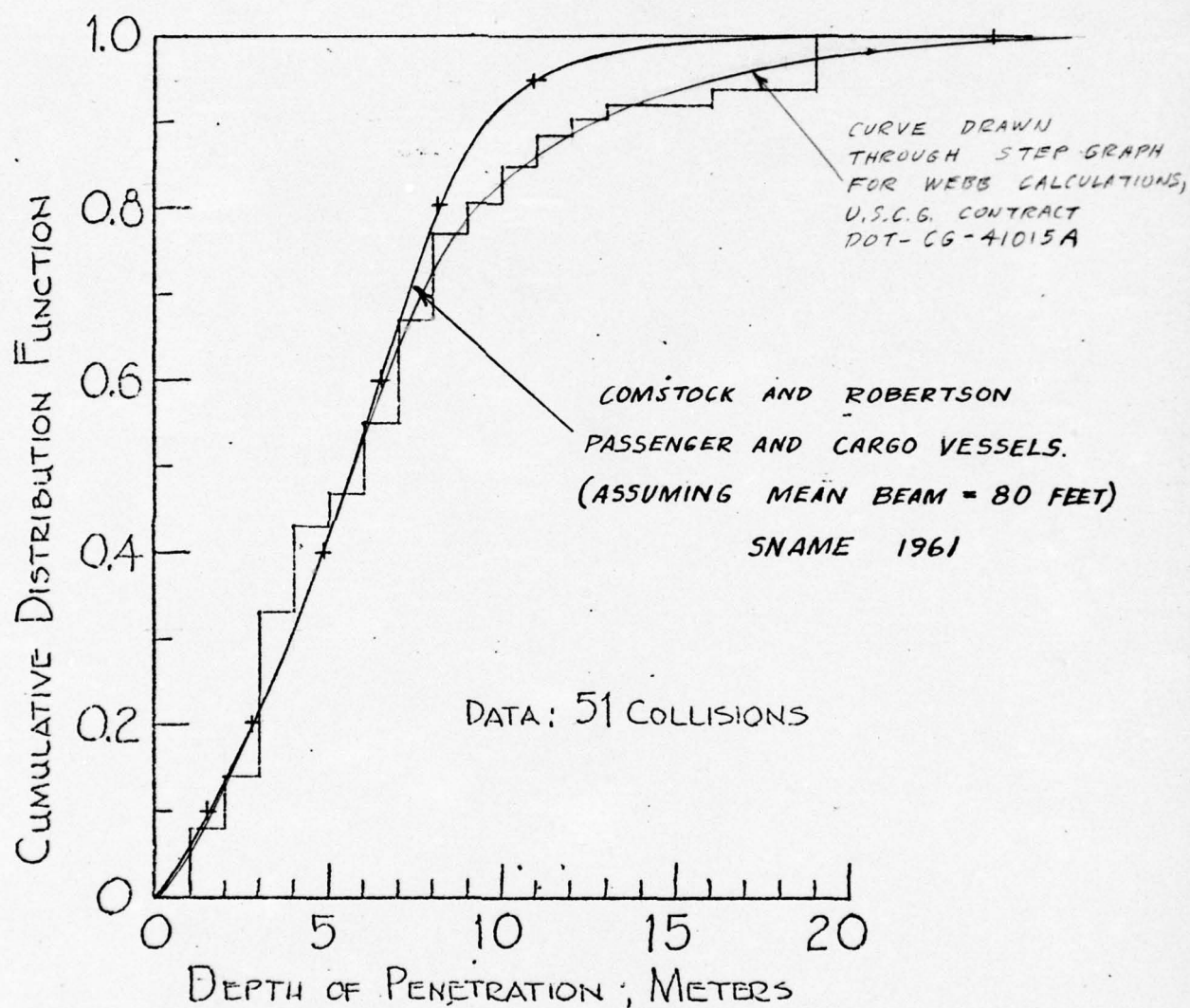


FIGURE 2



OBSERVED CUMULATIVE DISTRIBUTION OF DEPTH OF PENETRATION

Figure 1
 (FROM "PRELIMINARY ANALYSIS
 OF TANKER COLLISIONS"
 BY D.M. BOVET,
 U.S.C.G. OFFICE OF RESEARCH
 AND DEVELOPMENT, NOV. 30, 1970)

FIGURE 3

DISTRIBUTION OF PROBABLE OUTFLOW - BASE SHIP

DESIGN D75-A
763' x 125' x 54.5'

TO OBTAIN PROBABLE OUTFLOW FROM A COLLISION, FIND
AREA UNDER CURVE AND MULTIPLY BY 20, THERE BEING
(20) 5% INCREMENTS. THIS LEADS TO PROBABLE OUTFLOW = 6576 (METERS)³

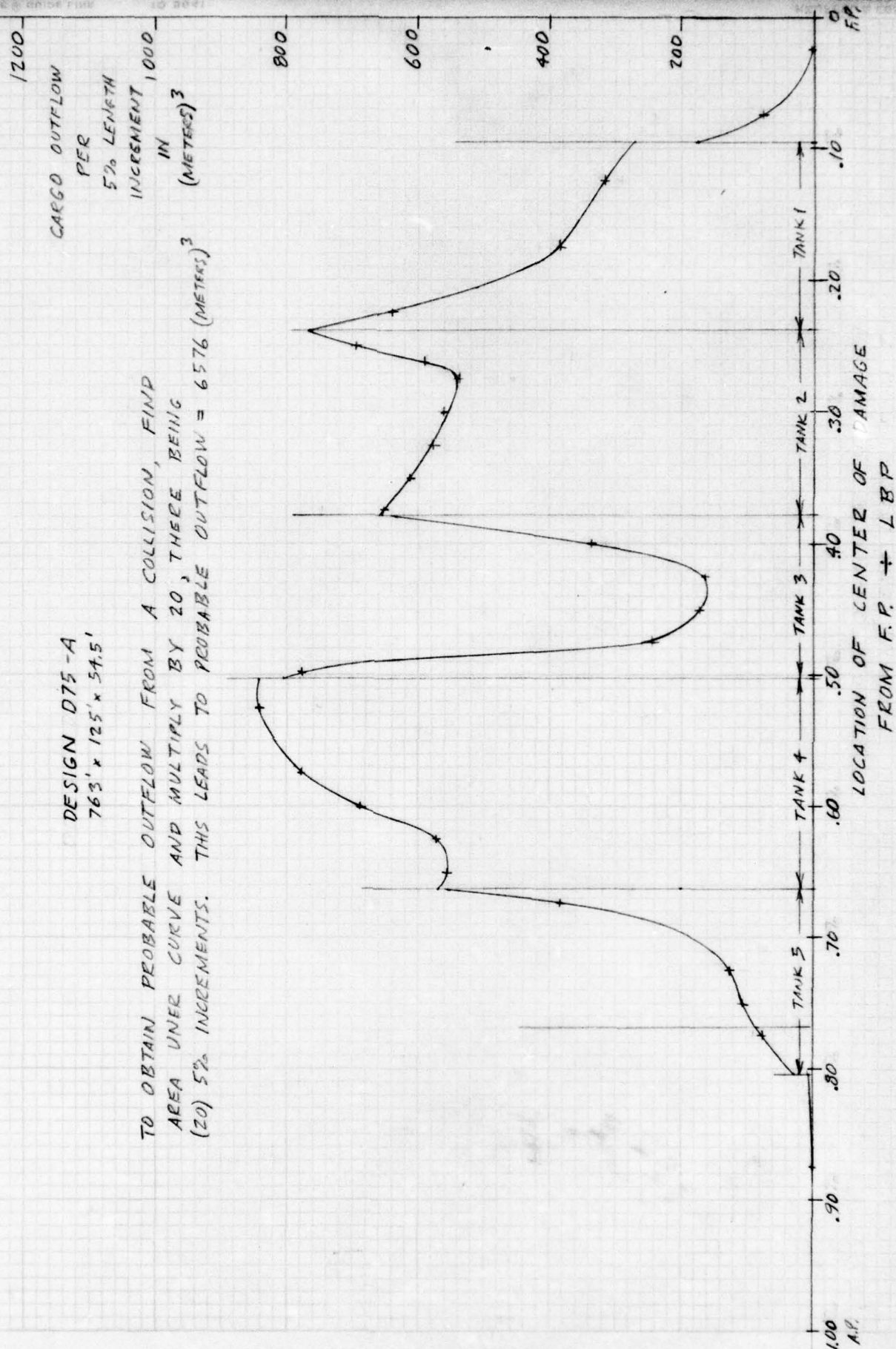


FIGURE 4

DISTRIBUTION OF PROBABLE OUTFLOW - CASE II

(BASE SHIP MODIFIED BY NON-STRUCTURAL BULKHEADS,
FREE-FLOODING AT FOOT, ON EVERY FRAME, IN
WING TANKS ONLY, EXTENDING TO HEIGHT TO
ACHIEVE OIL-WATER INTERFACE AT FOOT.

OIL S.G. = .85 ; WATER S.G. = 1.0256)

PROBABLE OUTFLOW FROM COLLISION
= AREA UNDER CURVE $\times 20 = 3451 \text{ (METERS)}^3$

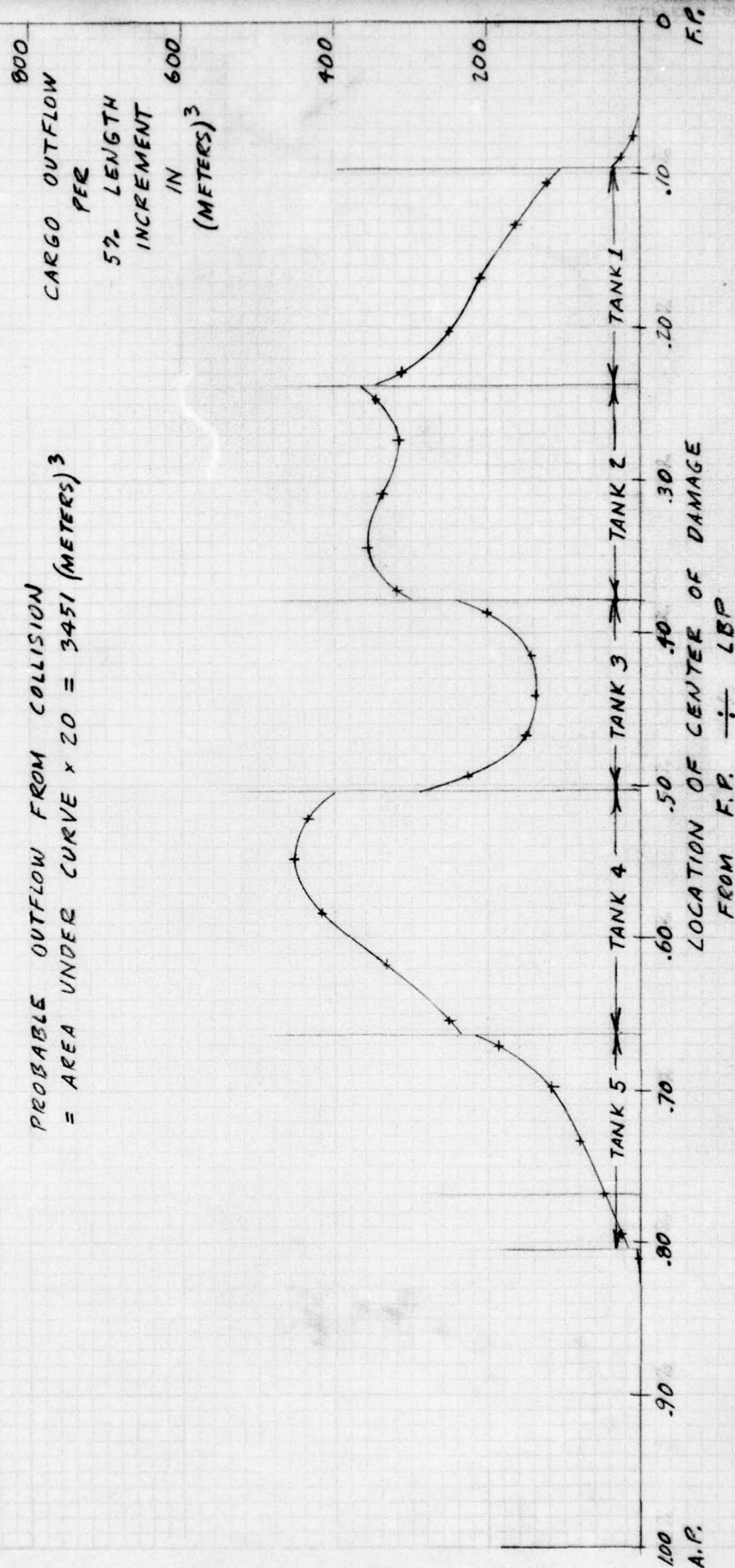


FIGURE 5

DISTRIBUTION OF PROBABLE OUTFLOW - CASE III
 (BASE SHIP MODIFIED BY NON-STRUCTURAL BULKHEADS,
 TIGHT AT BOTTOM AND SIDES TO ONE FOOT ABOVE
 PROBABLE W.L. AFTER DAMAGE, ON EVERY FRAME,
 IN WING TANKS ONLY)

PROBABLE OUTFLOW FROM COLLISION
 = AREA UNDER CURVE $\times 20 = 3432 \text{ (METERS)}^3$

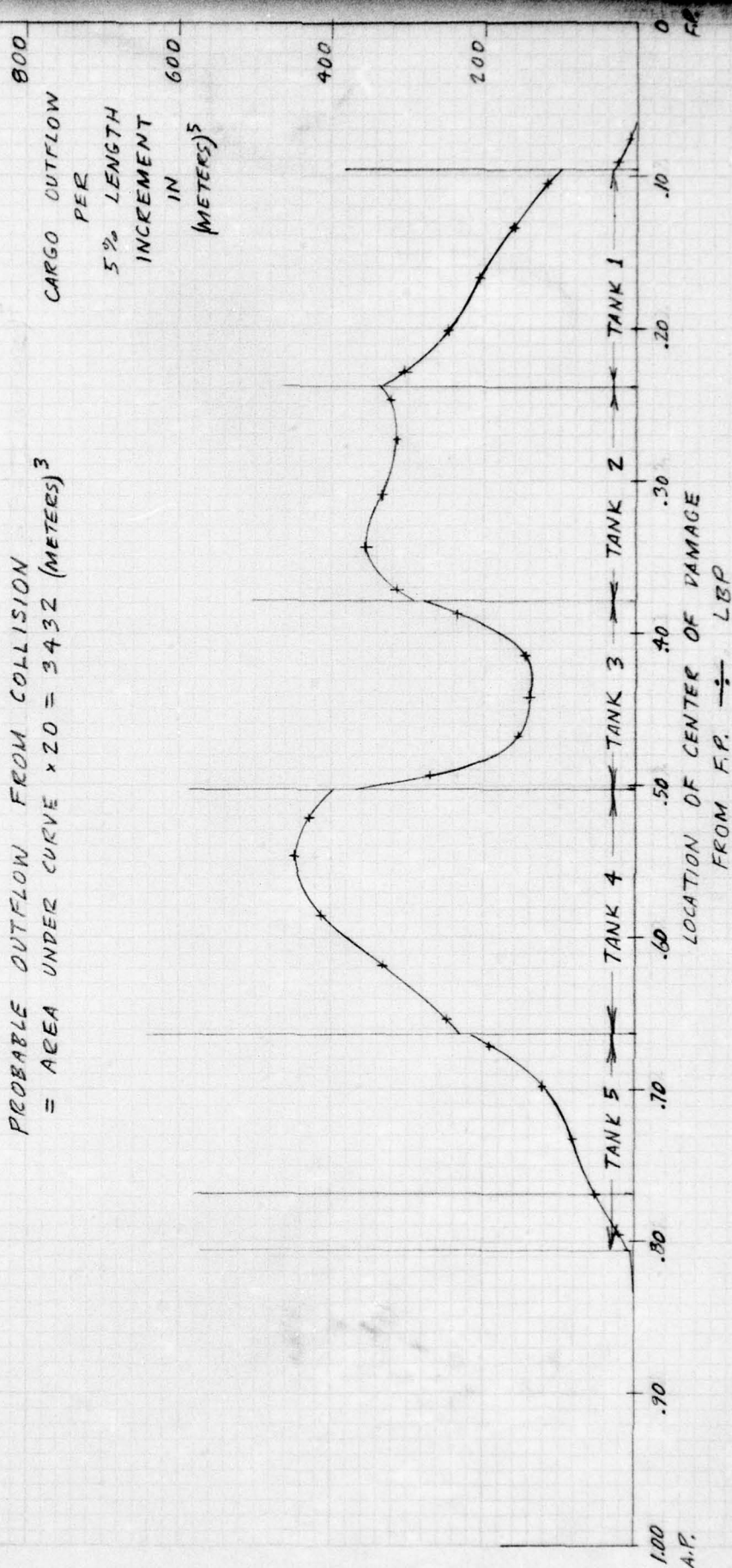


FIGURE 6

90%

DISTRIBUTION OF PROBABLE OUTFLOW - CASE IV

(BASE SHIP MODIFIED BY NON-STRUCTURAL BULKHEADS,
FREE-FLOODING AT FOOT, ON EVERY SECOND FRAME,
IN WING TANKS ONLY, EXTENDING TO HEIGHT TO
ACHIEVE OIL-WATER INTERFACE AT FOOT,
OIL S.G. = .85 ; WATER S.G. = 1.0256)

PROBABLE OUTFLOW FROM COLLISION
= AREA UNDER CURVE $\times 20 = 3829 \text{ (METERS)}^3$

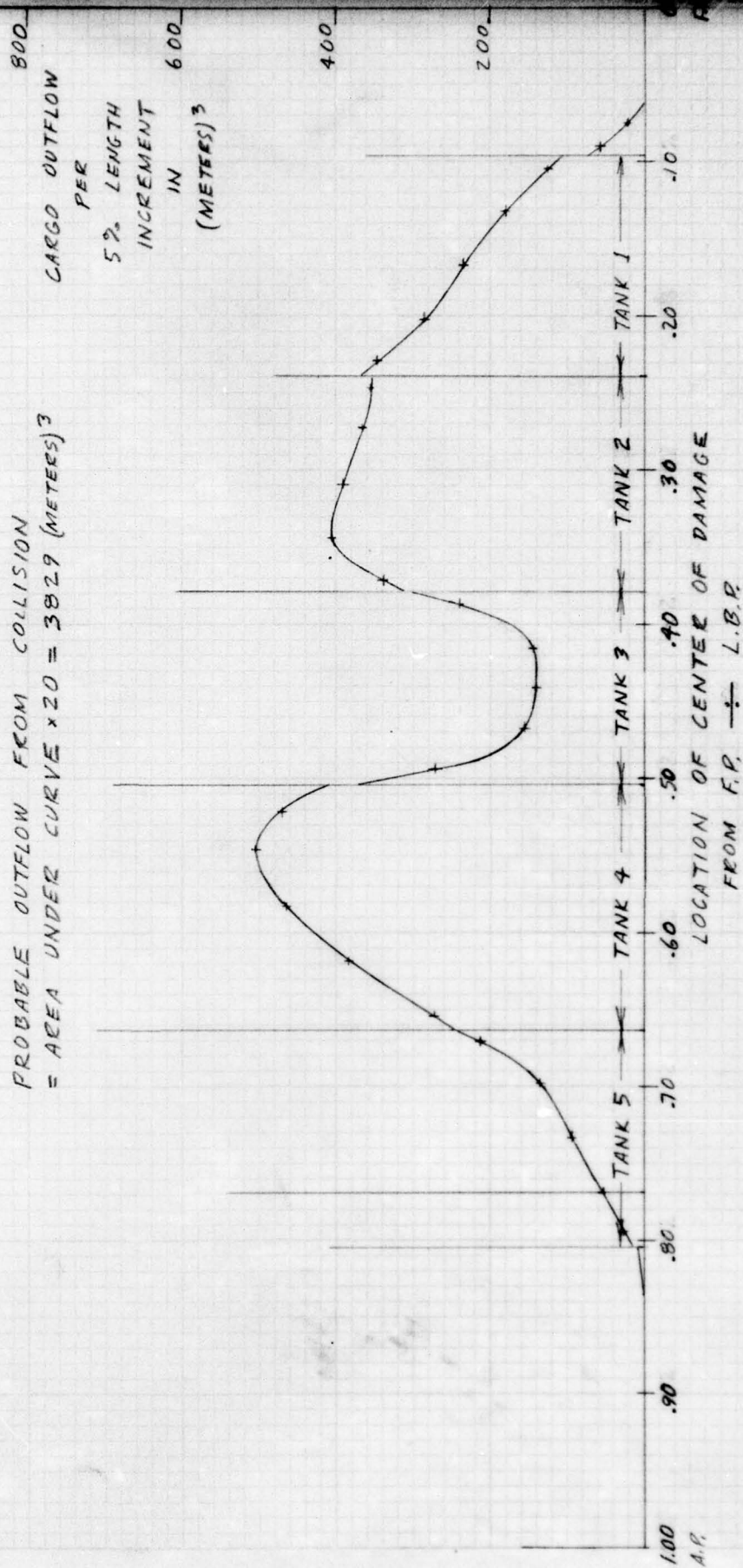


FIGURE 7

90%

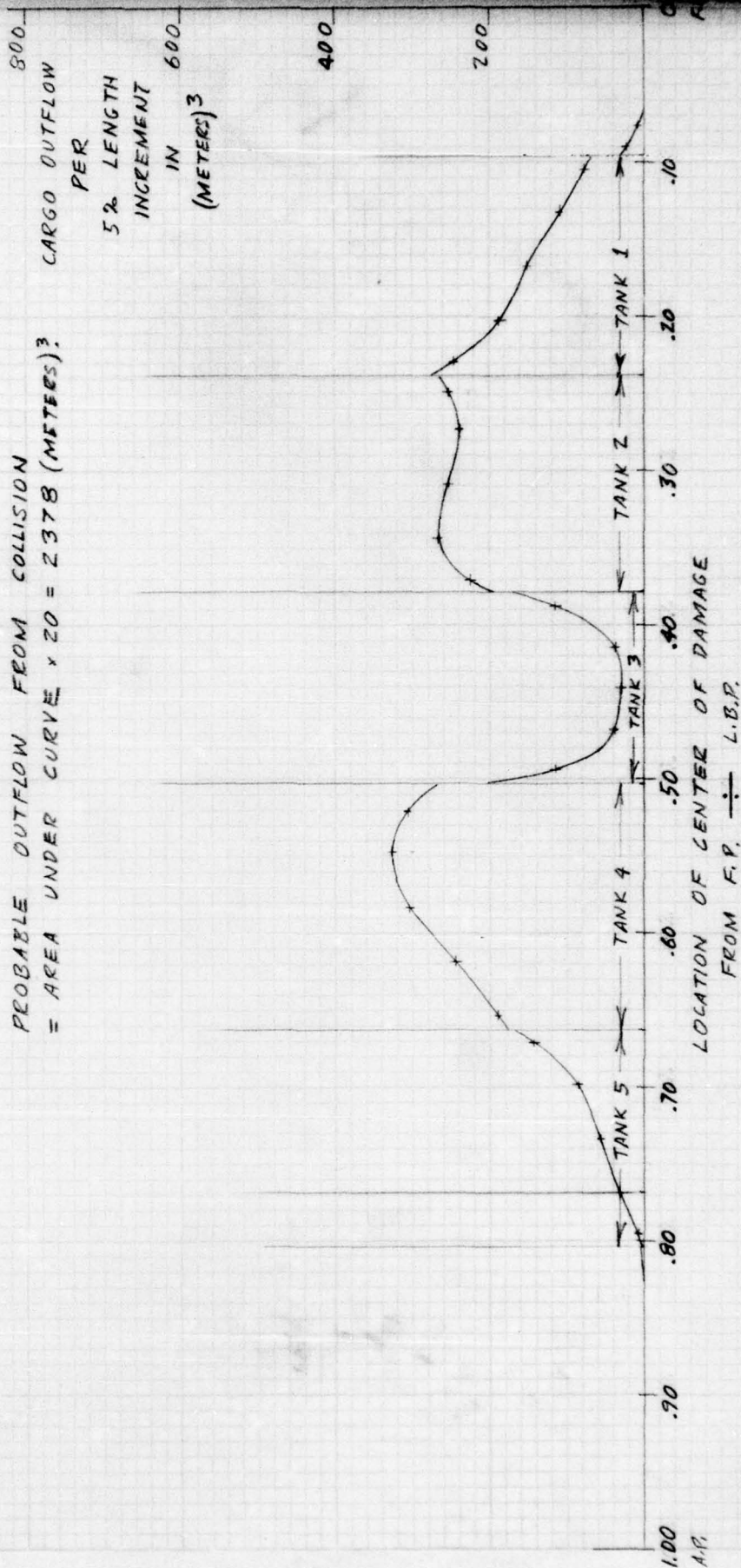
FIGURE 8

DISTRIBUTION OF PROBABLE OUTFLOW - CASE V

(BASE SHIP MODIFIED BY NON-STRUCTURAL BULKHEADS
FREE-FLOODING AT FOOT, ON EVERY FRAME, IN WING
TANKS AND CENTER TANKS, EXTENDING TO HEIGHT TO
ACHIEVE OIL-WATER INTERFACE AT FOOT.

OIL S.G. = .85 ; WATER S.G. = 1.0256.)

PROBABLE OUTFLOW FROM COLLISION
= AREA UNDER CURVE $\times 20 = 2378$ (METERS)³



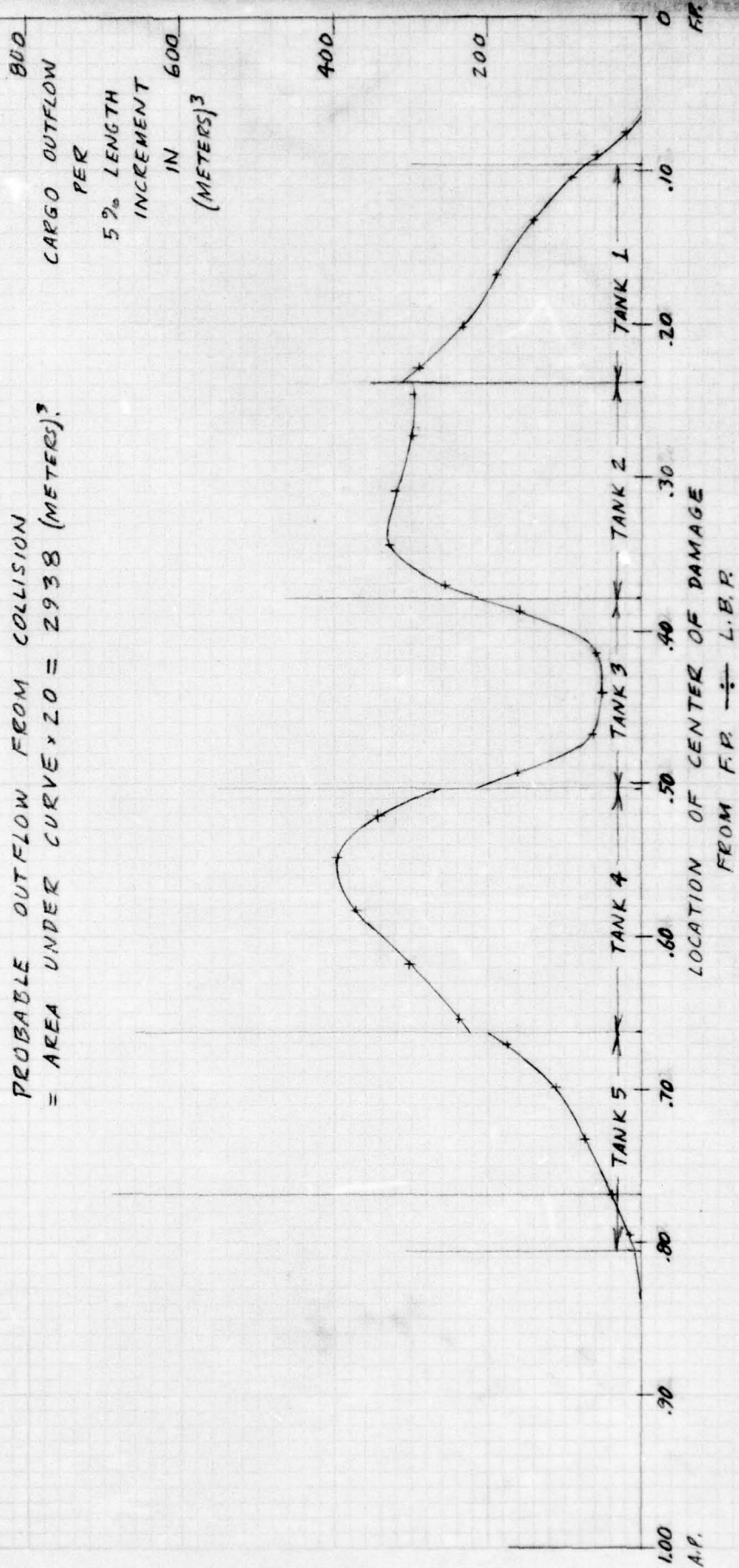
90%

63

DISTRIBUTION OF PROBABLE OUTFLOW - CASE VI

(BASE SHIP MODIFIED BY NON-STRUCTURAL BULKHEADS,
FREE-FLOODING AT FOOT, ON EVERY SECOND FRAME,
IN WING TANKS AND CENTER TANKS, EXTENDING
TO HEIGHT TO ACHIEVE OIL-WATER INTERFACE
AT FOOT. OIL S.G. = .85; WATER S.G. = 1.0256)

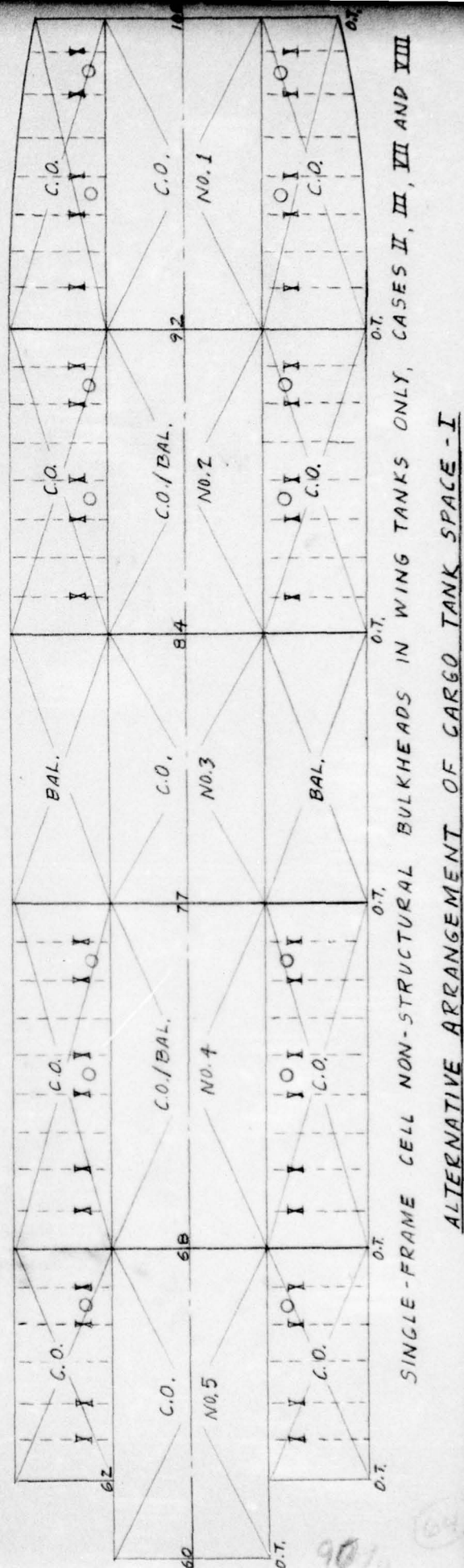
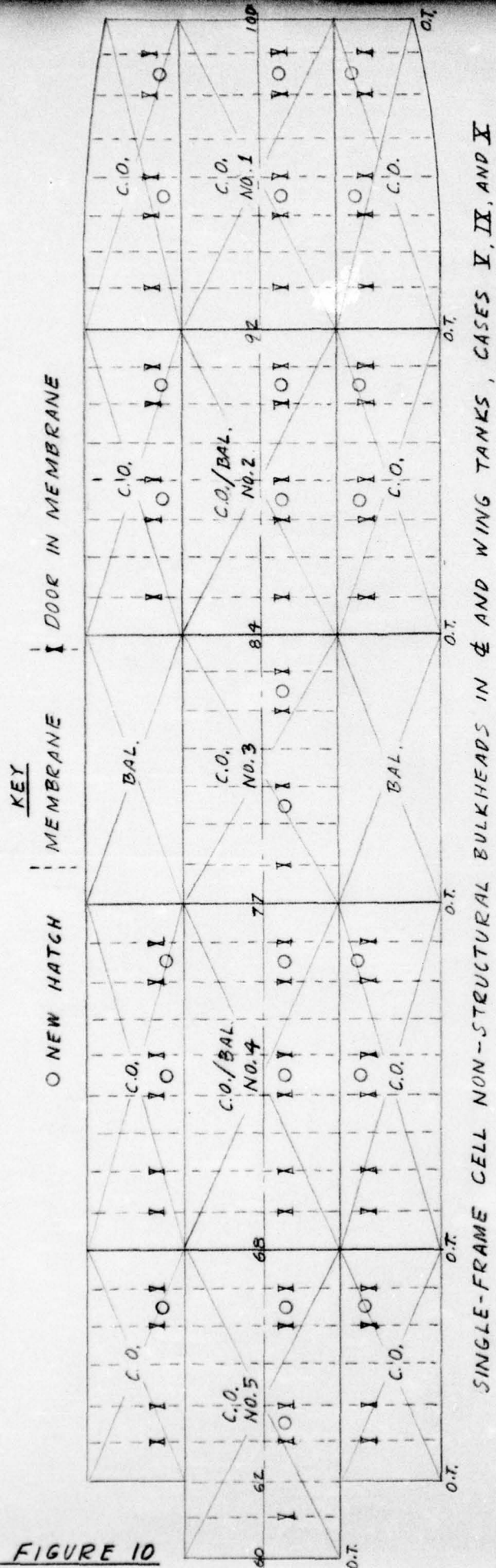
PROBABLE OUTFLOW FROM COLLISION
= AREA UNDER CURVE $\times 20 = 2938$ (METERS)³



90%

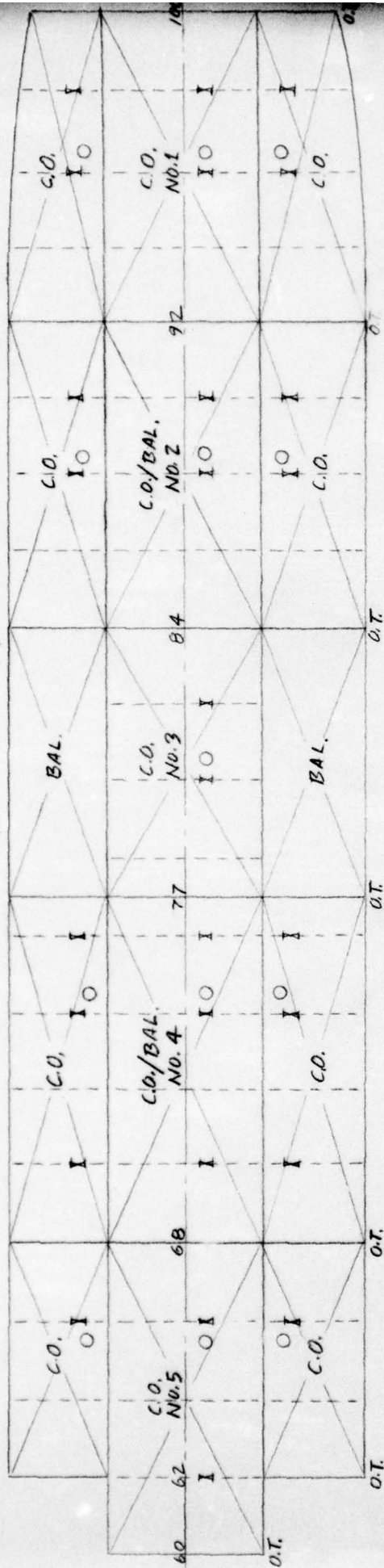
FIGURE 9

FIGURE 10

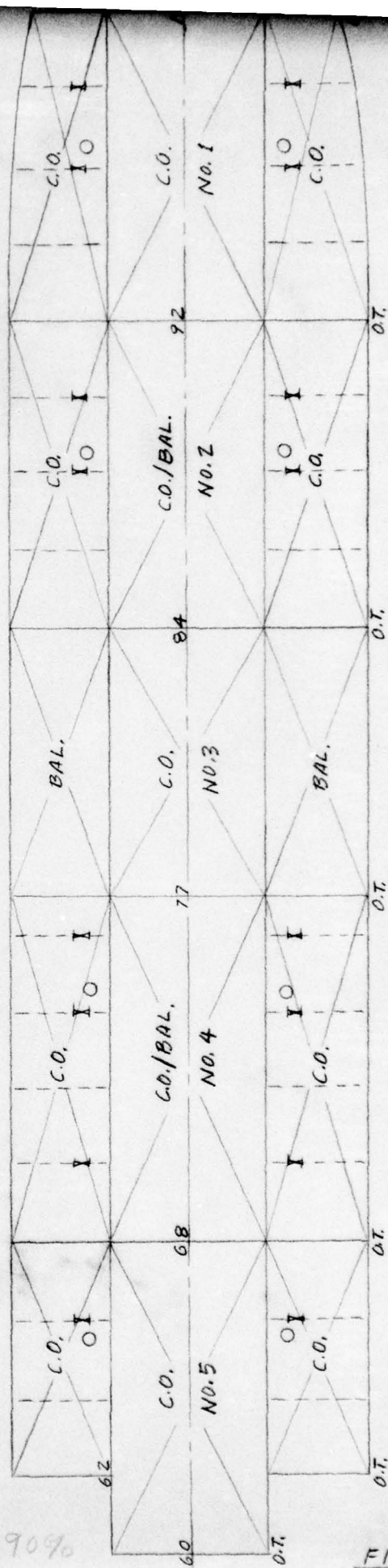


KEY

○ NEW HATCH | MEMBRANE | DOOR IN MEMBRANE

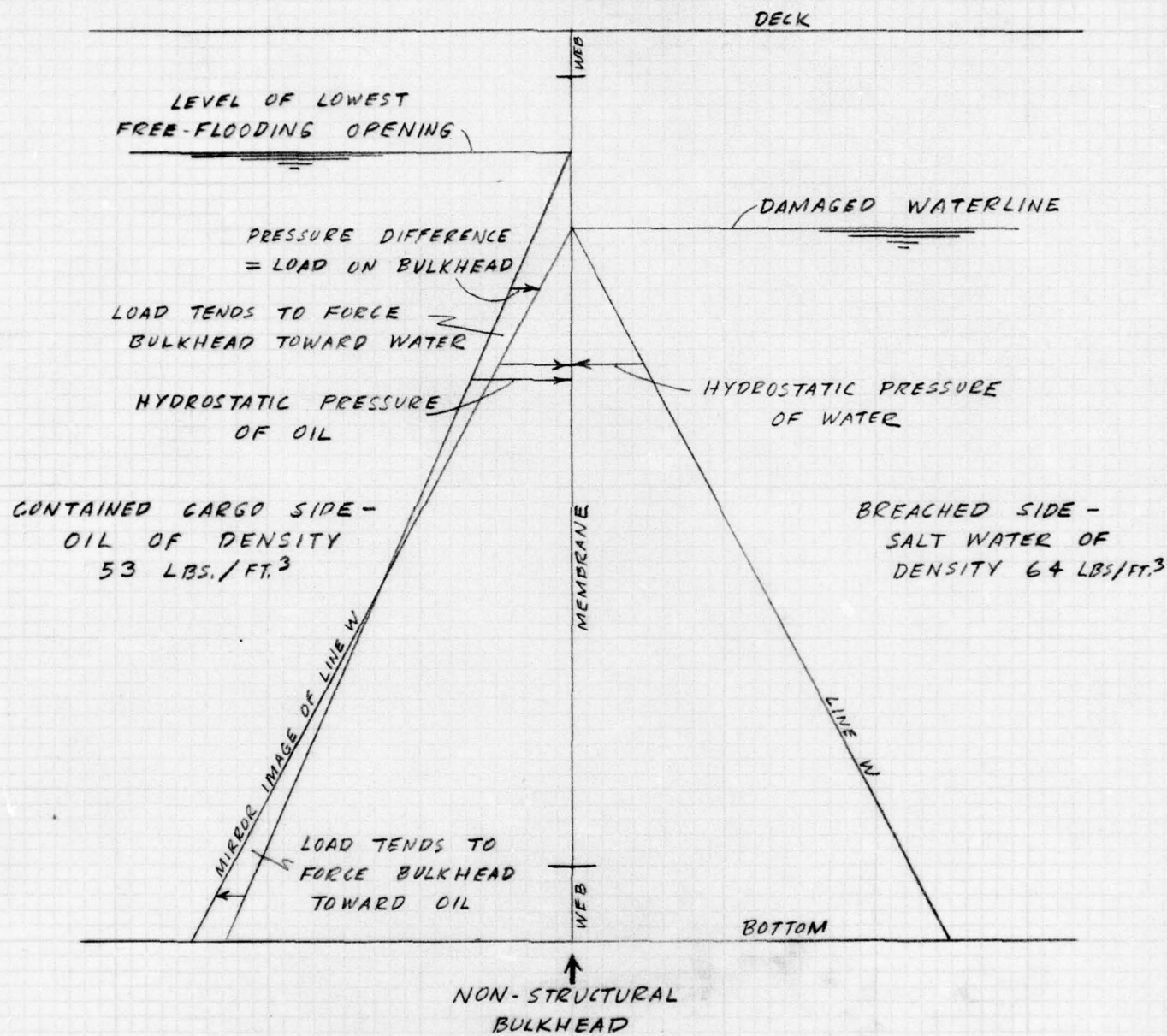


DOUBLE FRAME CELL NON-STRUCTURAL BULKHEADS IN WING TANKS, CASE VI



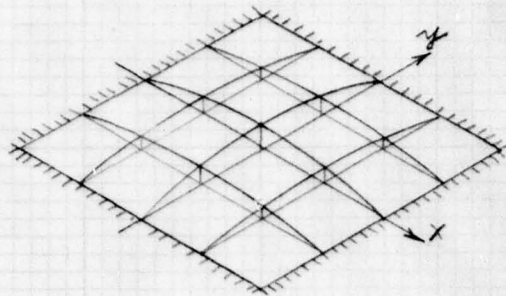
DOUBLE FRAME CELL NON-STRUCTURAL BULKHEADS IN WING TANKS ONLY, CASE IV

ALTERNATIVE ARRANGEMENT OF CARGO TANK SPACE-II

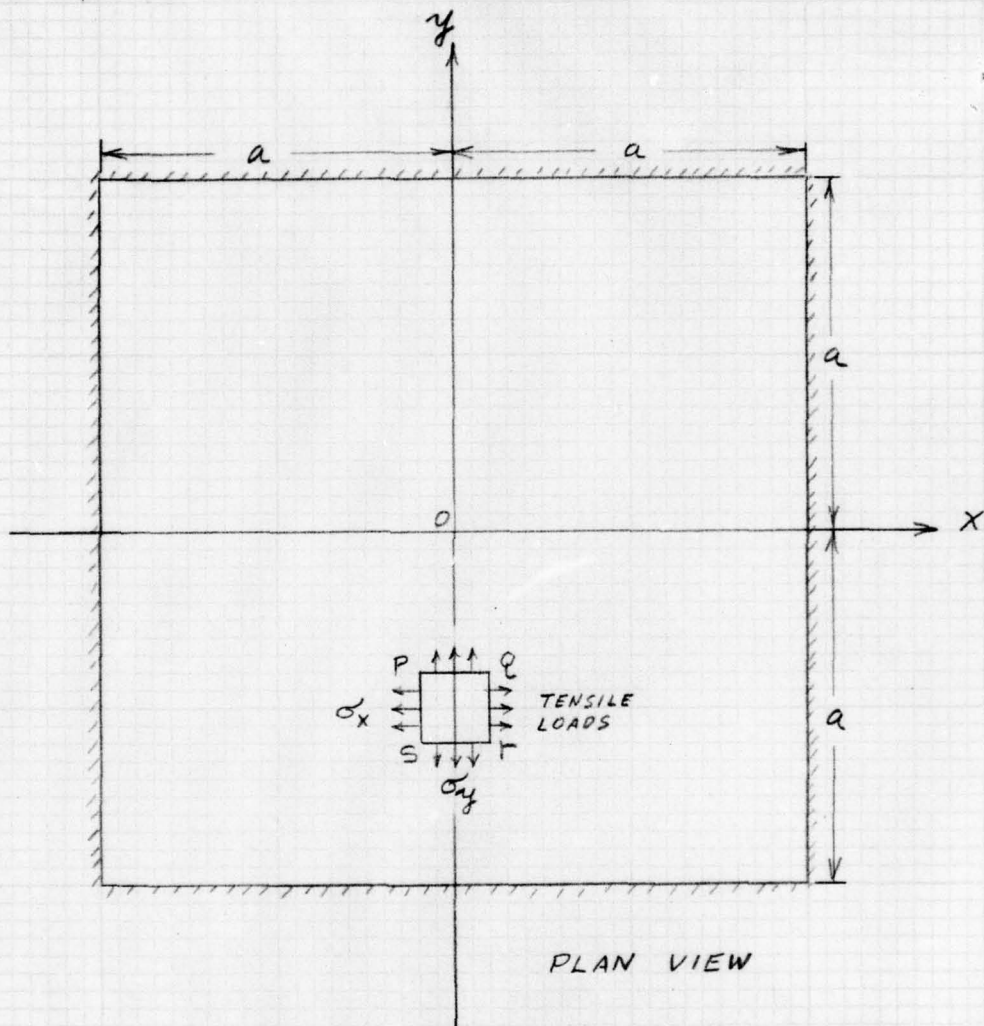


PRESSURE DISTRIBUTION ON
NON-STRUCTURAL BULKHEAD AFTER
DAMAGE - BULKHEAD TIGHT AT
BOTTOM AND SIDES

FIGURE 12



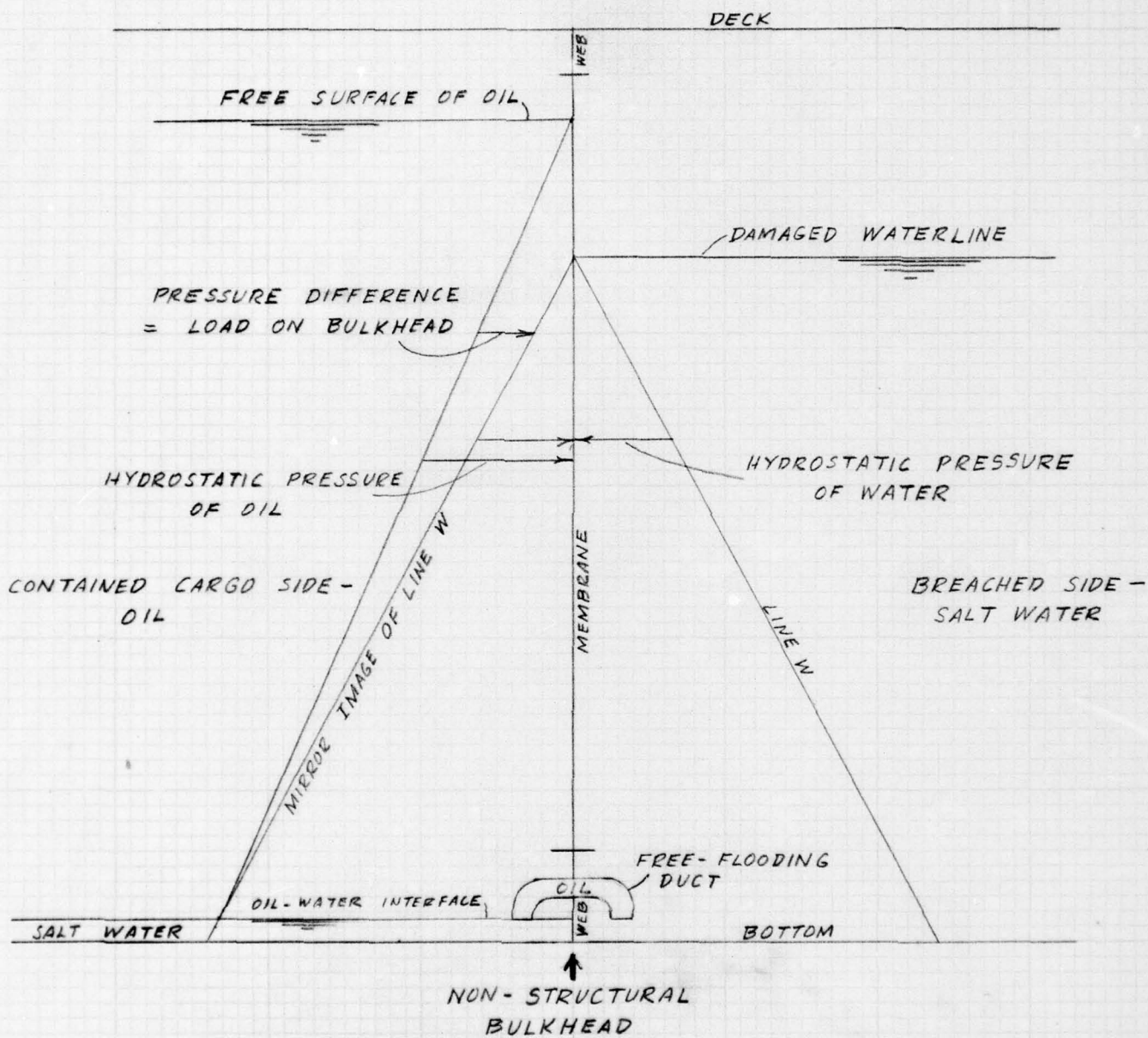
ISOMETRIC VIEW, SHOWING
SECTIONS DISTORTED BY
PRESSURE ON ONE FACE



PLAN VIEW

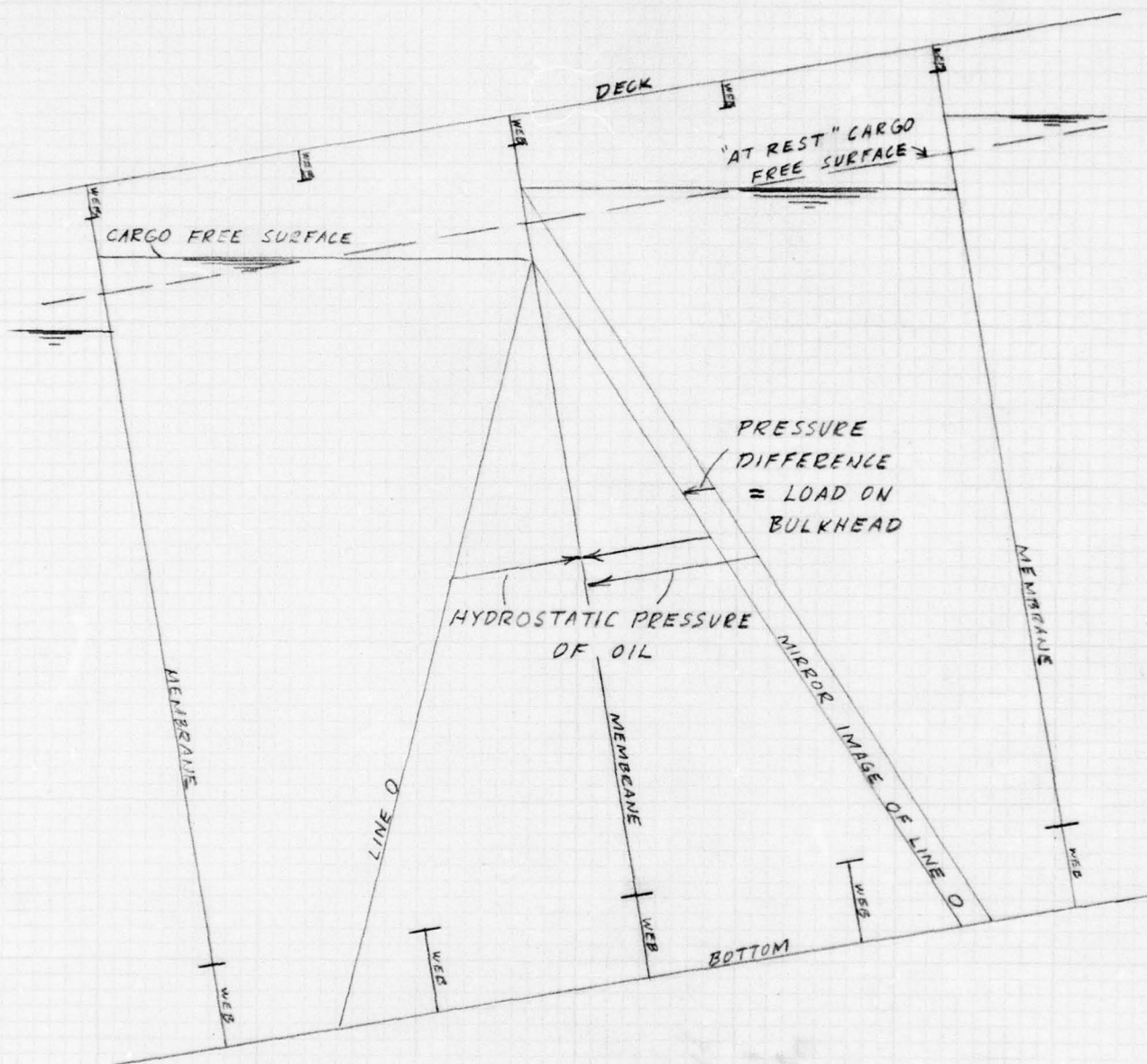
SQUARE MEMBRANE
CLAMPED AT ALL EDGES

FIGURE 13



PRESSURE DISTRIBUTION ON
NON-STRUCTURAL BULKHEAD AFTER
DAMAGE - BULKHEAD FREE FLOODING
AT FOOT

FIGURE 14



HYDROSTATIC PRESSURE DISTRIBUTION
DUE TO PITCH ANGLE ON 2-FRAME
CELL NON-STRUCTURAL BULKHEAD
WHEN CARRYING PARTIAL CARGO

FIGURE 15

FIGURE 16

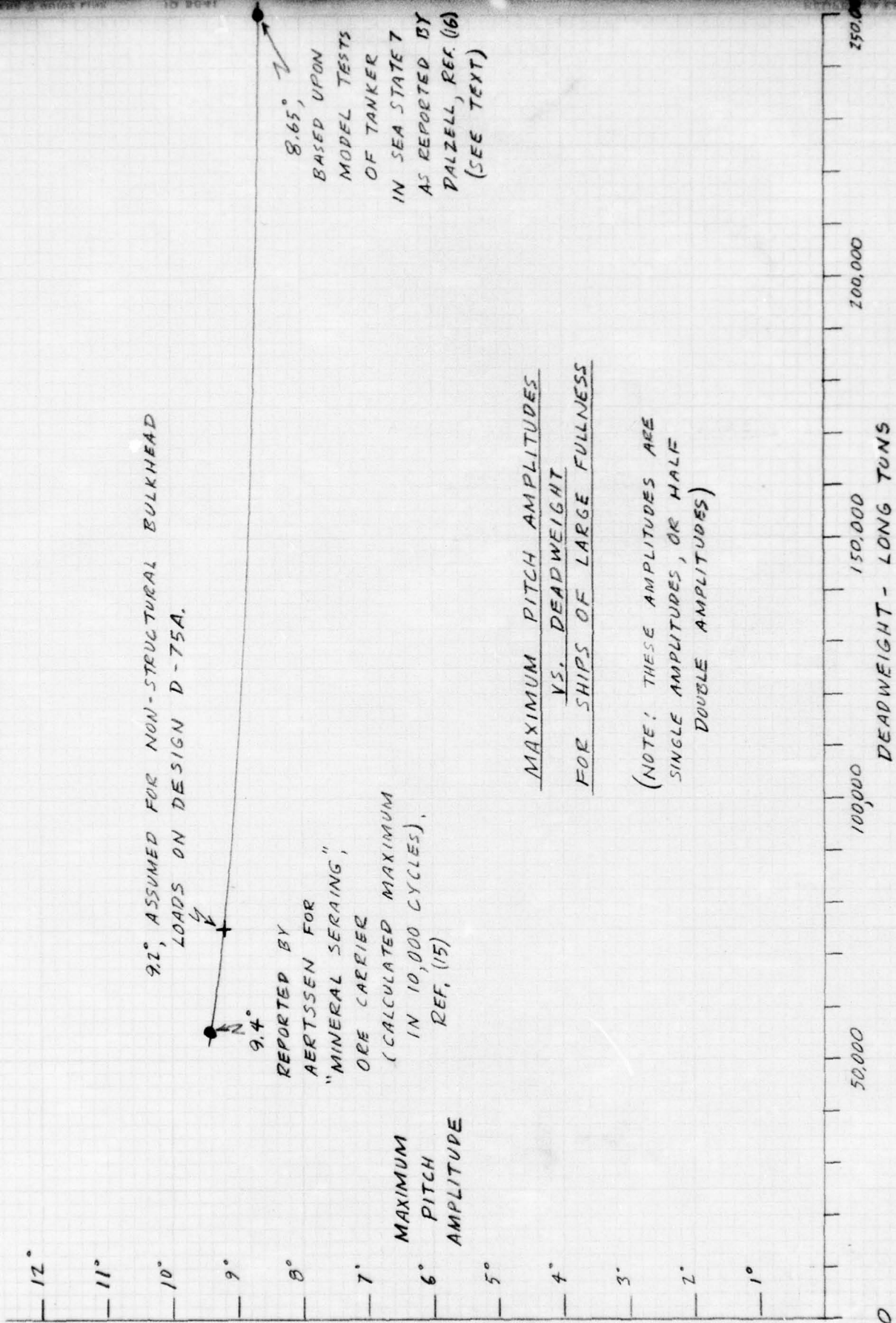
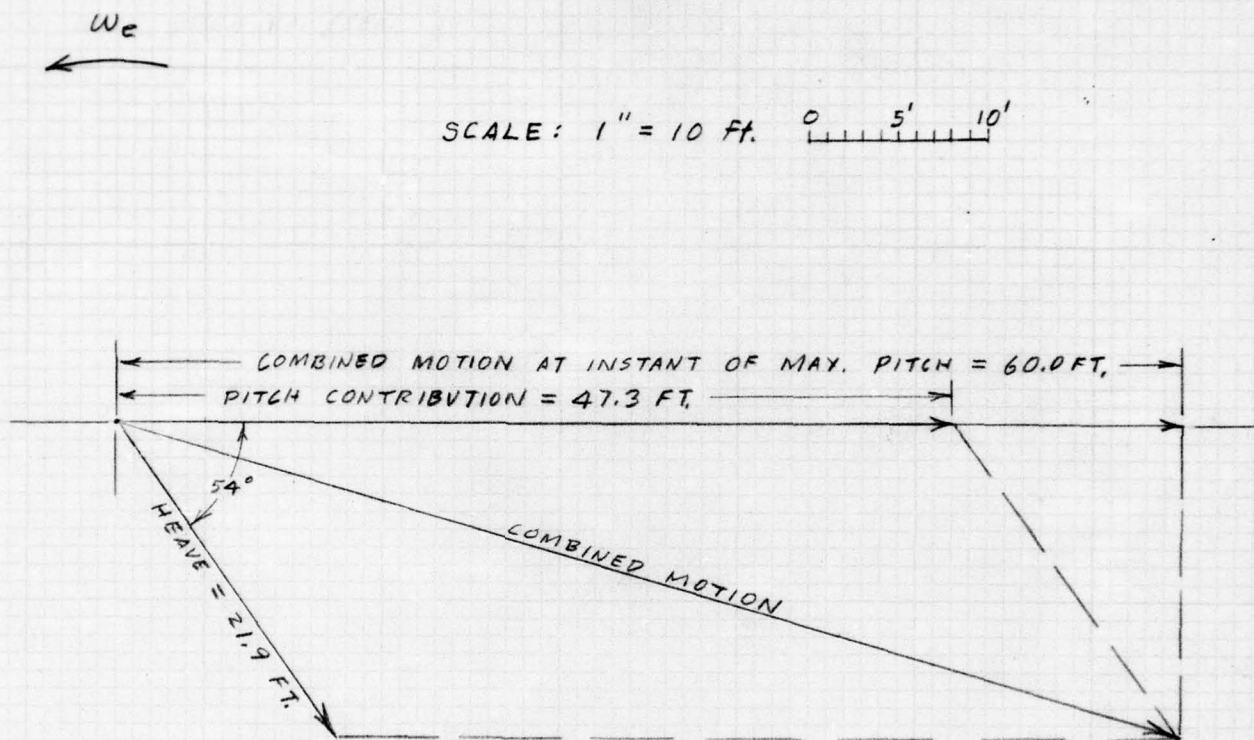


DIAGRAM ROTATES COUNTERCLOCKWISE AT
FREQUENCY OF ENCOUNTER ω_e

$$\omega_e = \frac{2\pi}{T_e} = \frac{2\pi}{9.97} = .6304 \text{ RAD./SEC.}$$

HORIZONTAL PROJECTION OF VECTOR IS
INSTANTANEOUS MOTION



$$\begin{aligned} \text{PITCH CONTRIBUTION VECTOR} &= \lambda \times \text{PITCH AMPLITUDE} \\ &= 294.5 \times \frac{9.2}{57.296} = 47.3 \text{ FT.} \end{aligned}$$

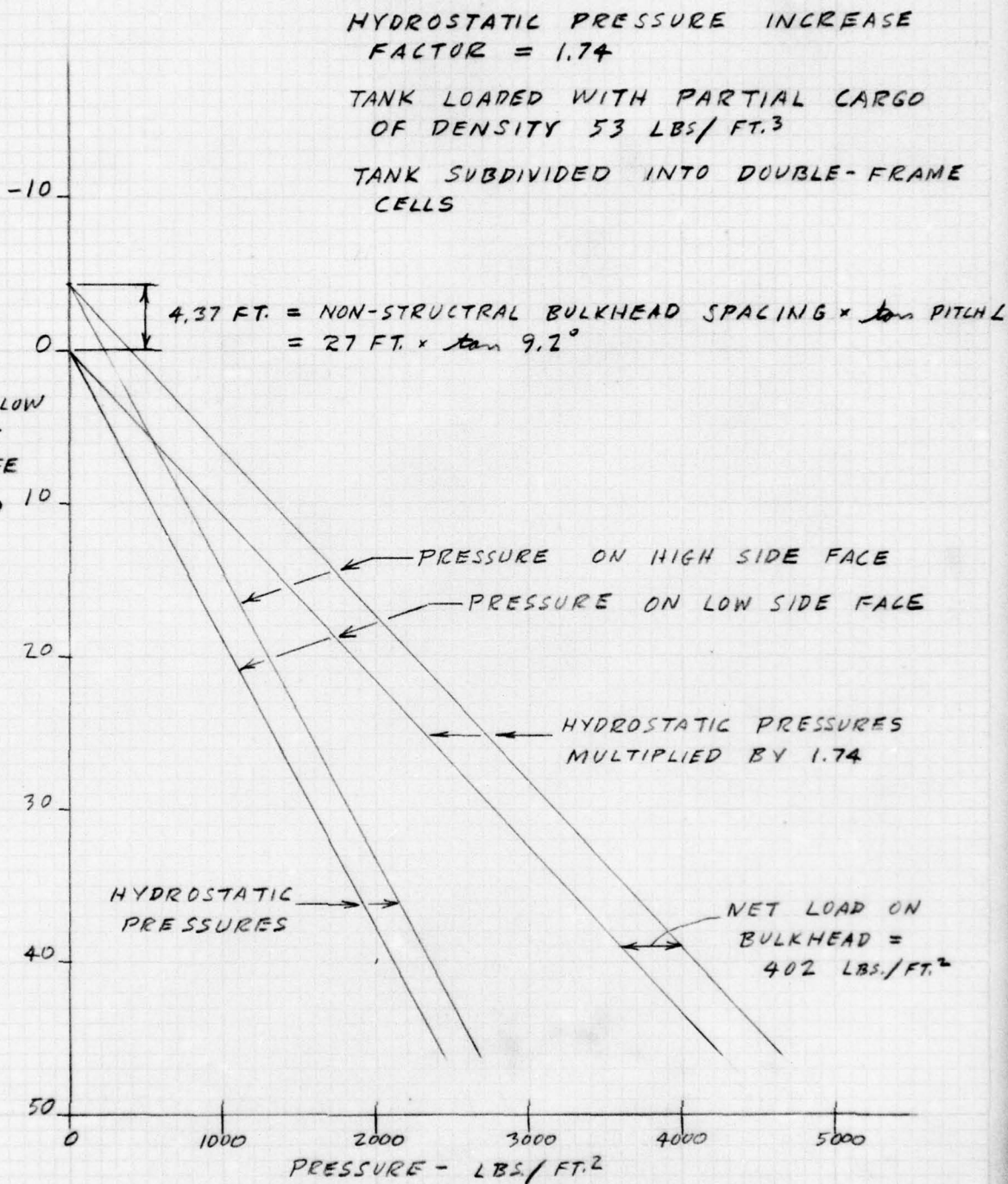
WHERE λ = DISTANCE FRAME 98 FORWARD OF AMIDS.

$$\begin{aligned} \text{NET UPWARD ACCELERATION AT FRAME 98 AT INSTANT} \\ \text{OF MAX. PITCH} &= \text{COMB. MOT.} \times \omega_e^2 = 60.0 \times (.6304)^2 \\ &= 23.84 \text{ FT/SEC.}^2 = .741 g \end{aligned}$$

VECTOR DIAGRAM SHOWING
MOTION AT FRAME 98 AT
INSTANT OF MAXIMUM PITCH

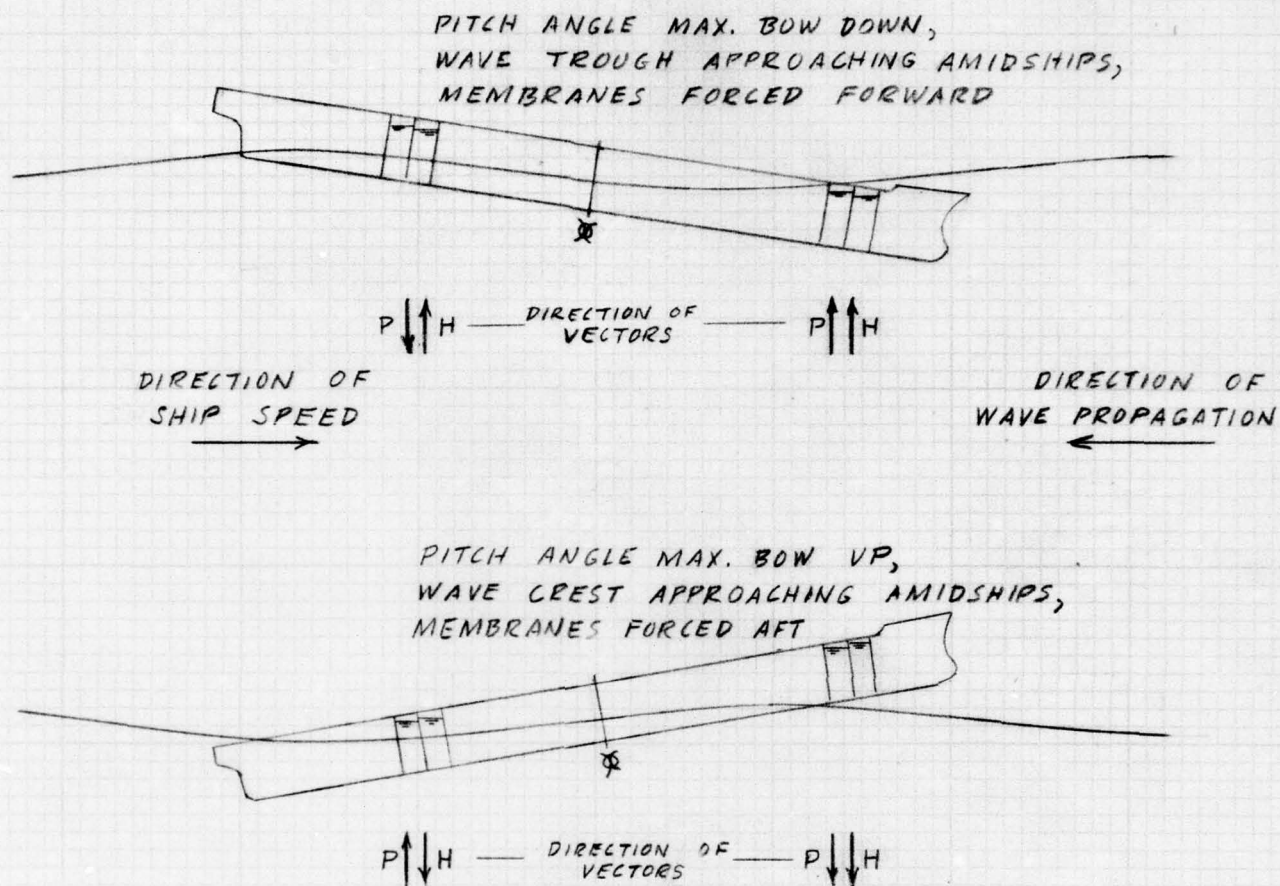
FIGURE 17

VERTICAL
DISTANCE BELOW
LOW SIDE
CARGO FREE
SURFACE, 10
FEET



HYDROSTATIC PRESSURES ON
NON-STRUCTURAL BULKHEAD
AT FRAME 98 AT INSTANT
OF MAXIMUM PITCH ANGLE

FIGURE 19



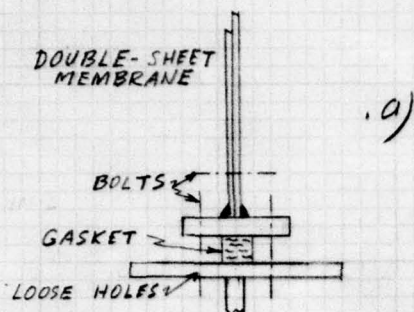
P = PITCH CONTRIBUTION VERTICAL ACCELERATION VECTOR
H = HEAVE ACCELERATION VECTOR

NOTE: VECTORS, SHIP, AND WAVE NOT TO SCALE.

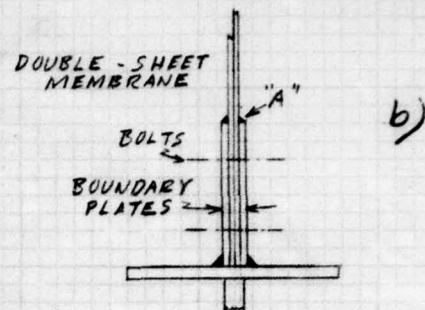
UPWARD ACCELERATION TENDS TO INCREASE
HYDROSTATIC PRESSURE LOAD ON MEMBRANES,
DOWNWARD ACCELERATION TENDS TO DECREASE IT.

DIAGRAMMATIC SKETCH SHOWING
DIRECTION OF VERTICAL ACCELERATION
COMPONENTS FORWARD AND AFT AT
INSTANT OF MAXIMUM PITCH ANGLE

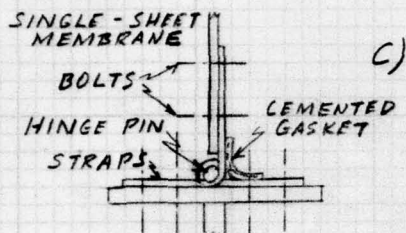
FIGURE 20



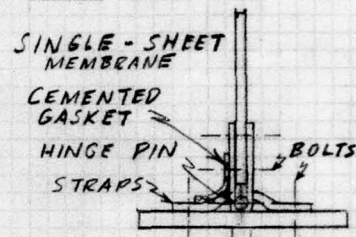
DIFFICULT TO WELD THIN SHEETS TO FACE PLATE; BENDING IN MEMBRANE AT WELD.



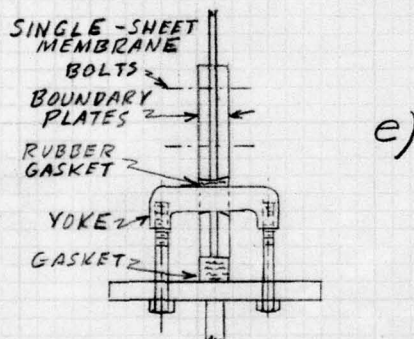
HARD SPOT AND BENDING IN MEMBRANE AT "A"; PRECISE FITTING NEEDED; NO WAY TO ADJUST IN SERVICE.



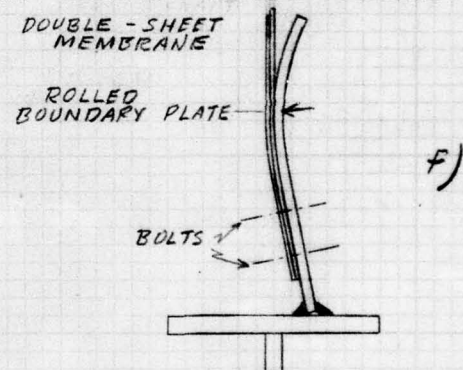
SAME DISADVANTAGES AS d).



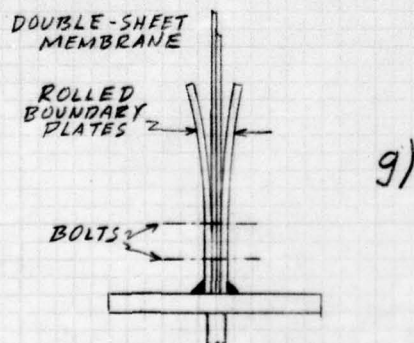
DIFFICULT TO FIT, ESPECIALLY IN CORNERS; AWKWARD GASKET.



SPECIAL YOKES NEEDED; YOKE HOLES MAY NOT STAY OIL-TIGHT.



LARGE BOUNDARY PLATE, AWKWARD TO FIT IN CORNERS; BENDING INDUCED IN WEB-FACE-PLATE CONNECTION.



PRECISE FITTING REQUIRED; NO WAY TO ADJUST IN SERVICE.

MEMBRANE EDGE-CONNECTIONS THAT WERE CONSIDERED AND REJECTED

FIGURE 21

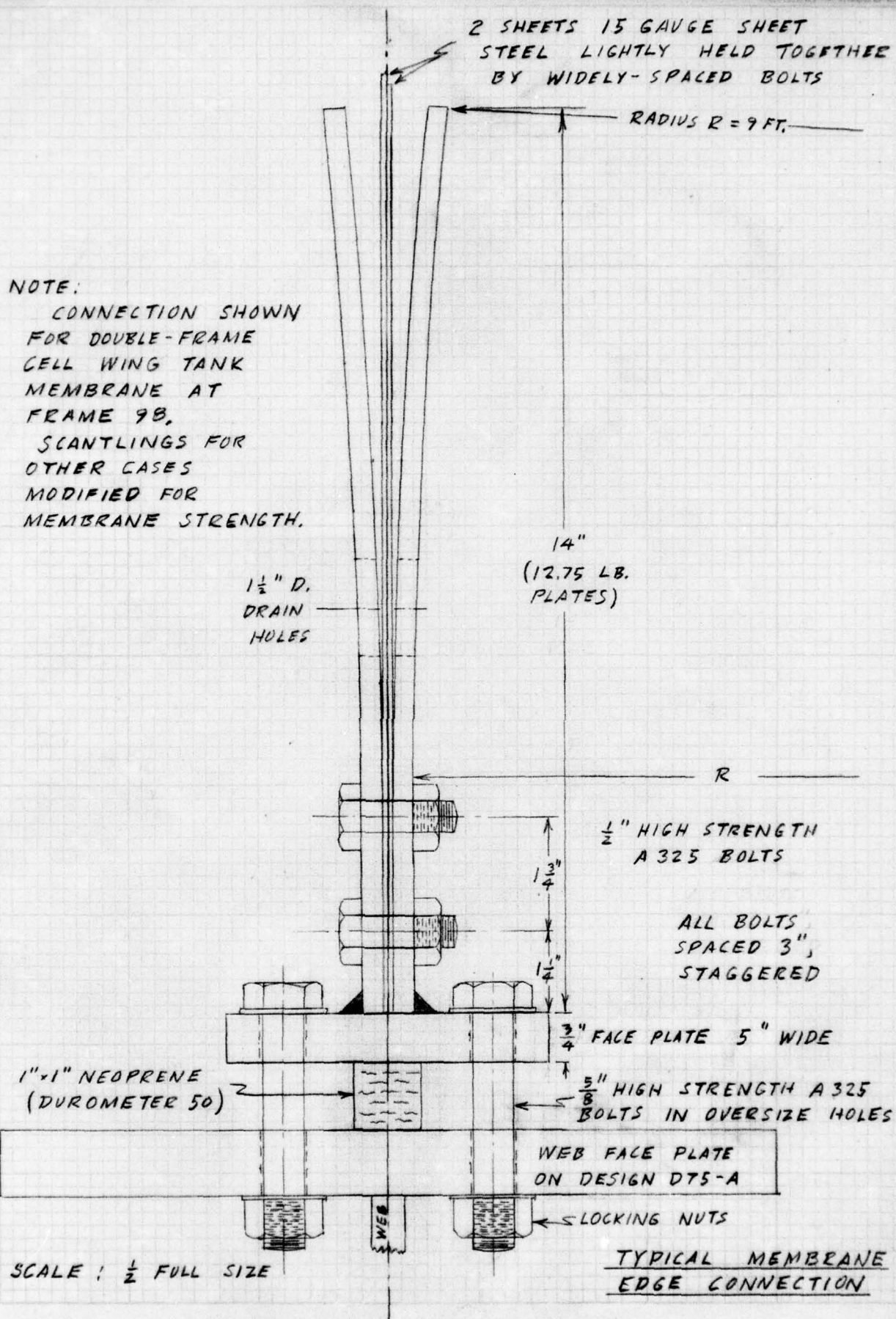
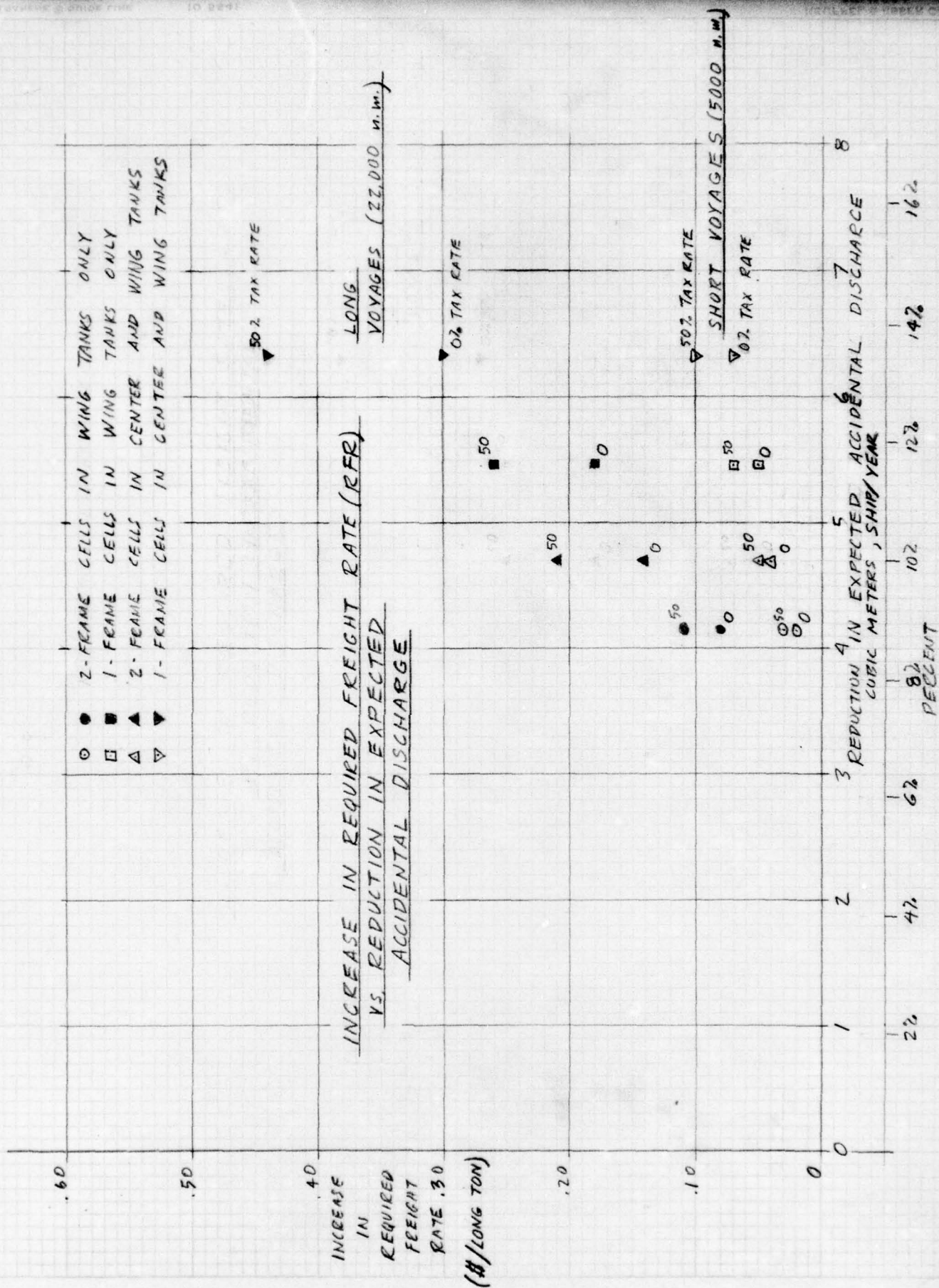
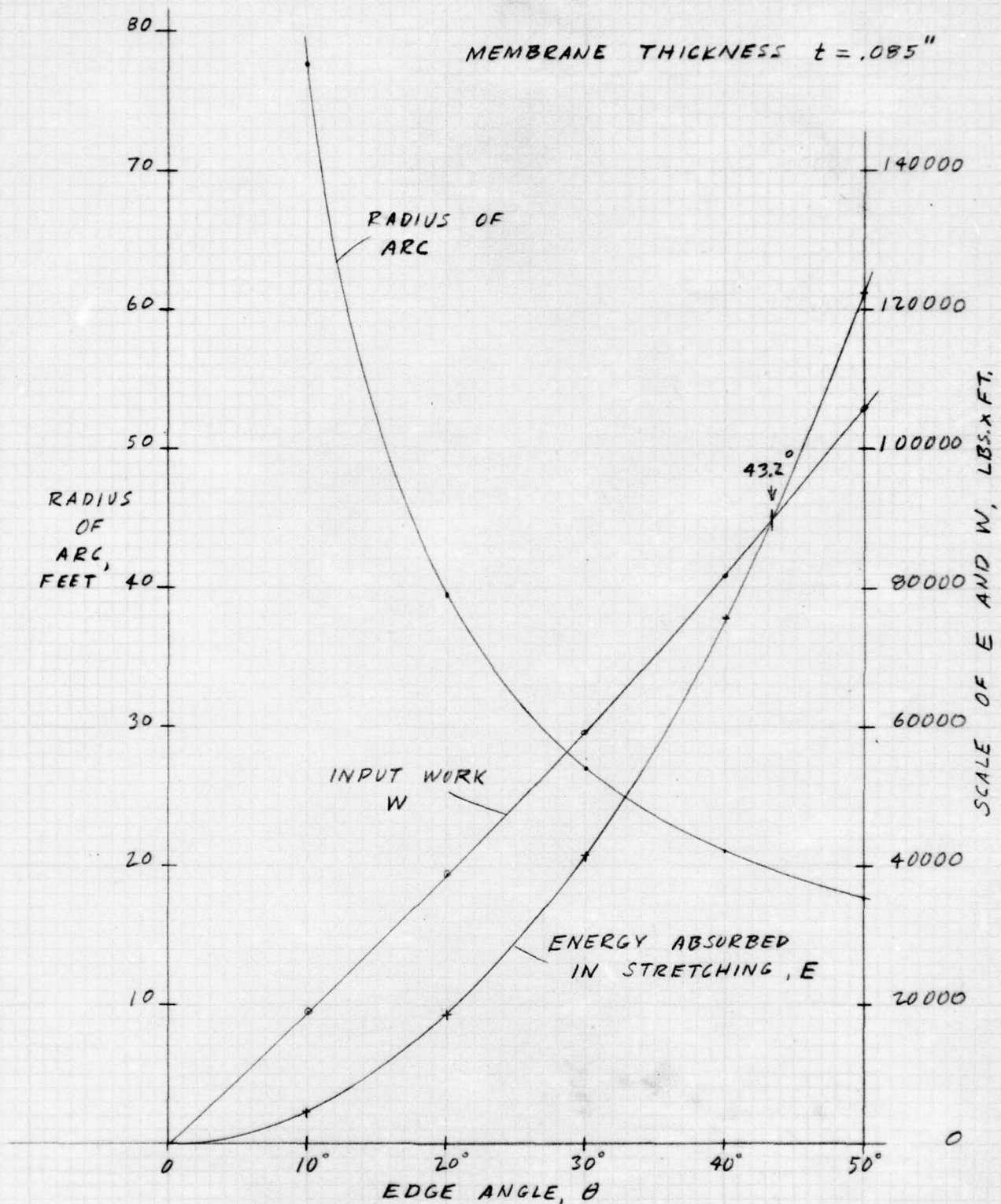


FIGURE 22

90%

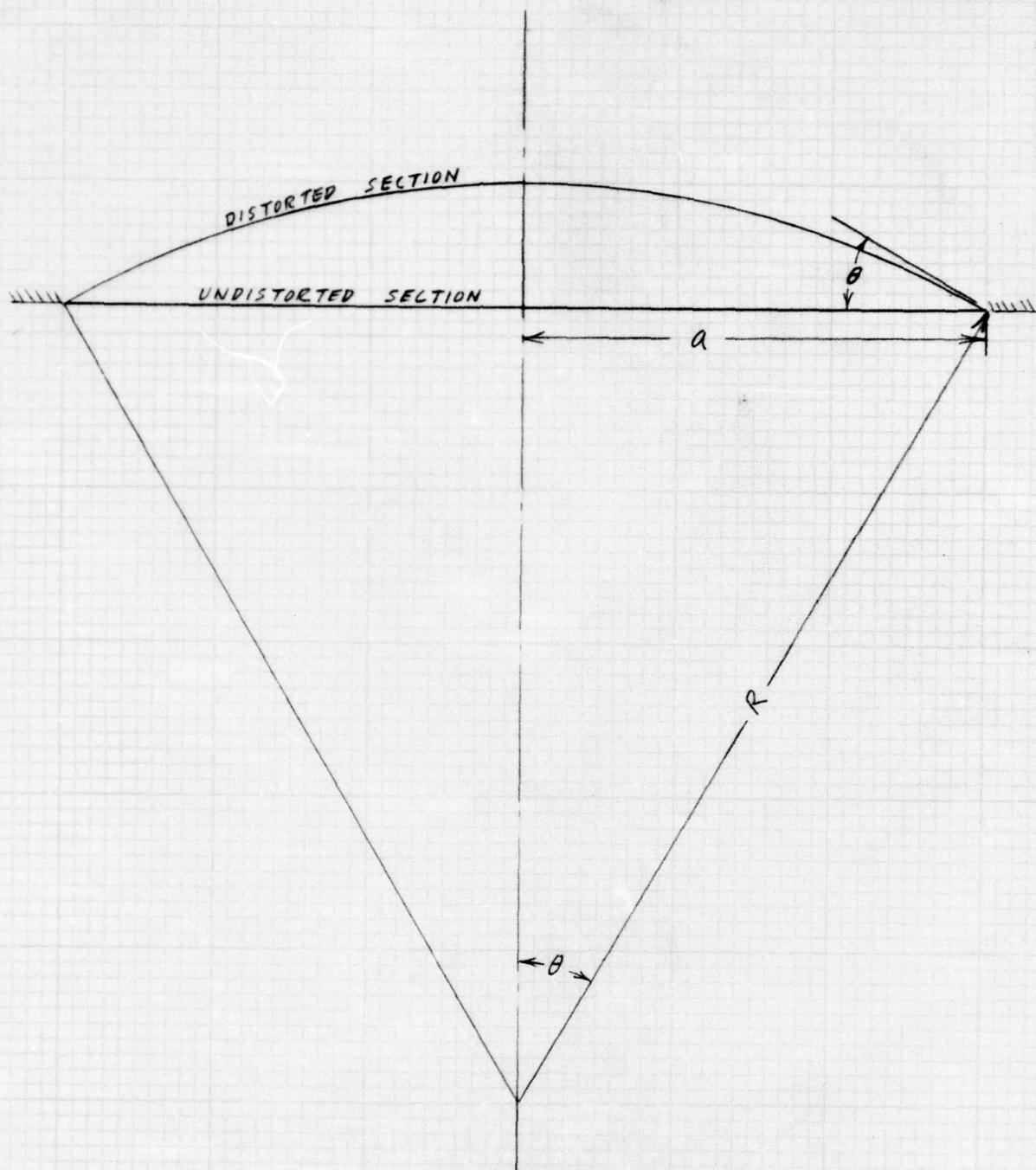
76





APPROXIMATION TO WORK DONE AND ENERGY ABSORBED IN YIELDING OF CENTER TANK MEMBRANE DUE TO PRESSURE LOAD OF 6.23 PSI

FIGURE 24



SECTION THROUGH
CLAMPED - EDGE SQUARE MEMBRANE
WITH PRESSURE ON ONE FACE
SHOWING APPROXIMATING CIRCULAR ARC

FIGURE 25

TABLE I

Percent of Damages vs. Damage Length

Mean Length of Damage (feet)	Incremental Damage Length (Feet)	Percent of Damages Occurring in Increment
2.5	5.0	3.7
7.5	"	5.6
12.5	"	10.2
17.5	"	14.3
22.5	"	14.2
27.5	"	12.3
32.5	"	9.5
37.5	"	8.5
42.5	"	5.7
47.5	"	3.6
52.5	"	2.7
57.5	"	1.5
62.5	"	1.3
67.5	"	1.0
72.5	"	.8
77.5	"	.6
82.5	"	.6
87.5	"	.5
92.5	"	.4
97.5	5.0	.4
110.0	20.0	.9
140.0	40.0	.7
180.0	"	.4
220.0	40.0	.4

 $\Sigma=100.0$

TABLE II

Percent of Damages vs. Depth of Penetration

Mean Depth of Penetration (meters)	Incremental Penetration Depth (meters)	Percent of Collisions Occurring in Increment
1	2	13.1
3	"	17.9
5	"	22.4
7	"	18.8
9	"	11.5
11	"	4.8
13	"	4.0
15	"	2.5
17	"	1.7
19	"	1.2
21	"	1.0
23	"	.6
25	2	.5

 $\Sigma=100.0$

TABLE III

Calculation Form for Determining Probable Outflow from
5% Length Damage Increment

Example is for Case II, with damage centered at Frame 68½, which is 65.4% length abaft F.P., and in Tank No. 4.

Mean Damage Length (ft)	Mean Damage ½ Length (ft)	Cells Breached	% Occurrence Incremental 100	Σ	Outflow (m) ³			Prod.
					From Cells	Above Cells	Below Duct	Total
2.5-22.5	1.25-11.25	h_{41}^i	.037+.056+.102+.143+.142	.480	1585.8	792.4	110.0	2488.2
27.5-52.5	13.75-26.25	g_{41}^{-i}	.125+.095+.085+.057+.036+.027	.425	2571.6	1321.5	183.4	4076.5
57.5-77.5	28.75-38.75	f_{41}^{-i}	.015+.013+.010+.008+.006	.052	3857.4	1321.5	183.4	5362.3
82.5-97.5	41.25-48.75	e_{41}^{-i}	.006+.005+.004+.004	.019	5143.2	1321.5	183.4	6648.1
110.0	55.0	d_{41}^{-i}	.009	.009	6429.0	1321.5	183.4	7933.9
140.0	70.0	c_{41}^{-i}	.007	.007	7714.8	1321.5	183.4	9219.7
180.0	90.0	b_{41}^{-i}	.004	.004	9000.6	1321.5	183.4	10505.5
220.0	110.0	a_{41}^{-i}	.004	.004	9643.5	1321.5	183.4	11148.4
				Σ = 1.000				Σ = 3554.4

Probability of damage centered within 5% length increment 65.4% length abaft F.P. = .048 (Figure 2).

Then probable outflow from wing tank damage = (3554.4) (.048) = 170.6 (m)³.

Capacity of No. 4 tank = 10,405 (m)³. Then probable outflow from damage penetrating center tank =
(3554.4 + 10405) (.048) = 670.0 (m)³.

Mean Depth of Penetration (m)	Σ Probability of Occurrence (Table II)	Outflow (m) ³	Prod.
1-9	.837	170.6	142.8
11-25	.163	670.0	109.2
		Σ = 252.0 (m) ³	Σ = Probable Outflow

TABLE IV

Summary of Outflow Calculations

(Listed in order of decreasing effectiveness of subdivision)

Case No.	No. of frames per cell	Tanks with cells	Type non-structural bulkheads	Height of cell	Probable Outflow (m) ³	
					From** damage centered at Fr. 72½ only	Considering all probable locations of damage
X	1	☐ and wings	tight	Full depth of tank	232	----
V	1	☐ and wings	free-flood	Interface 1 ft above ☐	304	2378
IX*	1	☐ and wings	tight	To 1 ft above WL	354	----
VI	2	☐ and wings	free-flood	Interface 1 ft above ☐	360	2938
VIII	1	wings only	tight	Full depth of tank	366	----
III	1	wings only	tight	To 1 ft above probable damaged WL	412	3432
II	1	wings only	free-flood	Interface 1 ft above ☐	418	3451
VII*	1	wings only	tight	To 1 ft above WL	455	----
IV	2	wings only	free-flood	Interface 1 ft above ☐	464	3829
I (base ship)	-	-----	none	-----	755	6576

For calculational purposes, a "cell" is defined as the oil-containing space between a pair of adjacent non-structural transverse bulkheads, or between a non-structural and an adjacent structural transverse bulkhead. This space may be bounded at the top by a free surface, and at the bottom by an oil-water interface.

For Case IV, a one-frame cell is located between Frames 76 and 77; for Case VI, one-frame cells are located between Frames 76 and 77, and between Frames 77 and 78 in the center tank.

* Not considered realistic cases, owing to probable submergence of tops of cells when ballast tanks are flooded from collision.

** Included for comparison only.

84
90%

TABLE V

Thickness of Wing Tank Membranes for Double-Frame Cells

Frame	Hydrostatic Pressure Increase Factor	Nominal Thickness (ins.)	Actual Thickness* (ins.)	2x Actual Thickness (ins.)	U.S. Std. Gauge
98	1.741	.1234	.0689	.1378	15
96	1.66	.1176	.0613	.1226	16
94	1.57	.1113	.0613	.1226	16
90	1.43	.1014	.0551	.1102	17
88	1.37	.0971	.0490	.0980	18
86	1.32	.0936	.0490	.0980	18
76	1.158	.0821	.0429	.0858	19
74	↓	↓	↓	↓	↓
72	↓	↓	↓	↓	↓
70	↓	↓	↓	↓	↓
66	↓	↓	↓	↓	↓
64	1.158	.0821	.0429	.0858	19

* Recommended thickness of each sheet of double-sheet laminate.

90%

(85)

TABLE VI

Thickness of Center Tank Membranes for Double-Frame Cells

Frame	Hydrostatic Pressure Increase Factor	Nominal Thickness (ins.)	Actual Thickness* (ins.)	2x Actual Thickness (ins.)	U.S. Std. Gauge
98	1.741	.228	.1225	.245	11
96**	1.66	.217	.1225	.245	11
94	1.57	.206	.1072	.2144	12
90	1.43	.187	.1072	.2144	12
88**	1.37	.179	.0919	.1838	13
86	1.32	.172	.0919	.1838	13
82	1.23	.160	.0919	.1838	13
80	1.20	.156	.0919	.1838	13
78	1.17	.153	.0919	.1838	13
76	1.158	.152	.0766	.1532	14
74	↓	↓	↓	↓	↓
72	↓	↓	↓	↓	↓
70	↓	↓	↓	↓	↓
66	↓	↓	↓	↓	↓
64**	↓	↓	↓	↓	↓
62	1.158	.152	.0766	.1532	14

* Recommended thickness of each sheet of double-sheet laminate.

** Swash bulkheads shown on Design D75-A.

90%

86

TABLE VII

Thickness of Wing Tank Membranes for Single-Frame Cells

Frame	Hydrostatic Pressure Increase Factor	Nominal Thickness (ins.)	Actual Thickness* (ins.)	2x Actual Thickness (ins.)	U.S. Std. Gauge
99	1.79	.063	.0337	.0674	21
98	1.741	.0617	.0337	.0674	21
97	1.70	.0602	.0306	.0612	22
96	1.66	.0588	.0306	.0612	22
95	1.65	.0585	.0306	.0612	22
94	1.57	.0556	.0306	.0612	22
93	1.54	.0546	.0276	.0552	23
91	1.47	.0519	.0276	.0552	23
90	1.43	.0507	.0276	.0552	23
89	1.40	.0494	.0276	.0552	23
88	1.37	.0486	.0245	.0490	24
87	1.34	.0475	.0245	.0490	24
86	1.32	.0468	.0245	.0490	24
85	1.29	.0457	.0245	.0490	24
76	1.158	.0410	.0214	.0428	25
75	↓	↓	↓	↓	↓
74					
73					
72					
71					
70					
69					
67					
66					
65					
64	↓	↓	↓	↓	↓
63	1.158	.0410	.0214	.0428	25

* Recommended thickness of each sheet of double-sheet laminate.

90%

87

TABLE VIII

Thickness of Center Tank Membranes for Single-Frame Cells

Frame	Hydrostatic Pressure Increase Factor	Nominal Thickness (ins.)	Actual Thickness* (ins.)	2x Actual Thickness (ins.)	U.S. Std. Gauge			
99	1.785	.117	.0613	.1226	16			
98	1.741	.114	.0613	.1226	16			
97	1.70	.111	.0613	.1226	16			
96**	1.66	.109	.0551	.1102	17			
95	1.62	.106	.0551	.1102	17			
94	1.57	.103	.0551	.1102	17			
93	1.54	.101	.0551	.1102	17			
91	1.47	.096	.0490	.0980	18			
90	1.43	.094	.0490	.0980	18			
89	1.40	.091	.0490	.0980	18			
88**	1.37	.090	.0490	.0980	18			
87	1.34	.088	.0490	.0980	18			
86	1.32	.086	.0490	.0980	18			
85	1.29	.085	.0429	.0858	19			
83	1.29	.082	↓	↓	↓			
82	1.23	.081						
81**	1.21	.079						
80	1.20	.078						
79	1.18	.077						
78	1.17	.077						
76	1.158	.076						
75	↓	↓						
74								
73**								
72								
71								
70	1.158	.076	.0429	.0858	19			

(Cont'd)

90%

88

TABLE VIII (Cont'd)

Thickness of Center Tank Membranes for Single-Frame Cells

Frame	Hydrostatic Pressure Increase Factor	Nominal Thickness (ins.)	Actual Thickness* (ins.)	2x Actual Thickness (ins.)	U.S. Std. Gauge
69	1.158	.076	.0429	.0858	19
67	↓	↓	↓	↓	↓
66					
65					
64**					
63					
62					
61	1.158	.076	.0429	.0858	19

* Recommended thickness of each sheet of double-sheet laminate.

** Swash bulkheads shown on Design D75-A.

TABLE IX

Summary of Estimated Ship Cost Increases

(Dollars)

	Non-Structural Bulkheads Free-Flooding at Foot of Web				Non-Structural Bulkheads Non Free-Flooding at Foot of Web			
	2	2	1	1	2	2	1	1
Frames per cell	wing tanks only	wings + tanks	wing tanks only	wings + tanks	wing tanks only	wings + tanks	wing tanks only	wings + tanks
Membrane location								
Membrane Material	7,080	26,780	7,970	33,240	7,080	26,780	7,970	33,240
Membrane Labor	33,650	74,710	75,720	178,390	33,650	74,710	75,720	178,390
Edge Connect. Matl.	23,850	62,600	26,980	65,630	23,850	62,600	26,980	65,630
Edge Connect. Bolts	18,750	26,330	41,200	70,830	18,750	26,330	41,200	70,830
Edge Connect. Gskts.	3,110	5,270	7,000	11,800	3,110	5,270	7,000	11,800
Edge Connect. Labor	44,980	84,990	71,680	163,980	44,980	84,990	71,680	163,980
Edge Conn. Coatings	17,110	31,400	38,500	69,800	17,110	31,400	38,500	69,800
Strut. Matl.	-----	12,740	-----	16,020	-----	12,740	-----	16,020
Strut. Labor	-----	6,370	-----	8,010	-----	6,370	-----	8,010
Hatch & Ladder Matl.	340	510	600	1,020	340	510	600	1,020
Hatch & Ladder Labor	980	1,420	1,680	2,820	980	1,420	1,680	2,820
Membrane Door Matl.	5,230	8,170	13,060	20,900	5,230	8,170	13,060	20,900
Membrane Door Labor	1,310	2,040	3,300	5,300	1,310	2,040	3,300	5,300
Sluice Valve Matl.	-----	-----	-----	-----	63,000	105,000	141,700	233,570
Sluice Valve Labor	-----	-----	-----	-----	6,830	11,030	14,170	23,360
Flooding Duct Matl.	5,810	11,770	9,030	16,550	-----	-----	-----	-----
Flooding Duct Lbr.	2,910	5,900	4,520	8,300	-----	-----	-----	-----
Inert Gas Pipe Matl.	6,020	7,210	13,500	16,240	6,020	7,210	13,500	16,240

TABLE IX (Cont'd)

	<u>Non-Structural Bulkheads Free-Flooding</u> at Foot of Web			<u>Non-Structural Bulkheads Non Free-Flooding</u> at Foot of Web		
Inert Gas Pipe Labor	6,020	7,210	13,500	16,240	6,020	7,210
Piping Rearrgmt. Matl.	-----	-----	-----	-----	-----	-----
Piping Rearrgmt. Labor	-----	-----	-----	-----	-----	-----
Web Cutout Closure	5,280	5,280	11,880	11,880	7,920	10,160
					17,820	22,720
Direct Shipyard Cost	182,430	380,700	340,120	716,950	246,180	487,060
Shipyard Delivery Price	228,040	475,900	425,150	896,190	307,700	608,800
Total Price for ship (millions of dollars)	14.93	15.18	15.13	15.60	15.01	15.31
					15.31	15.91

Note: Delivery Price of Base Ship, Design D75-A is \$14,700,000, Reference (4).

TABLE X

Required Freight Rates - Short Voyage

	Non-Structural Bulkheads Free-Flooding at Foot of Web				Non-Structural Bulkheads Non Free-Flooding at Foot of Web			
	2 wing tanks only	2 wings + tanks only	1 wing tanks only	1 wings + tanks only	2 wing tanks only	2 wings + tanks only	1 wing tanks only	1 wings + tanks only
Frames Per Cell	14,930,000	15,180,000	15,130,000	15,600,000	15,010,000	15,310,000	15,310,000	15,910,000
Membrane Location								
Delivery Price	75,608	75,265	75,588	75,196	75,608	75,265	75,588	75,196
Deadweight, long tons	344,000	345,000	345,000	347,000	345,000	345,000	346,000	349,000
Insurance, Annual	1,683,000	1,683,000	1,683,000	1,683,000	1,683,000	1,683,000	1,683,000	1,683,000
Additional Annual Oper. Cost (Fuel, Port charges, Manning, Prov./Stores)	2,027,000	2,028,000	2,028,000	2,030,000	2,028,000	2,028,000	2,029,000	2,032,000
Total Annual Oper. Cost	1,646,000	1,674,000	1,668,000	1,720,000	1,655,000	1,688,000	1,688,000	1,750,000
Amortization - 0 Tax	2,519,000	2,561,000	2,553,000	2,632,000	2,532,000	2,583,000	2,583,000	2,684,000
Amortization - 50 Tax	3,673,000	3,702,000	3,695,000	3,750,000	3,683,000	3,716,000	3,717,000	3,782,000
Total Annual Cost - 0 Tax	4,546,000	4,589,000	4,581,000	4,662,000	4,560,000	4,611,000	4,612,000	4,716,000
Total Annual Cost - 50 Tax	1,651,480	1,643,990	1,651,040	1,642,480	1,651,480	1,643,990	1,651,040	1,642,480
Cargo Delivered/Year	2.22	2.25	2.24	2.27	2.23	2.26	2.25	2.30
RFR - 0 Tax (\$/LT)	.9	2.3	1.8	3.2	1.4	2.7	2.3	4.5
% Increase*	2.75	2.79	2.77	2.82	2.76	2.80	2.79	2.87
RFR - 50 Tax (\$/LT)	1.1	2.6	1.8	3.7	1.5	2.9	2.6	5.5
% Increase*								

(All costs in dollars)

* RFR for Design D75-A = 2.20 for 0 Tax and 2.72 for 50 Tax.

TABLE XI

Required Freight Rates - Long Voyage

	Non-Structural Bulkheads Free-Flooding at Foot of Web				Non-Structural Bulkheads Non Free-Flooding at Foot of Web			
	2	2	1	1	2	2	1	1
Frames Per Cell	2	2	1	1	2	2	1	1
Membrane Location	wing tanks only	wings + tanks	wing tanks only	wings + tanks	wing tanks only	wings + tanks	wing tanks only	wings + tanks
Delivery Price	14,930,000	15,180,000	15,130,000	15,600,000	15,010,000	15,310,000	15,310,000	15,910,000
Deadweight, long tons	75,608	75,265	75,588	75,196	75,608	75,265	75,588	75,196
Insurance, Annual	344,000	345,000	345,000	347,000	345,000	345,000	345,000	349,000
Add'l Annual Oper. Cost (Fuel, Port charges, Manning, Prov/Stores)	1,519,000	1,519,000	1,519,000	1,519,000	1,519,000	1,519,000	1,519,000	1,519,000
Total Annual Oper. Cost	1,863,000	1,864,000	1,864,000	1,866,000	1,864,000	1,864,000	1,865,000	1,868,000
Amortization - 0 Tax	1,646,000	1,674,000	1,668,000	1,720,000	1,655,000	1,688,000	1,688,000	1,750,000
Amortization - 50 Tax	2,519,000	2,561,000	2,553,000	2,632,000	2,532,000	2,583,000	2,583,000	2,684,000
Total Annual Cost - 0 Tax	3,509,000	3,538,000	3,532,000	3,586,000	3,519,000	3,552,000	3,553,000	3,618,000
Total Annual Cost - 50 Tax	4,382,000	4,425,000	4,417,000	4,498,000	4,396,000	4,447,000	4,447,000	4,552,000
Cargo Delivered/Year	430,140 long tons	428,190 long tons	429,570 long tons	427,790 long tons	430,140 long tons	428,190 long tons	429,570 long tons	427,790 long tons
RFR - 0 Tax (\$/LT)	8.16	8.26	8.22	8.38	8.18	8.30	8.27	8.46
% Increase*	1.0	2.2	1.7	3.7	1.2	2.7	2.4	4.7
RFR - 50 Tax (\$/LT)	10.19	10.33	10.28	10.51	10.22	10.39	10.35	10.59
% Increase*	1.2	2.6	2.1	4.4	1.5	3.2	2.8	5.2

(All costs in dollars)

* RFR for Design D75-A = 8.08 for 0 Tax and 10.07 for 50 Tax.

TABLE XII

Decrease in Expected Annual Accidental DischargeDesign D75-A (Base ship)

Expected accid. discharge - collisions - per ship per year	9.90 (m) ³
Expected accid. discharge - strandings, rammings - per ship per year	37.10 (m) ³
Expected accid. discharge - total - per ship per year	47.00 (m) ³
Probable outflow from collision	6576 (m) ³

Base Ship with Double-Frame Cells in Wing Tanks Only

Probable outflow from collision	3829 (m) ³
Expected accid. discharge - collisions - per ship per year	5.76 (m) ³
Expected accid. discharge - total - per ship per year	42.86 (m) ³
Reduction in expected accid. discharge - per ship per year	4.14 (m) ³
Reduction in expected accid. discharge - percent	8.8
Increase in total annual cost per ship*	\$26,000
Cost of reduction in expected accid. outflow	\$6280/(m) ³

Base Ship with Double-Frame Cells in Center and Wing Tanks

Probable outflow from collision	2938 (m) ³
Expected accid. discharge - collisions - per ship per year	4.42 (m) ³
Expected accid. discharge - total - per ship per year	41.42 (m) ³
Reduction in expected accid. discharge - per ship per year	5.48 (m) ³
Reduction in expected accid. discharge - percent	11.7
Increase in total annual cost per ship*	\$55,000
Cost of reduction in expected accid. outflow	\$10,036/(m) ³

Base Ship with Single-Frame Cells in Wing Tanks Only

Probable outflow from collision	3451 (m) ³
Expected accid. discharge - collisions - per ship per year	5.20 (m) ³
Expected accid. discharge - total - per ship per year	42.30 (m) ³
Reduction in expected accid. discharge - per ship per year	4.70 (m) ³

TABLE XII (Cont'd)

Reduction in expected accid. discharge - percent	10.0
Increase in total annual cost per ship*	\$49,000
Cost of reduction in expected accid. outflow	\$13,617/(m) ³

Base Ship with Single-Frame Cells in Center and Wing Tanks

Probable outflow from collision	2378 (m) ³
Expected accid. discharge - collisions - per ship per year	3.58 (m) ³
Expected accid. discharge - total - per ship per year	40.68 (m) ³
Reduction in expected accid. discharge - per ship per year	6.32 (m) ³
Reduction in expected accid. discharge - percent	13.4
Increase in total annual cost per ship*	\$103,000
Cost of reduction in expected accid. outflow	\$16,297/(m) ³

* Short voyage, 0 tax case.

TABLE XIII

Calculation of Mean Operational Discharge per Voyage

Ballasted Displacement Tank Cleaning Method	<u>45% Full Load Displ.</u>		<u>60% Full Load Displ.</u>	
	1	2	1	2
<u>Base Ship, Design D75-A, Reference (4)</u>				
Mean operational discharge per voyage	3.77(m) ³	2.01(m) ³	4.62(m) ³	2.85(m) ³
Discharge per voyage from dirty ballast	.33(m) ³	.33(m) ³	1.18(m) ³	1.18(m) ³
Discharge per voyage from tank washings	3.44(m) ³	1.68(m) ³	3.44(m) ³	1.68(m) ³
Dirty ballast carried, long tons	5,330	5,330	18,930	18,930
Cargo/ballast tank surface area, (ft) ²	143,970	143,970	143,970	143,970
<u>Base Ship with Double-Frame Cells in Wing Tanks Only</u>				
Cargo/ballast tank surface area, (ft) ²	143,970	143,970	143,970	143,970
16-voyage discharge from dirty ballast	5.28(m) ³	5.28(m) ³	18.88(m) ³	18.88(m) ³
Cargo only tank surface area, (ft) ²	906,410	906,410	906,410	906,410
3-voyage cargo only tank wash-disch.	30.70(m) ³	14.98(m) ³	30.70(m) ³	14.98(m) ³
16-voyage cargo/ballast tank wash-disch.	26.01(m) ³	12.69(m) ³	26.01(m) ³	12.69(m) ³
Total 16-voyage operational disch.	61.99(m) ³	32.95(m) ³	75.59(m) ³	46.55(m) ³
Mean operational discharge per voyage	3.87(m) ³	2.06(m) ³	4.72(m) ³	2.91(m) ³
<u>Base Ship with Double-Frame Cells in Center and Wing Tanks</u>				
Cargo/ballast tank surface area (ft) ²	178,130	178,130	178,130	178,130
16-voyage discharge from dirty ballast	6.57(m) ³	6.57(m) ³	23.36(m) ³	23.36(m) ³
Cargo only tank surface area, (ft) ²	945,450	945,450	945,450	945,450
3-voyage cargo only tank wash-disch.	32.02(m) ³	15.63(m) ³	32.03(m) ³	15.63(m) ³
16-voyage cargo/ballast tank wash-disch.	32.18(m) ³	15.70(m) ³	32.18(m) ³	15.70(m) ³
Total 16-voyage operational disch.	70.77(m) ³	37.90(m) ³	87.56(m) ³	54.69(m) ³
Mean operational discharge per voyage	4.42(m) ³	2.37(m) ³	5.47(m) ³	3.42(m) ³

TABLE XIII (Cont'd)

Base Ship with Single-Frame Cells in Wing Tanks Only

Cargo/ballast tank surface area, (ft) ²	143,970	143,970	143,970	143,970
16-voyage discharge from dirty ballast	5.28(m) ³	5.28(m) ³	18.88(m) ³	18.88(m) ³
Cargo only tank surface area, (ft) ²	966,410	966,410	966,410	966,410
3-voyage cargo only tank wash. disch.	32.73(m) ³	15.97(m) ³	32.73(m) ³	15.97(m) ³
16-voyage cargo/ballast tank wash. disch.	<u>26.01(m)³</u>	<u>12.69(m)³</u>	<u>26.01(m)³</u>	<u>12.69(m)³</u>
Total 16-voyage operational disch.	64.02(m) ³	33.94(m) ³	77.62(m) ³	47.54(m) ³
Mean operational discharge per voyage	4.00(m) ³	2.12(m) ³	4.85(m) ³	2.97(m) ³

Base Ship with Single-Frame Cells in Center and Wing Tanks

Cargo/ballast tank surface area, (ft) ²	217,170	217,170	217,170	217,170
16-voyage discharge from dirty ballast	7.96(m) ³	7.96(m) ³	28.48(m) ³	28.48(m) ³
Cargo only tank surface area (ft) ²	1,064,000	1,064,000	1,064,000	1,064,000
3-voyage cargo only tank wash. disch.	36.04(m) ³	17.58(m) ³	36.04(m) ⁴	17.58(m) ³
16-voyage cargo/ballast tank wash. disch.	<u>39.23(m)³</u>	<u>14.90(m)³</u>	<u>39.23(m)³</u>	<u>14.90(m)³</u>
Total 16-voyage operational disch.	83.23(m) ³	40.44(m) ³	103.75(m) ³	60.96(m) ³
Mean operational discharge per voyage	5.20(m) ³	2.53(m) ³	* 6.48(m) ³	3.81(m) ³

* Fails to meet limit of Cargo dwt/15,000 = 5.91 -- Table 10, Reference (4).

AD-A032 868

WEBB INST OF NAVAL ARCHITECTURE GLEN COVE N Y
NON-STRUCTURAL BULKHEADS TO CONTROL TANKER OIL SPILLS.(U)
AUG 74 N A HAMLIN

F/G 13/10

UNCLASSIFIED

USCG-D-112-76

DOT-CG-41015-A

NL

2 OF 2

AD
A032868



END

DATE
FILMED
1 - 77

TABLE XIV

Fleetwise Oil Outflow Estimates from Operational and Accidental
Discharges Apportioned on a Per Ship, Per Year Basis,
Assuming 12 Voyages Per Year

Ballasted Displacement Tank Cleaning Method	<u>45% Full Load Displ.</u>		<u>60% Full Load Displ.</u>	
	1	2	1	2
<u>Base Ship - Design D75-A</u>				
Probable outflow from collision	6576 (m) ³	6576 (m) ³	6576 (m) ³	6576 (m) ³
Mean operational discharge per voyage	3.77(m) ³	2.01(m) ³	4.62(m) ³	2.85(m) ³
Expected accid. disch.-collisions-ship/yr.	9.90(m) ³	9.90(m) ³	9.90(m) ³	9.90(m) ³
Expected accid. disch.- other - ship/year	37.10(m) ³	37.10(m) ³	37.10(m) ³	37.10(m) ³
Operational discharge - ship/year	<u>45.20(m)³</u>	<u>24.10(m)³</u>	<u>55.40(m)³</u>	<u>34.18(m)³</u>
Expected total discharge - ship/year	92.20(m) ³	71.10(m) ³	102.40(m) ³	81.18(m) ³
<u>Base Ship with Double-Frame Cells in Wing Tanks Only</u>				
Probable outflow from collision	3829 (m) ³	3829 (m) ³	3829 (m) ³	3829 (m) ³
Mean operational discharge per voyage	3.87(m) ³	2.06(m) ³	4.72(m) ³	2.91(m) ³
Operational discharge - ship/year	46.40(m) ³	24.70(m) ³	56.60(m) ³	34.90(m) ³
Expected accid. disch.-collisions-ship/yr.	<u>5.76(m)³</u>	<u>5.76(m)³</u>	<u>5.76(m)³</u>	<u>5.76(m)³</u>
Expected total discharge - ship/year	89.26(m) ³	67.56(m) ³	99.46(m) ³	77.76(m) ³
Reduction in expected total disch.-ship/yr.	2.94(m) ³	3.54(m) ³	2.96(m) ³	3.42(m) ³
Increase in total annual cost - 0 tax*	\$26,000	\$26,000	\$26,000	\$26,000
Cost of reduction in expected total outflow	\$8843/(m) ³	\$7345/(m) ³	\$8843/(m) ³	\$7602/(m) ³
<u>Base Ship with Double-Frame Cells in Center and Wing Tanks</u>				
Probable outflow from collision	2938 (m) ³	2938 (m) ³	2938 (m) ³	2938 (m) ³
Mean operational discharge per voyage	4.42(m) ³	2.37(m) ³	5.47(m) ³	3.42(m) ³
Operational discharge - ship/year	52.99(m) ³	28.42(m) ³	65.59(m) ³	41.02(m) ³
Expected accid. disch.-collisions-ship/yr.	<u>4.43(m)³</u>	<u>4.43(m)³</u>	<u>4.43(m)³</u>	<u>4.43(m)³</u>
Expected total disch. - ship year	94.52(m) ³	69.95(m) ³	107.12(m) ³	82.55(m) ³
Reduction in expected total disch.-ship/yr.	-2.32(m) ³	1.15(m) ³	-4.72(m) ³	-1.37(m) ³
Increase in total annual cost - 0 tax*	\$55,000	\$55,000	\$55,000	\$55,000
Cost of reduction in expected total outflow	-----**	\$47,826/(m) ³	-----**	-----**

TABLE XIV (Cont'd)

Base Ship with Single-Frame Cells in Wing Tanks Only

Probable outflow from collision	3451 (m) ³	3451 (m) ³	3451 (m) ³	3451 (m) ³
Mean operational discharge per voyage	4.00(m) ³	2.12(m) ³	4.85(m) ³	2.97(m) ³
Operational discharge - ship/year	47.96(m) ³	25.42(m) ³	58.16(m) ³	35.62(m) ³
Expected accid. disch.-collisions-ship/yr.	<u>5.20(m)³</u>	<u>5.20(m)³</u>	<u>5.20(m)³</u>	<u>5.20(m)³</u>
Expected total discharge - ship/year	90.26(m) ³	67.72(m) ³	100.46(m) ³	77.92(m) ³
Reduction in expected total disch.-ship/yr.	1.94(m) ³	3.38(m) ³	1.94(m) ³	3.26(m) ³
Increase in total annual cost - 0 tax *	\$49,000	\$49,000	\$49,000	\$49,000
Cost of reduction in expected total outflow	\$25,257/(m) ³	\$14,497/(m) ³	\$25,257/(m) ³	\$15,031/(m) ³

Base Ship with Single-Frame Cells in Center and Wing Tanks

Probable outflow from collision	2378 (m) ³	2378 (m) ³	2378 (m) ³	2378 (m) ³
Mean operational discharge per voyage	5.20(m) ³	2.53(m) ³	***6.48(m) ³	3.81(m) ³
Operational discharge - ship/year	62.34(m) ³	30.33(m) ³	77.70(m) ³	45.69(m) ³
Expected accid. disch.-collisions-ship/yr.	<u>3.58(m)³</u>	<u>3.58(m)³</u>	<u>3.58(m)³</u>	<u>3.58(m)³</u>
Expected total disch. - ship/year	103.02(m) ³	71.01(m) ³	118.38(m) ³	86.37(m) ³
Reduction in expected total disch.-ship/yr.	-10.82(m) ³	.09(m) ³	-15.98(m) ³	-5.19(m) ³
Increase in total annual cost - 0 tax *	\$103,000	\$103,000	\$103,000	\$103,000
Cost of reduction in expected total outflow	-----**	\$1,144,444/(m) ³	-----**	-----**

* Assumes short voyage case, Table X

** Cost of reduction in expected total outflow omitted where reduction is increased.

*** Fails to meet limit of cargo dwt/15,000 = 5.91

(99)
100X
all